MICROBIAL ELECTROSYNTHESIS IN *SHEWANELLA ONEIDENSIS* MR-1

By

Kathryne Caldwell Ford

A DISSERTATION

Submitted to
Michigan State University
in partial fulfillment of the requirements
for the degree of

Microbiology and Molecular Genetics – Doctor of Philosophy

2023

ABSTRACT

Shewanella oneidensis MR-1 is a model electroactive bacterium that has been extensively studied for both foundational mechanisms and biotechnology. Despite this, the extent and complexity of the extracellular electron transport (EET) pathway is still being unraveled. This field of study is further complicated because cells modulate the flow of electrons based on rate of flux, redox partner, and whether electrons are being exported or imported into the cell. In this work, I explore the EET pathway of *S. oneidensis* in the context of microbial electrosynthesis (MES) optimization. MES technology aims to use microorganisms as biocatalysts to drive the formation of useful chemical products in a bioelectrochemical system (BES), ideally using carbon dioxide (CO_2) as the substrate. Here, I will examine the native EET systems and synthetic biology efforts to engineer a strain of *S. oneidensis* capable of such electroautrophy for bioproduction.

In Chapter 2, I look at the influence of oxygen (O_2) on MES efficiency for 2,3-butanediol generation in *S. oneidensis*. To do this, butanediol dehydrogenase is expressed in wild-type (WT) *S. oneidensis* cells to catalyze the NADH-dependent reduction of acetoin to 2,3-butanediol. Our research group previously showed that electron uptake from a cathode to form NADH is an energetically unfavorable reaction and overcame this thermodynamic barrier through expression of the proton pump proteorhodopsin (PR). In the new design, the reaction is coupled to the energetically favorable reduction of O_2 by native oxidase; during this bidirectional electron transfer, electrons from the cathode power both reactions.

In Chapter 3, I use this same system to reassess the contribution of major cytochrome proteins in the EET pathway during MES. I demonstrate that the outer membrane MtrCAB complex is essential for this process, while other components like CymA and FccA have a more flexible role. Importantly, I show that exogenous flavins are unable to compensate for the loss of natively produced flavins for 2,3-butanediol production, despite their apparent influence on cathodic current. Finally, I reexamine the role of hydrogenases in this process, demonstrating their importance for cell survival on the electrode.

Chapters 4 and 5 of this dissertation focus on the use of synthetic biology techniques to install a CO_2 fixation pathway in the heterotrophic *S. oneidensis.* To achieve this goal, I combine *in silico* metabolic modeling with a CRISPRi knockdown system to create a strain in which multiple substrates are required for biomass synthesis and energy acquisition. By then expressing RuBisCO and PrkA in this strain (Δ*gpmA* pCBB), I then devise a laboratory evolution experiment to generate a strain that will use CO_2 to build biomass.

In summary, there is still much to be understood about EET in *S. oneidensis* and an increasing array of bioengineering tools that can be used to this end. This work does just this by exploring the energetics and physiology of *S. oneidensis*'s EET network, as well as laying the groundwork for a functional electroautotrophic chassis for carbon-neutral bioproduction.

This work is dedicated to my friends and loved ones.
Those who made me food when I was too busy to cook, spent long days working alongside me, traveled across the world with me, and had social distance hangouts when we couldn't be together. Though we continue to go our separate ways as we grow older, I will always carry your love with me.

This is also dedicated to my oldest companion, Buttons, and my newest family members who arrived during my graduate school, Zachary, Abigail, and Gabriel.

ACKNOWLEDGEMENTS

There are many people I would like to thank for their support, mentorship, and guidance during my nine years at Michigan State University. I would like to thank the Michigan State University Honors College for offering me a spot in their Professorial Assistantship program, allowing me to begin my scientific journey in my first year of undergraduate studies. Similarly, the Bailey Scholars program and Clean Water Action, two communities that nurtured my interest in environmental protection and provided a space to both live and grow. These opportunities put me on my path towards pursuing applicable solutions to the environmental issues we currently and will continue to face.

I am grateful to the Microbiology and Molecular Genetics, and Biochemistry and Molecular Biology departments that have been a welcoming environment to foster collaboration and growth during my tenure. Their financial support has enabled me to travel to research conferences around the world and maintain connections with exceptional researchers. Thank you to the National Science Foundation for the Graduate Student Research Fellowship that gave me the freedom to pursue work that inspired me, as well as their trust in my scientific future.

I express my deepest gratitude to those who mentored me, fostering my scientific skills, nurturing integrity, and cultivating critical thinking abilities. My senior undergraduate work with Dr. Matthew Schrenk and the members of his research team inspired me to remain at Michigan State for graduate school. As well as his continued mentorship as a member of my thesis committee, alongside two inspirational scientists, Dr. Gemma Reguera and Dr. Robert Hausinger. Thank you for pushing my research abilities forward and help me create a scientific body of work of which I am immensely

proud. Additional thanks to those in the department who kept me sane through many a coffee break and commiserating chat, especially Dr. Kazem Kashefi, (soon-to-be-Dr.) Osama Alian, and Dr. Kody Duhl.

There are not enough words to express my appreciation and gratitude for my mentor Dr. Michaela TerAvest and the members of our research team; Shaylynn Miller, Megan Gruenberg, Nicholas Tefft, Dr. Magda Felczak, and everyone who passed through during my time. Though I was hesitant to join a biochemistry and electromicrobiology lab, I am so glad that I did. Michaela's mentorship has been invaluable to my growth as a scientist, collaborator, and person. She helped me maintain focus on my project while giving me the freedom to explore my crazy ideas. I am grateful to her for being an inspiration to what effective, successful, and thoughtful academic mentorship can be. To my lab mates: thank you for being there to bounce ideas off of, help me finish an experiment, and moral support for every time a bioreactor leaked or the HPLC errored. I know that without your help and company, my time in graduate school would have been difficult and lonely.

Finally, I want to thank my loved ones. For my family that pushed me to excel and always believed in me. For my friends who kept me sane through food, movie nights, and great company. I will hold your friendships close to my heart as we grow and move away, change careers, experience loss, and find others we care for. Thank you to my partner John Shook, who has been my rock and my light at the end of the tunnel. You are one of the most naturally gifted scientists I have ever known, your laughter is infectious and always brings me joy, and I am excited to start the next chapter of my life with you. Last but not least, thank you to my little man and Zoom companion, Buttons.

TABLE OF CONTENTS

LIST OF ABBREVIATIONS

2,3-BDO	2,3-butanediol
apo-	‘without cofactor’
ATP	Adenonine triphosphate
BES	Bioelectrochemical system
BDH (Bdh)	Butanediol dehydrogenase
CB(B)C	Calvin-Benson(-Bassham) Cycle
CCCP	Carbonyl cyanide m-chlorophenylhydrazone
CMF	Carbon microfiber
CNF	Carbon nanofiber
CRISPRi	Clustered regularly interspaced short palindromic repeats – interference
CRISPRa	Clustered regularly interspaced short palindromic repeats - activation
DMSO	Dimethyl sulfoxide
DO	Dissolved oxygen
eDNA	Extracellular DNA
FAD	Flavin adenine dinucleotide
FBA	Flux balance analysis
FMN	Flavin mononucleotide
EAB	Electroactive bacteria
EET	Extracellular electron transport
EOC	Exported organic carbon
EPS	Exopolymeric substances
ETC	Electron transport chain

holo-	‘with cofactor’
HPLC	High performance liquid chromotagraphy
IPTG	Isopropylthio-β-galactoside
MES	Microbial electrosynthesis
MEC	Microbial electrosynthesis cell
MFC	Microbial fuel cell
NAD^+	Nicotinamide adenine dinucleotide (oxidized form)
NADH	Nicotinamide adenine dinucleotide (reduced form)
NAG	N-acetylglucosamine
NDH	NADH dehydrogenase
OMC	Outer membrane cytochrome
OME	Outer membrane extension
OMV	Outer membrane vesicle
PMF	Proton motive force
PR	Proteorhodopsin
ROS	Reactive oxygen species
RF	Riboflavin
sgRNA	Small guide RNA
SMF	Sodium motive force
SNP	Small nucleotide polymorphism
TCA	Tricarboxcylic acid
TMAO	Trimethylamine N-oxide
WT	Wildtype

Chapter 1: Microbial Electrosynthesis in *Shewanella oneidensis* MR-1

Kathryne C. Ford[1,2], Michaela A. TerAvest[1]*

[1]Department of Biochemistry and Molecular Biology, Michigan State University, East Lansing, MI, 48824, USA

[2]Department of Microbiology and Molecular Genetics, Michigan State University, East Lansing, MI, 48824, USA

1.1 Abstract

Human reliance on fossil fuels is unsustainable. As alternative technologies such as wind and solar electricity generation develop, researchers are simultaneously designing systems to store the electricity as chemical energy. Microbial electrosynthesis (MES) is a burgeoning field that offers a platform to do just this. In MES, electrons are taken up by microorganisms to drive targeted chemical reactions to produce useful products such as acetic acid and ethanol. This work will discuss the history and future of MES, specifically through the use of the exoelectrogenic bacterium *Shewanella oneidensis* MR-1. We will examine the physiology of electron transport in *S. oneidensis*, as well as how synthetic biology tools are being leveraged to optimize these pathways.

1.2 Introduction to Microbial Electrosynthesis

The exchange of electrons is a fundamental biochemical process, ubiquitous and essential for life to exist. Cells rely on the uptake of electrons from feedstocks during catabolism, and the deposition of electrons onto readily available compounds. Understanding this flow of electrons, and how different species facilitate this flow, is fundamental to our knowledge of physiology, community interactions, and developing biotechnology. In natural environments, microorganisms evolve specialized mechanisms to fill specific ecosystem niches. This specificity means that the physiological capabilities of different bacterial species are closely tied to where they live. One of the strongest determinants is availability of terminal electron acceptors for respiration. Humans, most animals, and many microorganisms rely on aerobic respiration, utilizing oxygen as the terminal electron acceptor. In the absence of oxygen, organisms can use other molecules like nitrate or sulfate for anaerobic respiration, or internal redox

reactions to gain energy in a process called fermentation[1]. Some microorganisms have also evolved to use extracellular electron acceptors. This process requires specialized protein machinery to transport electrons from internal energy pools, across cellular membranes onto the cell surface to reduce available acceptors. This mechanism, termed extracellular electron transport (EET), allows microbes to use solid metal oxides like Fe(III) and Mn(IV) for anaerobic respiration. Researchers discovered that EET-capable microbes can extend this ability to use electrodes as electron acceptors and donors. As understanding of EET pathways expanded, so did the potential to use these electroactive bacteria (EAB) for biotechnology.

A common technology that employs EAB is a process called microbial electrosynthesis (MES). In MES, EAB are used as biocatalysts to convert chemical energy into electrical energy, and vice versa. With increased interest in using renewable sources of energy such as wind and solar, being able to transform the electrical energy produced to chemical energy will be invaluable. Additionally, many MES systems aim to use autotrophs as the biocatalysts to capture and store atmospheric carbon dioxide (CO_2)[2–4]. This diverse field has leveraged native and engineered microbes for bioremediation, carbon capture, biofuel production, and more.

This work will discuss the energetic considerations for using a MES platform for the carbon-neutral generation of industrially relevant chemical products by the bacterium *Shewanella oneidensis* MR-1. This strain contains a complex and diverse network of EET proteins, so we will also look at the role of key players during electron transport to generate NADH. Additionally, we will discuss a synthetic biology pipeline for enacting difficult genetic modifications. Lastly, we will demonstrate how this

bioengineering pipeline can be applied to *S. oneidensis* for future work towards integrating this system with carbon capture (**Figure 1.1**).

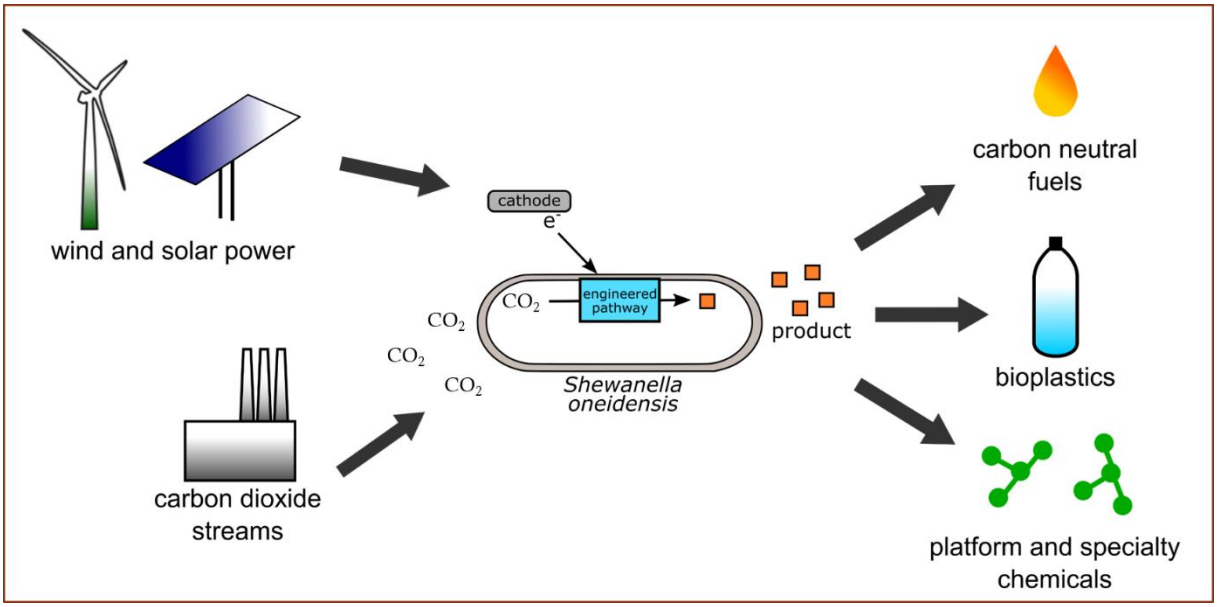

Figure 1.1 Goal of MES in *S. oneidensis*. An overarching goal of the TerAvest research group is to engineer a strain of *S. oneidensis* MR-1 that can be used in MES to produce industrially relevant chemical products. This organism is naturally capable of using a cathode as an electron donor. Therefore, research aims for this project include: (1) Understanding and optimizing electron uptake, (2) Introducing exogenous pathways for bioproduction, (3) Installing a CO_2 fixation pathway in this heterotroph. Figure adapted from Tefft and TerAvest 2019[5].

1.3 Technology Meets Microbiology

While the term 'microbial electrosynthesis' was first coined in 2010 by Nevin et al.[3], the basis for this technology goes back over a hundred years[6]. During that time, many research developments employed bioelectrochemical systems (BES) as microbial fuel cells (MFCs). In an MFC, microorganisms are used as biocatalysts to convert chemical energy into electricity on an electrode[7–9]. This system offers an alternative means for energy generation from a wide range of sources outside of fossil fuels, including undesirable feedstocks like wastewater[10,11]. In principle, as bacteria liberate electrons from carbon substrates during metabolism, they generate reducing

equivalents (NADH, NADPH) or reduced cytochromes, which in turn reduce the soluble mediators that shuttle the electrons to the anode, while O_2 and H^+ react at the cathode to form H_2O[12,13]. Beyond this core structure, the design of MFCs can vary greatly based on electrode material, vessel dimensions, bacterial species or consortia, and feedstock[14]. Often, early iterations of MFCs would rely on redox-active mediators to facilitate electron movement between the cells and the electron accepting electrode (anode)[15,16]. This was because the mechanisms of electron transfer by bacteria were poorly understood. Commonly used mediators include neutral red, methylene blue, and anthraquinone-2,6-disulfonate (AQDS).

Eventually, interest grew in using this process in reverse, using electricity to power biochemical reactions. To do this, a BES is used as a microbial electrosynthesis cell (MEC), where bacteria on the cathode take up electrons to create reducing power such as NADH that can be used to drive a specific chemical reaction (**Figure 1.2**). This approach was enticing as a potential means of storing the electricity generated from renewable sources like wind and solar, a sort of biochemical battery. Additionally, depending on the physiological capabilities of the microbes, MECs are used to produce other useful chemicals, including acetic acid, ethanol, and even pharmaceuticals[2,17–20]. Since then, this process known as microbial electrosynthesis (MES) has undergone significant expansion, driven by researchers' efforts to improve the design and efficiency of MECs. This work encompasses three primary developmental approaches: material and structural design of BES, broadening the range of potential products, and characterizing and improving the electron transport pathways of the microbes on the cathode[21].

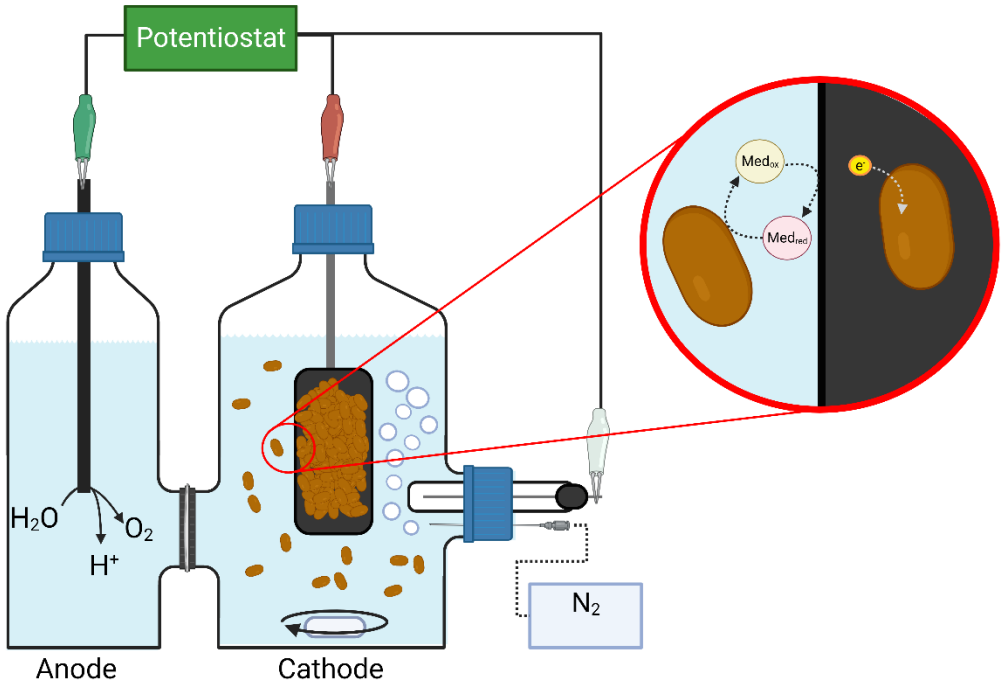

Figure 1.2 *S. oneidensis* on a Cathode in a BES. In a 2-chamber MEC, *S. oneidensis* cells are inoculated into the working chamber with the cathode, while the anode is in the counter chamber, separated by an ion exchange membrane. In the counter chamber, water is split into O_2 and H^+ by energy provided by the anode. The working chamber, often sparged with inert gases such as N_2 to prevent O_2 intrusion, has cells in suspension and attached to the cathode. *S. oneidensis* will take up electrons either through direct contact with the cathode, or via redox-reversible mediators (inset). In the depicted design, the anode is a carbon rod, the cathode is a carbon felt sheet attached to a Pt wire, and the reference electrode, which acts as a reference point to maintain a constant potential in the MEC, is a silver wire saturated by KCl (Ag/AgCl).

Though many early MFC designs had a limited understanding of how bacteria were capable of electron exchange with electrodes, the innate link between EET and anaerobic respiration was ultimately uncovered. In parallel with MFC research, it was discovered that there are bacteria capable of anaerobic respiration using extracellular materials such as U(VI), Mn(IV) and Fe(III)[22–26]. Microbes capable of this extracellular electron transport (EET) are referred to as dissimilatory metal reducing bacteria (DMRB), as they do not assimilate the reduced metals into cell components or protein structures. As the physiological mechanisms behind EET were elucidated, it was shown

that DMRB have the capacity to use an anode as a terminal electron acceptor and produce electrical energy[27,28]. Two of the first well-studied genera capable of this process were *Geobacter* (first described as strain GS-15) and *Shewanella* (previously *Alteromonas*)[22,25,28–30]. While there has since been found a wide variety of electroactive bacteria (EAB) capable of directly or indirectly interacting with electrodes (*Desulfovibrio, Sporomusa, Clostridia, Pseudomonads,* etc.), a vast majority of our understanding of the physiology of EET comes from these two foundational organisms[9,31,32]. Additionally, as a γ-proteobacterium, *S. oneidensis* is genetically tractable. Due to this, much work has utilized this organism as the basis for work on electrode-driven bioproduction.

Since its inception, there has been interest in exploring the potential for combining autotrophy with EET for MES. Organisms with 'electroautotropic' metabolism could be fed carbon dioxide (CO_2) and energy from electrodes as the sole inputs for bioproduction systems. This approach is the end goal for many MES system designs; consumption of CO_2 that would otherwise be emitted while generating high-value chemical products using energy derived from renewable sources. In this dissertation, both EET and carbon fixation will be addressed, along with bioengineering strategies that have been developed to improve these systems in *S. oneidensis* for application in MES. First, we will examine the current understanding of EET in *S. oneidensis*, including the major components, how they are regulated, and how researchers have improved upon the native pathway.

1.4 EET Pathways

As the ability to generate electricity by bacteria is a byproduct of native bio-reduction (respiration) and bio-oxidation pathways, there is not a single consensus

mechanism for performing reversible EET among EAB. Although the EET systems in *S. oneidensis* and *Geobacter* sp. are the most comprehensively studied, research has revealed a diverse field of microorganisms capable of EET. For instance, over a dozen genera have been identified to be capable of the bio-reduction of aqueous U(VI) to the insoluble form U(IV), a process which could be employed for removal of the metal from contaminated soils[33]. While there is overlap in general strategies and shared homologs of different pathways, the diversity in this ability allows for a deeper understanding of the reasons behind their evolution and the mechanisms involved.

A significant portion of our knowledge of microbe-electrode interactions stems from research done under anodic potentials, where the electrode functions as an electron acceptor. Due to interest in using these organisms for MES, more work is being done towards understanding these pathways under cathodic, electron-uptake conditions[5,34–40]. In general, *S. oneidensis* employs two primary mechanisms of EET that have been differentiated: direct and indirect[9,16,31,41]. Direct EET involves outer membrane cytochrome (OMC) proteins on the cell surface directly interacting with an electrode to exchange electrons, whereas indirect utilizes extracellular mediators. While endogenous excreted flavins are the dominant mediators in *S. oneidensis* cultures, artificial electron shuttles like methyl viologen, neutral red, and methylene blue have been used to enhance EET[16]. *S. oneidensis* grows as biofilms on the electrode surface, allowing for a combination of direct and indirect EET through its conductive exopolymeric substances matrix (EPS)[42–45]. Additionally, the role of ‘nanowires’ in EET has garnered interest because it allows cells to deposit electrons over long distances. To optimize EET, understanding flavin chemistry, biofilm formation, nanowires, and

flexibility of proteome and regulatory pathways is essential (**Figure 1.3**).

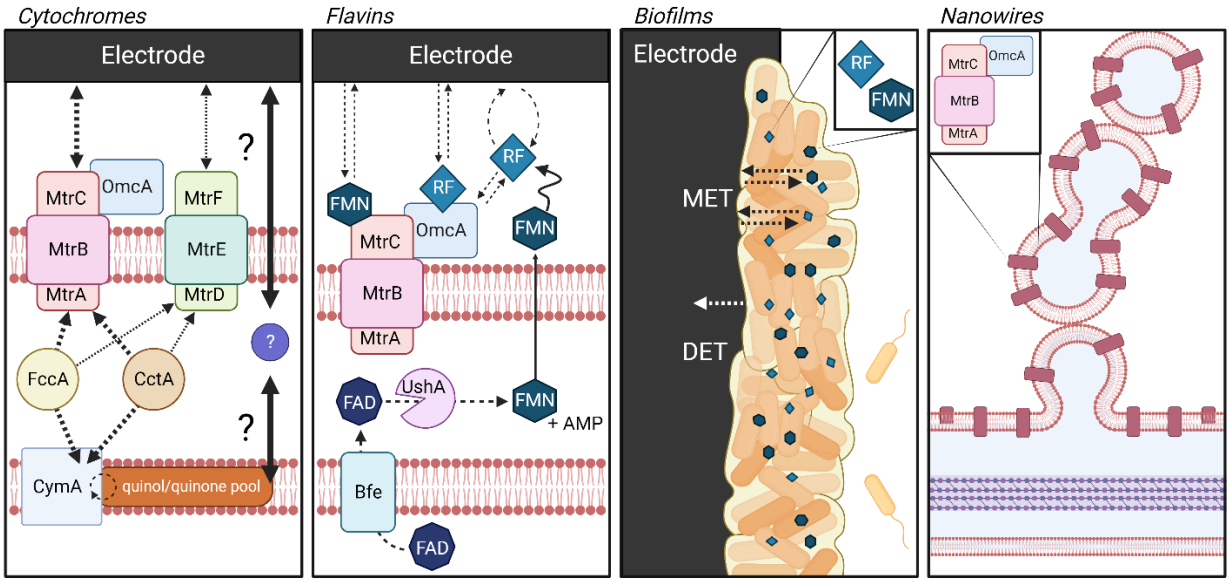

Figure 1.3 Considerations for Improving EET in *S. oneidensis*. When examining potential avenues for improving EET in *S. oneidensis*, four major areas of research are: streamlining the cytochrome network, clarifying the contribution of flavins, improving biofilm formation and conductivity, and understanding electron transport along nanowires. The primarily discussed electron pathway in *S. oneidensis* is electrons being passed from quinol-linked CymA to MtrCAB (+ OmcA, or the less efficient homologous MtrDEF) via periplasmic electron carriers (FccA, CctA). However, *S. oneidensis* has many more cytochromes, and recent work has suggested alterative pathways between the electrode and cell, within the periplasm, and quinol-linked proteins besides CymA[34,46–49]. In *S. oneidensis*, flavin adenosine dinucleotide (FAD) is created in the cytoplasm and transported into the periplasm via Bfe to be cleaved by UshA to form flavin mononucleotide (FMN) and adenosine monophosphate (AMP). FMN is exported through an unknown transporter, where it will act as cofactor for outer membrane cytochromes (OMCs) or abiotically convert to riboflavin (RF) to associate with OMCs or freely shuttle electrons[50–52]. While flavins have been known as important for EET for years, recent data have suggested they contribute more as OMC cofactors for OmcA and MtrC than as free flavins[53–55]. These flavins are also found within the EPS of electrode-attached biofilms[42]. Similarly, it has also been shown that the EPS matrix of *S. oneidensis* biofilms is rich in redox-active cytochrome proteins[56]. This creates a conductive environment that facilitates direct or mediated electron transfer (DET, MET). Over longer distances, cells will build so-called nanowires to transport electrons. In *S. oneidensis*, these are chains of outer membrane vesicles (OMVs) that are rich in cytochromes like MtrCAB[57,58].

1.4.1 Cytochrome-rich pathway

S. oneidensis contains over 40 cytochrome rich proteins. Approximately 80% of these proteins are localized to the outer membrane and can potentially aid in EET; the most well studied EET cytochromes are those in the Mtr pathway[16,46,59,60]. During anaerobic respiration, electrons enter the quinol pool, where they can be passed from the reduced quinols to the inner-membrane bound electron hub CymA[49,61–65]. From here, the electrons can then be passed directly to periplasmic terminal reductases (FccA, NapAB, SirA, NrfA, TorA, etc.) or shuttling cytochrome proteins (FccA, CctA)[66–68]. These shuttling proteins will chauffeur the electrons from the inner membrane to the Mtr complex in the outer membrane. Mtr is a 3-protein complex that spans the outer membrane, including a beta-barrel porin (MtrB) and two heme-rich cytochromes (MtrA, MtrC), and is often found associating with the surface attached protein OmcA[69–73]. Together these OMCs form an EET wire, with OmcA situated to the outside of the cell and MtrC reaching up to ~90 Å above the surface of the cell[74]. MtrC has a trifurcated heme structure, optimizing the distribution of electrons to potential electron acceptors. *S. oneidensis* also excretes the redox reversible flavin compounds riboflavin (Rf) and flavin mononucleotide (FMN) which shuttle electrons from the cell surface to electron acceptors during indirect EET[50,52]. Additionally, OmcA and MtrC associate with Rf and FMN to form flavocytochrome complexes, aiding in direct EET[53–55,75,76].

One important characteristic of the EET cytochrome network in *S. oneidensis* is its redundancy and versatility[77,78]. Though it would be intuitive that the cell uses the same pathway for reduction of similar compounds (e.g., Fe(II)-oxide and ferric citrate), this is not the case. In addition to the cytochrome proteins already mentioned, *S.*

oneidensis also contains two homologs of MtrCAB (MtrDEF, DmsEFABGH) which can complement the primary complex to varying degrees of success [47,48]. Loss of either major periplasmic electron carrier, FccA or CctA, shows no phenotype on an anode and each is likely able to compensate for loss of the other[68,79,80]. CymA is essential for reduction of Fe(III), nitrate, nitrite, fumarate, DMSO, arsenate (V), and manganese (IV), but not for trimethylamine N-oxide (TMAO), sulfite, or thiosulfate[63]. There is also increasing evidence that the inward EET pathway diverges from the outward EET pathway[34,39]. *S. oneidensis* also expresses two hydrogenase complexes, which could potentially facilitate hydrogen-mediated EET.

The flexibility of the *Shewanella* EET system has also been demonstrated and optimized through informed genetic manipulations. Delgado et al. showed that replacing several redox active periplasmic protein encoding genes (*nrfA, ccpA, napA, napB*) with *cctA*, thereby simplifying the network, led to a ~1.7-fold increase in Fe (III) reduction, and ~1.5-fold increase in current after 24 h[80]. More recently, Sun et al. showed that it is the specific tailoring of the network, and not merely excess cytochromes, that aids in EET; overexpression of cytochrome *c* maturation machinery (*ccm*) was slightly inhibitory compared to WT. However, they similarly saw improvements through the deletion of *fccA, napB,* and *tsdB*, and over expression of *cctA*[66]. This work highlights a promising avenue of research for improving EET by optimizing the native proteome.

The reversibility of the MtrCAB pathway in *S. oneidensis* enables it to generate reducing power and drive formation of ATP[5,81,82]. Interestingly, recent work by Rowe et al. showed that deletion of five previously uncharacterized genes (SO0841, SO0181, SO0400, SO3660, SO3662) caused a significant defect in electron uptake from a

cathode[34]. These genes were predicted to encode proteins involved in cell signaling, regulation of a putative oxidoreductase, a quinol-monooxygenase, a transcriptional regulator, and an inner membrane ferredoxin, respectively. Of these, all but SO0841 showed a defect solely in inward EET, with no defect in outward transfer. This highlights that despite all the understanding of EET in *S. oneidensis*, there is still much to learn about this complex cytochrome network. One aspect that further obscures our study of EET proteins is their association with the redox active molecules Rf, FMN, and FAD.

1.4.2 Flavins

Some iron oxide-reducing organisms were capable of doing so at a distance, and this was first demonstrated in *S. oneidensis* cells by Lies et al[83]. However, at the time it was unknown by what mechanism this was occurring, and researchers inferred that it was likely due to soluble redox-active molecules, specifically within a biofilm matrix. These redox active molecules were identified as flavins by Marsili et al. in 2008. Since then, there has been extensive work done to understand the role these redox molecules play in EET[50,84]. Researchers noted that unlike in experiments previously done in *Geobacter spp.*, replacement of BES medium with fresh electrolyte decreased oxidation currents by ~73%. To determine if this reduction was due to soluble redox compounds, spent medium was filter sterilized and returned to the BES, restoring ~95% of anodic current. This redox compound was identified as Rf. This work was quickly followed by work describing the flavin profile of Rf, FMN, and FAD in *S. oneidensis* cells and supernatant, as well as their impact on extracellular ET[51,72,84]. Together, this tells us that FAD is manufactured in the cytoplasm, exported to the periplasm via a flavin transporter (Bfe) before being cleaved by UshA to FMN and AMP[51,85]. FMN is actively secreted

outside the cell and is abiotically transformed into Rf, while FAD remains inside the cell, acting as an essential cofactor for enzymes like fumarate reductase (FccA). The level of flavin secretion is closely associated with the redox state of the environment, as well as availability of carbon substrate and electron acceptor species[86,87].

Following these discoveries, researchers sought to understand the mechanism behind flavins' role in ET. All three species of flavins mentioned here are freely redox reversible, so the prevailing theory for many years was that flavins acted as mediators, shuttling electrons between the cell and electron acceptor across long distances[50,51,88–90]. This was supported by data such as that described in Marsili et al. 2008, that when medium containing soluble flavins was removed, the current decreased, and recovered upon their return. Similarly, deletion of the flavin transporter (Δ*bfe*) resulted in a ~75% decrease in anodic current versus WT *S. oneidensis*. However, there is increasing evidence suggesting that a more prominent role for flavins during EET is as bound cofactors for outer membrane cytochromes (OMC)[38,39,53,54,56,75,76,88,91–93].

Much of the work done to determine the role of specific compounds or proteins on EET has been interpretation of current generated on an anode; very often these working electrodes are also made of carbon materials. This design ignores a variety of confounding variables that can greatly influence data interpretation. One such example is abiotic interactions with the electrode by soluble molecules. Notably, flavins adsorb onto carbon electrode surfaces[53,56]. This leads to conflicting results between work done with carbon electrodes versus electrodes made from indium tin oxide, gold, or other materials. Additionally, because many conclusions are drawn from electrochemical data, it can be difficult to separate abiotic and biotic effects without thorough controls. To this

end, researchers have sought to resolve the binding relationship between OMCs (MtrC, OmcA) and flavins[53,75,93,94]. FMN and Rf associates with MtrC and OmcA, respectively, and these associations can either be transient or stable. A factor influencing this bond is the formation of a disulfide bond in the presence of oxygen, preventing flavin binding to MtrC[75,93]. Therefore, affinity for flavins to bind MtrC is tightly controlled by the redox state of the protein, flavins, and environment. To this end, later work parsed apart the influence of free versus bound flavins to ET. By using a carbon felt electrode, researchers were able to, for the first time, demonstrate the presence of free flavins, flavocytochromes, and OMCs in a single system. Because of this, they could demonstrate that while secreted flavins show a strong electrochemical response, they do not significantly contribute to the biotic current. Instead, it is cytochromes and flavocytochromes that contribute to a majority of the ET[53]. In experiments similar to those that first identified soluble mediators as important to ET, it was shown that in addition to free flavins, released flavin-bound OMCs are found in the bulk medium and capable of electron shuttling[95]. Importantly, while this body of work demonstrates the overestimation of the role of free flavins in the system, it does not negate the fact that flavins are vital for ET; they are simply more important as OMC-bound cofactors.

Flavins also stimulate increased biofilm formation[38,42,91,96,97]. While the physiological mechanism has not been determined, evidence suggests that as the concentration of extracellular Rf increases (>15 nM), it initiates a regulatory shift affecting biofilm-related genes[42]. Biofilms act as an electroactive network, enabling increased EET using redox active molecules trapped within the EPS matrix[92]. Notably, quantification of flavins trapped within biofilms show ~10-fold increase in concentration

compared to the bulk medium. The amount of Rf in the biofilm (2.21×10^{15} molecules) falls within the range of potential OMC binding sites (3.49×10^{14} - 1.05×10^{16}). Taken together, it can be inferred that even if a flavin is not tightly bound to an OMC, it can act as an electron shuttle to a much smaller degree, remaining within the biofilm rather than diffusing over long distances. Work characterizing the role of flavins during EET to an acceptor behind a barrier (cells cannot attach) supported this, showing that a loss of MtrC/OmcA cannot be complemented by exogenous flavin addition. This work reiterated that flavins can be recycled for shuttling but rely on OMCs and operate over short distances[98]. Keeping this in mind, we will next look at the importance of biofilm formation during EET.

1.4.3 Biofilms

In natural environments, it is crucial for bacteria to form biofilms for protection, resource sharing and access, and horizontal gene transfer[99]. *S. oneidensis* forms biofilms on mineral surfaces, such as Fe-oxide, to promote anaerobic respiration using the insoluble minerals[100]. A biofilm consists of whole cells trapped within a matrix of EPS, DNA, proteins, and other secreted molecules. Cells can shift between motile and attached lifestyles via regulatory changes triggered by environmental stimuli. While motile, cells chemotactically sense their environment, and when encountering a favorable environment, such as Fe-oxide, adhere to the surface and initiate biofilm formation[101]. When grown in a BES using an anode as an electron acceptor, cells similarly form biofilms on the electrode surface. Cell attachment and subsequent biofilms are vital to the efficiency of EET between the cell and electrode[102]. Therefore,

much work has been done to understand both the structure and composition of the EPS, as well as the regulatory mechanisms that control them.

Under dynamic conditions with flow, *S. oneidensis* cells develop biofilms, while in static aerobic cultures, they form surface pellicles[103]. Formation is stimulated by the presence of oxygen, and dispersal occurs upon oxygen depletion[104,105]. Genes identified as vital to biofilm formation include agglutination proteins (AggA), extracellular adhesion proteins (BpfA), pili proteins (MshA/PilD, Mxd operon), and the transformation and export systems for them[106–109]. Additionally, as with many microorganisms, the regulation of the small molecule messenger c-di-GMP impacts biofilm formation[99,110,111]. While EPS composition varies from organism to organism, *S. oneidensis* EPS is dominated by proteins, but also contains extracellular DNA (eDNA)[103,112–114]. The biofilm also transforms over time, resulting in changes in composition, thickness, conductivity, shape, and stability[96,111–113,115,116].

During growth on an anode, more current is generated when more cells are attached to the electrode. In nutrient rich, aerobic environments, *S. oneidensis* biofilms can grow relatively thick (100+ μM) and form 3-dimensional, mushroom like structures[106,117,118]. On electrodes in anoxic conditions however, the cells tend to form much thinner biofilm, only monolayers in many cases. This behavior is explained by the need for cells to be in physical contact with the electron acceptor to best survive. Attempts to increase EET by biofilm modulation have seen the most success by increasing the area of attachment and conductivity of the EPS matrix[102,109,116,119–121]. This increase was demonstrated as biofilms grown on electrodes at 0.0 V_{SHE} or aerobically with no current applied will form the mushroom structures, while those grown

at 0.4 V_{SHE} were flat and even, covering more of the electrode[118]. Additionally, even in thicker, electrode attached biofilms, a vast majority of the current (95%) was attributable to the tightly attached bottom layer of cells[56]. A unique example of this was reported by Zhao et al., who showed that overexpression of SulA, which inhibits FtsZ ring formation during cell division, resulted in biofilms with larger surface area coverage and EET. These increases were attributed to the morphological changes that resulted in bigger and elongated cells, therefore increasing the area covered per cell[91]. Another approach focuses instead on optimizing electrode material. Sanchez et al. demonstrated that by using carbon nanofiber (CNF) electrodes over carbon microfiber (CMF), there was increased surface area, creating more cell attachment locations, leading to thicker biofilms and more current generation[119].

Regulation of biofilm formation also impacts the structure and conductivity. Internally, many of the regulatory systems for attachment are controlled by the small messenger c-di-GMP. This signaling molecule can act as both a transcription and post-translational controller in a majority of well-studied bacteria[99,111,122]. It is formed by diguanylate cyclases and degraded by phosphodiesterases; high concentrations increase biofilm formation, and low concentrations signal for detachment[123,124]. Attempts to alter the internal concentration, through expression or deletion of diguanylate cyclases or phosphodiesterases, have shown that more c-di-GMP increases biofilms and current[110,111]. Interestingly, Ng et al. also showed that c-di-GMP increases expression of the Mtr pathway, resulting in thicker and more conductive biofilms[99]. This can also be achieved through external signaling cues. In the work showing biofilm formation at different anodic potentials, those grown at 0.4 V_{SHE} had a lower EPS

content but higher concentrations of electroactive components[118]. Regulation of exonucleases is also important, as there is a required balance between having enough to degrade eDNA that could impact conductivity in older biofilms, but not so much as to abolish its role in attachment for young ones[112]. Another interesting demonstration of regulatory impact is the gene *bolA*. Overexpression of this transcriptional regulator increases biofilm and current generation, but a deletion of *bolA* did not have a phenotype compared to WT. The authors suggest that *bolA* is only expressed under harsh growth conditions, aiding in attachment under dire environmental situations[116]. The electroactive components of biofilms consist of flavins, cytochromes, and flavocytochromes. Work by Edel et al. showed that there was roughly ~10-fold more flavin compounds trapped within the biofilm matrix than in the effluent[42]. As previously mentioned, the amounts of flavins measured falls within the feasible concentration range of cytochrome proteins. Edel et al. suggest that this could corroborate the assertion that even in biofilms, flavins are bound to OMCs, facilitating 'electron hopping' between the redox centers. Whether the cells are using direct or mediated transfer is also significantly affected by regulation. Investigations into biofilm conductivity over time by Choi et al. suggest that younger biofilms mainly use direct EET, while the role of flavin mediated transfer increases as the biofilm ages and increases in thickness[115]. When considering regulatory impact on EET processes, a growing area of interest is the role of 'nanowires', both in their formation and their electroactive composition.

1.4.4 Nanowires

Geobacter spp. are well known for their long electroactive pili structures capable of transporting electrons over long distances. These structures, named nanowires, were

believed to also be formed by *S. oneidensis* cells for EET. *S. oneidensis* can form type IV pili structures with high homology to those of *Geobacter* spp[125]. However, early evidence demonstrated that while *S. oneidensis* forms 'nanowires' capable of EET, these are not pili, and therefore not nanowires[126,127]. It was later demonstrated that outer membrane extensions (OMEs) form the observed conductive filaments[128]. This has led to some contention regarding nomenclature, with other researchers instead suggesting the names 'nanopods' or 'nanocables'[129,130]; for consistency with literature, they will be referred to here as nanowires. Pirbadian et al. provided the first evidence that the nanowires are OMEs, made of chains of outer membrane vesicles (OMVs), containing periplasm (but not cytoplasm) and do not involve pili[131]. The nanowires form under anaerobic conditions and production is stimulated by surface attachment, regardless of substrate availability, surface type, and mixing conditions[132,133]. The conductive nature of the extensions is attributed to OMCs located along the cell surface, including OmcA and MtrC[57,134]. During nanowire formation, expression of Mtr pathway cytochromes, and a variety of periplasmic cytochrome proteins are greatly up regulated, highlighting the correlation between cell surface area and cytochrome usage[133]. While inclusion of OMCs is widely accepted as the physiological structure of nanowires, the mechanism behind the EET properties is more elusive. The prevailing theory supported by both the composition of the nanowires and energetics calculations, is that they facilitate 'electron hopping'. Electrons are passed between the redox active centers of cytochromes embedded in the OM, with a calculated conductivity akin to artificial silicon nanowires (0.01-1 S/cm)[129,130,134].

As much of the work on *S. oneidensis* nanowires is comparatively recent, OME contributions to EET, compared to flavin mediated and non-OME surface cytochromes, have not been thoroughly investigated. Some considerations when determining the relative importance should include the apparent discrepancies between these two established mechanisms. On one side, long distance EET has been attributed to secreted flavin molecules, both due to the distance traversed, and the ability to reduce compounds behind a physical barrier[50–52,72,83,98]. Conversely, evidence suggesting that a majority of flavins are bound to cytochromes as cofactors implies that they may not be as effective at long distance EET as previously thought[39,42,53,56]. Nanowires may fill this gap as they use cytochromes and flavocytochromes to transfer electrons and have been shown to reach up to 9 μm in length[131]. Additionally, if OMVs become detached from the larger nanowire structure, they could facilitate electron shuttling over distances similar to those proposed by free flavins. Work by Liu et al. potentially demonstrates this process, showing that large exported organic components (EOCs), meaning 'excreted' cytochromes and not flavins, are responsible for more than half (~56%) of extracellular reduction of Cr(VI)[95]. These components could potentially represent OMVs that were formed from nanowires. As this system diverges so greatly from our understanding of *Geobacter* spp. nanowires, it will be imperative to understand the contribution of *S. oneidensis* nanowires to EET.

1.5 Bioengineering Techniques

The fields of synthetic biology and biotechnology are inextricably linked as researchers aim to harness biological tools to tackle challenges such as climate change. Synthetic biology incorporates tools from engineering, computer science, and

chemistry to redesign biological processes. *S. oneidensis*, as a model electroactive organism,[135] has garnered significant interest as researchers aim to develop tools for its use during growth with electrodes. Being a γ-proteobacterium and closely related to *Escherichia coli*, *S. oneidensis* offers the advantage of genetic manipulability and the utilization of tools developed for *E. coli*. In this section, we will discuss different bioengineering approaches ranging from small genetic modifications like single nucleotide point mutations (SNP) to entire libraries of novel DNA constructs. Specifically, we will look at bioengineering approaches aimed at increasing EET between cell and electrode through optimization of native processes or genetic toolkit development.

1.5.1 Native Optimization

As discussed, *S. oneidensis* contains many genes that play a role in EET. These encode conductive cytochromes, extracellular components, and metabolic enzymes, many of which have multiple homologous copies within the genome (e.g., MtrCAB & MtrDEF). We have already discussed a variety of approaches researchers have used to improve EET, including simplifying the cytochrome network, increasing biofilm formation or flavin excretion, and modulating the metabolome[66,91,108,110,111,116,136–138]. Other approaches have focused on increasing NADH concentration through enhanced synthesis pathways or substrate utilization. In this way, more electrons (in the form of more NADH) will lead to an increase in reduced quinols and increased electron export. Li et al. aimed to increase the pool of NAD^+/NADH through expression of five non-native genes aimed at increasing import and synthesis of NADH precursors[139]. This modification led to a 4.4-fold increase in power output compared to WT cells. Work by Ding et al. aimed to increase NADH concentrations by increased expression of native

proteins found in central carbon metabolism[140]. Their targets include lactate importers, NADH-generating steps (GapA, Mdh), and NADH dehydrogenases (Ndh), leading to a 62% increase in power density when all four are overexpressed. A recent study implemented genetic alterations from a variety of research groups that have demonstrated various levels of improved EET[141]. A combination of gene knockouts (Δ*SO3171*[108], Δ*exeS*[114], Δ*SO1942*[99,142], Δ*SO3491*), expression of *Geobacter* OMCs and *B. subtilis* flavin synthesis genes[38], and use of an 'artificial biofilm electrode' increased the power density to ~39-fold more than WT *S. oneidensis*. This study illustrates that by combining various engineering techniques, including the utilization of established approaches, it is possible to achieve significantly enhanced output compared to using any of these techniques individually.

1.5.2 Tool Development

While many tools that were first developed in *E. coli* can be adapted to *S. oneidensis*, the development of these systems to optimally operate in *S. oneidensis* can save time and effort that would otherwise be used for troubleshooting. Researchers have addressed this goal through thoughtful plasmid design and employing a wide variety of CRISPR-based editing systems. When constructing plasmids for expression, or overexpression, of different genes, considerations include induction system, copy number, plasmid compatibility, and more. Two commonly used induction systems include isopropyl ß-D-1-thiogalactopyranoside (IPTG)induction using the *lac* promoter, or arabinose induction. However, there is an interest in expanding these options as these systems can be poorly repressed (i.e., 'leaky') or have off-target metabolic effects. This effort has included leveraging native TMAO respiration enzymes for TMAO-based

induction and adapting a rhamnose-inducible system from *E. coli*[143,144]. While the TMAO based approach has the benefit of using native proteins, it is inefficient because it is leaky and inducer concentration dwindles with time. Conversely, the rhamnose-inducible system is beneficial as rhamnose is non-toxic and cannot be metabolized in *S. oneidensis*. However, many researchers prefer constitutive systems to prevent off target effects of inducers, and potentially poorly controlled expression. Yi et al. addressed this concern through introduction of T7 RNA polymerase into *S. oneidensis*, which enables the use of the widely-used constitutive T7 promoter system[145]. Meanwhile, Cao et al. comprehensively tested expression and control of a library of vectors, including 9 promoters of different strengths, 4 origins of replication, 2 shuttle genes for genetic transfer, and various antibiotic selection markers[146]. This knowledge allows researchers to choose which plasmid characteristics they need. Understanding of vector design is crucial when designing more complex systems, such as those using CRISPR.

Many strategies for increasing EET involve gene deletions. Sucrose counter selection is a commonly used technique but can take weeks to result in a single knockout due to time needed for plasmid construction, conjugation, and screening[147]. Depending on the gene target, thousands of colonies may need to be screened to generate the desired mutant. CRISPR-based systems have been engineered to simplify screening, vector construction, and range of potential modifications. Corts et al. developed a clever design in which a Cas9 enzyme targets un-modified genomes, therefore killing any WT revertants and ensuring that only the desired mutant can survive[148]. An alternative to gene deletion can be single base conversions to generate premature stop codons, thereby preventing translation[149,150]. In 2022, Chen et al.

published two research papers that expanded the coverage of the editable genome (from 89% to 100%) by increasing recognized protospacer adjacent motif (PAM) sites[151,152]. This expansion is important because Cas9 enzymes require PAM sites (e.g. 5'-NGG-3') to associate with the genome, and this development allows binding in AT-rich regions that were previously unsuitable. They also engineered a vector to enable simultaneous activation (CRISPRa) and inactivation (CRISPRi) of two different genes. The use of CRISPRi, where a sgRNA binds to a gene target and associates with an inactive Cas9 to block transcription, is also desirable as it can allow for inducible repression of genes as opposed to outright deletion. Such systems have been successfully developed in both *S. oneidensis* and *E. coli*[153,154]. Ford et al. adapted the *E. coli*-based CRISPRi system in conjunction with *in silico* metabolic modeling to generate a difficult knockout in a gene previously considered essential[155]. This result demonstrates the flexibility with which these different genetic tools can be operated. Many of these tools are developed in the context of increasing EET between *S. oneidensis* cells and the electrode. It is important to remember that the greater goal behind this is to improve MES systems to produce biofuels, bioplastics, and more.

1.6 MES for Bioproduction

Development of effective, scalable MES platforms requires an intimate understanding of the biological processes involved. There are a variety of tactics researchers have used to approach this goal, including using mixed-cultures, engineering electron uptake in organisms that naturally generate valuable products, and engineering production pathways in electroactive organisms[156,157]. While each approach

has merit, we believe that the approach of engineering bioproduction in electroactive bacteria, and specifically *S. oneidensis*, is the best path forward[158].

A key challenge when using microbial communities for MES is the lack of specificity in product generation. Mixed-cultures typically rely on methanogens and acetogens as the bio-producers. This requirement presents a problem because though these designs use CO_2 as the initial feedstock, poor electron uptake and subsequent energy loss as methane make them ineffective. Any attempts to improve these systems requires engineering of not only multiple, potentially uncharacterized, organisms, but of the interactions between organisms in the community. This requires additional time and effort to troubleshoot complex community systems. For these reasons, we find the flexible and rapid ability to adapt pure cultures to be a better alternative.

Engineering EET pathways in pure cultures of organisms already capable of producing a specific product can face equally complex problems. Namely, understanding the intricacies of EET in their native host is already challenging. Deciding which pathway to use, how it will be regulated, and its impact on native processes are just some of the considerations needed. For example, researchers have implemented the MtrCAB pathway in the model organism *E. coli*, which has the benefits of being well characterized and genetically tractable[89,159,160]. Though this strain could achieve extracellular EET, it was slow, reducing extracellular iron at 2% the rate of *S. oneidensis*[89]. While other organisms have been modified to interact with electrodes, none are as efficient as native systems, and the only chemical produced in many instances is acetic acid. As highlighted in Prèvoteau et al., to make these designs economically feasible there cannot be ‘wasted electrons’ in the form of off-target

products or poor EET rates[2]. While it is tempting to use model organisms like *E. coli*, the growing field for bioengineering in *S. oneidensis*, as detailed above, demonstrates a diminishing disparity in terms of genetic manipulation. To this end, there has been an increase in publications illustrating *S. oneidensis*'s use for bioproduction and even bioremediation[161]. Flynn et al. showed electrode-dependent conversion of glycerol to ethanol at 82% efficiency[162,163]. Other work has shown production of *n*-butanol and methane, two other useful fuels[164,165]. More complex engineering has capitalized on the intricate redox network within *S. oneidensis* to overproduce the heme precursor and cancer drug 5-aminolevulinic acid (ALA) and recycle electron shuttles for redox-based polymerization[166,167]. This wide range of research exemplifies the diversity of potential products possible when developing bioproduction, rather than optimizing non-electroactive organisms to produce acetic acid. To this end, the work discussed in this dissertation addresses many of the questions broached above. My efforts include investigating the physiological properties of *S. oneidensis* during electron uptake (Chapter 2), the flexibility of the inward electron pathway (Chapter 3), a pipeline for characterizing and deleting conditionally essential genes (Chapter 4), and a look at work towards implementing a functional Calvin-Benson Cycle in *S. oneidensis* (Chapter 5).

1.7 Research Overview

Previously published work by the TerAvest lab has demonstrated the ability for *S. oneidensis* to take up electrons from a cathode to drive 2,3-butanediol production from the precursor acetoin. Chapter 2 of this dissertation builds on this research by characterizing native processes. This investigation is essential because as noted above, understanding the roles and interactions of the EET network within an organism will be

instrumental in future work aimed at increasing product output. Specifically, I have demonstrated that proton motive force (PMF) is imperative for NADH generation; production increases with high levels of PMF and ceases when the proton gradient is collapsed [5,81]. In this work, I expand on this result by ensuring that all 2,3-butanediol produced is electrode-dependent, and showing that the native oxidases can sustain PMF. This work demonstrates a feasible application for bidirectional EET, coupling unfavorable NADH production to the energetically downhill reduction of oxygen. Additionally, it details potential hurdles related to the presence of oxygen in a BES and how to overcome them.

Similarly, Chapter 3 investigates the contribution of known EET pathway components in the context of MES. Often, conclusions on the contribution of different proteins, shuttles, or structures are drawn solely from electrochemical data. This can be misleading due to the abiotic interactions these redox molecules can have with electrodes. For this reason, I investigated how the loss of certain essential EET proteins impacts 2,3-butanediol generation. Using this model, I can more accurately assess how much of the current is biotic and going towards creating reducing power such as NADH during electron uptake from a cathode. From the components I examined, I determined that MtrCAB is essential for electron uptake. Interestingly, I found CymA and endogenous flavins to be important, while loss of FccA and exogenous flavins had no impact. I also demonstrated the value of the native hydrogenases, not in the context of hydrogen mediated EET, but for increased cell viability on the electrode. Together, this work both supports many established claims but also demonstrates the impracticality of using current data alone to interpret biological processes.

Chapter 4 discusses a pipeline that combines *in silico* metabolic modeling with CRISPRi based gene knockdown to quickly generate difficult knockouts[155]. Using OptKnock with a previously designed model for *S. oneidensis* central metabolism, I identified a genetic strategy for evolving a carbon dioxide fixing module within *S. oneidensis*[168–173]. This strategy relied on the deletion of the gene *gpmA* to sever the flow of carbon between gluconeogenesis and the TCA cycle. However, this gene has been characterized as expected essential and numerous attempts to generate a knockout were unsuccessful. Generating this mutant failed because there was not sufficient substrate to power these two modules (gluconeogenesis and TCA) separately. To address this, I used a CRISPRi knockdown system to characterize the potential phenotype of a Δ*gpmA* strain growing on different carbon substrates. I found that supplementing the medium with inosine and lactate restored a *gpmA* knockdown growth defect to WT levels. The gene deletion protocol was amended with the additional substrates, allowing for the isolation of a mutant. The rate of mutate formation during this was approximately half of all colonies screened (46%) further showing that this method worked and it was not merely chance that the mutant was made. The research in this chapter focuses on the development of this pipeline, while Chapter 5 will briefly cover the current stage of using this strain to evolve a carbon fixing pathway.

Overall, this work will address the current challenges in using *S. oneidensis* for practical development of MES and how I are working to overcome them. I have demonstrated bidirectional EET to power unfavorable reactions, characterized the EET pathway during MES, and developed genetic engineering strategies to continuously push this field forward.

REFERENCES

(1) Müller, V. (2009) Bacterial Fermentation. *Encyclopedia of Life Sciences* 1–7.

(2) Prévoteau, A., Carvajal-Arroyo, J. M., Ganigué, R., and Rabaey, K. (2020, April 1) Microbial electrosynthesis from CO_2: forever a promise? *Curr Opin Biotechnol*. Elsevier Ltd.

(3) Nevin, K. P., Woodard, T. L., Franks, A. E., Summers, Z. M., and Lovley, D. R. (2010) Microbial Electrosynthesis: Feeding Microbes Electricity To Convert Carbon Dioxide and Water to Multicarbon Extracellular Organic Compounds. *mBio 1*, 1–4.

(4) Rabaey, K., and Rozendal, R. A. (2010) Microbial electrosynthesis - Revisiting the electrical route for microbial production. *Nat Rev Microbiol 8*, 706–716.

(5) Tefft, N. M., and TerAvest, M. A. (2019) Reversing an Extracellular Electron Transfer Pathway for Electrode-Driven Acetoin Reduction. *ACS Synth Biol 8*, 1590–1600.

(6) Potter, M. C. (1911) Electrical effects accompanying the decomposition of organic compounds. *Proceedings of the Royal Society of London. Series B, Containing Papers of a Biological Character 84*, 260–276.

(7) Allen, R. M., and Bennetto, H. P. (1993) Microbial fuel-cells - Electricity production from carbohydrates. *Appl Biochem Biotechnol 39–40*, 27–40.

(8) Bennetto, H. P., Stirling, J. L., Tanaka, K., and Vega, C. A. (1983) Anodic reactions in microbial fuel cells. *Biotechnol Bioeng 25*, 559–568.

(9) Thapa, B. Sen, Kim, T., Pandit, S., Song, Y. E., Afsharian, Y. P., Rahimnejad, M., Kim, J. R., and Oh, S. E. (2022) Overview of electroactive microorganisms and electron transfer mechanisms in microbial electrochemistry. *Bioresour Technol 347*, 126579.

(10) Venkata Mohan, S., Mohanakrishna, G., Reddy, B. P., Saravanan, R., and Sarma, P. N. (2008) Bioelectricity generation from chemical wastewater treatment in mediatorless (anode) microbial fuel cell (MFC) using selectively enriched hydrogen producing mixed culture under acidophilic microenvironment. *Biochem Eng J 39*, 121–130.

(11) Venkata Mohan, S., Mohanakrishna, G., Srikanth, S., and Sarma, P. N. (2008) Harnessing of bioelectricity in microbial fuel cell (MFC) employing aerated cathode through anaerobic treatment of chemical wastewater using selectively enriched hydrogen producing mixed consortia. *Fuel 87*, 2667–2676.

(12) Logan, B. E., and Regan, J. M. (2006) Microbial Fuel Cells - Challenges and Applications. *Environ Sci Technol* 5172–5180.

(13) Logan, B. E., Hamelers, B., Rozendal, R., Schröder, U., Keller, J., Freguia, S., Aelterman, P., Verstraete, W., and Rabaey, K. (2006, September 1) Microbial Fuel Cells: Methodology and Technology. *Environ Sci Technol*.

(14) Jourdin, L., and Burdyny, T. (2021) Microbial Electrosynthesis: Where Do We Go from Here? *Trends Biotechnol 39*, 359–369.

(15) Ieropoulos, I. A., Greenman, J., Melhuish, C., and Hart, J. (2005) Comparative study of three types of microbial fuel cell. *Enzyme Microb Technol 37*, 238–245.

(16) Sydow, A., Krieg, T., Mayer, F., Schrader, J., and Holtmann, D. (2014, October 1) Electroactive bacteria—molecular mechanisms and genetic tools. *Appl Microbiol Biotechnol*. Springer Verlag.

(17) Steinbusch, K. J. J., Hamelers, H. V. M., Schaap, J. D., Kampman, C., and Buisman, C. J. N. (2010) Bioelectrochemical ethanol production through mediated acetate reduction by mixed cultures. *Environ Sci Technol 44*, 513–517.

(18) Shi, M. M., Jiang, Y. G., and Shi, L. (2019, October 1) Electromicrobiology and biotechnological applications of the exoelectrogens Geobacter and Shewanella spp. *Sci China Technol Sci*. Springer Verlag.

(19) Shin, H. J., Jung, K. A., Nam, C. W., and Park, J. M. (2017, December 1) A genetic approach for microbial electrosynthesis system as biocommodities production platform. *Bioresour Technol*. Elsevier Ltd.

(20) Hasany, M., Mardanpour, M. M., and Yaghmaei, S. (2016) Biocatalysts in microbial electrolysis cells: A review. *Int J Hydrogen Energy 41*, 1477–1493.

(21) Lovley, D. R. (2006, June) Microbial fuel cells: novel microbial physiologies and engineering approaches. *Curr Opin Biotechnol*.

(22) Myers, C. R., and Nealson, K. H. (1988) Bacterial manganese reduction and growth with manganese oxide as the sole electron acceptor. *Science Science 240*, 1319–1321.

(23) Lovley, D. R., Phillips, E. J. P., Gorby, Y. A., and Landa, E. R. (1991) Microbial reduction of uranium. *Nature*.

(24) Nealson, K. H., and Saffarini, D. (1994) Iron and manganese in anaerobic respiration: Environmental significance, physiology, and regulation. *Annu Rev Microbiol 48*, 311–343.

(25) Lovley, D. R., Stolz, J. F., Nord Jr, G. L., and Phillips, E. J. P. (1987) Anaerobic production of magnetite by a dissimilatory iron-reducing microorganism. *Nature 330*, 252–254.

(26) Lovley, D. R., and Phillips, E. J. P. (1988) Novel mode of microbial energy metabolism: organic carbon oxidation coupled to dissimilatory reduction of iron or manganese. *Appl Environ Microbiol 54*, 1472–1480.

(27) Kim, B. H., Kim, H. J., Hyun, M. S., and Park, D. H. (1999) Direct electrode reaction of Fe(III)-reducing bacterium, Shewanella putrefaciens. *J Microbiol Biotechnol*.

(28) Bond, D. R., Holmes, D. E., Tender, L. M., and Lovley, D. R. (2002) Electrode-reducing microorganisms that harvest energy from marine sediments. *Science (1979) 295*, 483–485.

(29) Lovley, D. R., and Phillips, E. J. P. (1992) Reduction of Uranium by Desulfovibrio desulfuricans. *Appl Environ Microbiol 58*, 850–856.

(30) Kim, B. H., Ikeda, T., Park, H. S., Kim, H. J., Hyun, M. S., Kano, K., Takagi, K., and Tatsumi, H. (1999) Electrochemical activity of an Fe(III)-reducing bacterium, Shewanella putrefaciens IR-1, in the presence of alternative electron acceptors. *Biotechnology Techniques 13*, 475–478.

(31) Karthikeyan, R., Singh, R., and Bose, A. (2019) Microbial electron uptake in microbial electrosynthesis: a mini-review. *J Ind Microbiol Biotechnol 46*, 1419–1426.

(32) Mateos, R., Sortes, A., Alonso, R. M., Moran, A., and Escapa, A. (2019) Enhanced CO 2 Conversion to Acetate through Microbial Electrosynthesis (MES) by Continuous Headspace Gas Recirculation. *Energies (Basel) 12*.

(33) Newsome, L., Morris, K., and Lloyd, J. R. (2014) The biogeochemistry and bioremediation of uranium and other priority radionuclides. *Chem Geol 363*, 164–184.

(34) Rowe, A. R., Salimijazi, F., Trutschel, L., Sackett, J., Adesina, O., Anzai, I., Kugelmass, L. H., Baym, M. H., and Barstow, B. (2021) Identification of a pathway for electron uptake in *Shewanella oneidensis*. *Commun Biol 4*, 1–10.

(35) Rowe, A. R., Rajeev, P., Jain, A., Pirbadian, S., Okamoto, A., Gralnick, J. A., El-Naggar, M. Y., and Nealson, K. H. (2018) Tracking electron uptake from a cathode into Shewanella cells: Implications for energy acquisition from solid-substrate electron donors. *mBio 9*, 1–19.

(36) Madsen, C. S., and TerAvest, M. A. (2019) NADH dehydrogenases Nuo and Nqr1 contribute to extracellular electron transfer by Shewanella oneidensis MR-1 in bioelectrochemical systems. *Sci Rep 9*.

(37) Feng, J., Jiang, M., Li, K., Lu, Q., Xu, S., Wang, X., Chen, K., and Ouyang, P. (2020) Direct electron uptake from a cathode using the inward Mtr pathway in *Escherichia coli*. *Bioelectrochemistry 134*, 1–8.

(38) Yang, Y., Ding, Y., Hu, Y., Cao, B., Rice, S. A., Kjelleberg, S., and Song, H. (2015) Enhancing Bidirectional Electron Transfer of *Shewanella oneidensis* by a Synthetic Flavin Pathway. *ACS Synth Biol 4*, 815–823.

(39) Yi, Y., Zhao, T., Zang, Y., Xie, B., and Liu, H. (2021) Different mechanisms for riboflavin to improve the outward and inward extracellular electron transfer of *Shewanella loihica*. *Electrochem commun 124*, 1–7.

(40) Gu, T., Wang, D., Lekbach, Y., and Xu, D. (2021) Extracellular electron transfer in microbial biocorrosion. *Curr Opin Electrochem 29*, 1–7.

(41) Shi, L., Dong, H., Reguera, G., Beyenal, H., Lu, A., Liu, J., Yu, H. Q., and Fredrickson, J. K. (2016) Extracellular electron transfer mechanisms between microorganisms and minerals. *Nat Rev Microbiol 14*, 651–662.

(42) Edel, M., Sturm, G., Sturm-Richter, K., Wagner, M., Ducassou, J. N., Couté, Y., Horn, H., and Gescher, J. (2021) Extracellular riboflavin induces anaerobic biofilm formation in *Shewanella oneidensis*. *Biotechnol Biofuels 14*, 1–14.

(43) Zhou, G., Yuan, J., and Gao, H. (2015) Regulation of biofilm formation by BpfA, BpfD, and BpfG in *Shewanella oneidensis*. *Front Microbiol 6*, 1–11.

(44) Reguera, G., Nevin, K. P., Nicoll, J. S., Covalla, S. F., Woodard, T. L., and Lovley, D. R. (2006) Biofilm and nanowire production leads to increased current in Geobacter sulfurreducens fuel cells. *Appl Environ Microbiol 72*, 7345–7348.

(45) Saunders, S. H., Tse, E. C. M., Yates, M. D., Otero, F. J., Trammell, S. A., Stemp, E. D. A., Barton, J. K., Tender, L. M., and Newman, D. K. (2020) Extracellular DNA Promotes Efficient Extracellular Electron Transfer by Pyocyanin in *Pseudomonas aeruginosa* Biofilms. *Cell 182*, 919–932.

(46) Coursolle, D., and Gralnick, J. A. (2010) Modularity of the Mtr respiratory pathway of *Shewanella oneidensis* strain MR-1. *Mol Microbiol 77*, 995–1008.

(47) Edwards, M. J., White, G. F., Butt, J. N., Richardson, D. J., and Clarke, T. A. (2020) The Crystal Structure of a Biological Insulated Transmembrane Molecular Wire. *Cell 181*, 665–673.

(48) Coursolle, D., and Gralnick, J. A. (2012) Reconstruction of Extracellular Respiratory Pathways for Iron(III) Reduction in *Shewanella oneidensis* Strain MR-1. *Front Microbiol 3*, 56.

(49) Xiao, X., Li, C. X., Peng, J. R., Fan, Y. Y., and Li, W. W. (2023) Dynamic roles of inner membrane electron-transfer hub of *Shewanella oneidensis* MR-1 in response to extracellular reduction kinetics. *Chemical Engineering Journal 451*.

(50) Marsili, E., Baron, D. B., Shikhare, I. D., Coursolle, D., Gralnick, J. A., and Bond, D. R. (2008) *Shewanella* secretes flavins that mediate extracellular electron transfer. *Proc Natl Acad Sci U S A 105*, 3968–3973.

(51) Kotloski, N. J., and Gralnick, J. A. (2013) Flavin electron shuttles dominate extracellular electron transfer by Shewanella oneidensis. *mBio 4*, 553–565.

(52) Brutinel, E. D., and Gralnick, J. A. (2012) Shuttling happens: Soluble flavin mediators of extracellular electron transfer in Shewanella. *Appl Microbiol Biotechnol 93*, 41–48.

(53) Xu, S., Jangir, Y., and El-Naggar, M. Y. (2016) Disentangling the roles of free and cytochrome-bound flavins in extracellular electron transport from *Shewanella oneidensis* MR-1. *Electrochim Acta 198*, 49–55.

(54) Okamoto, A., Hashimoto, K., and Nealson, K. H. (2014) Flavin Redox Bifurcation as a Mechanism for Controlling the Direction of Electron Flow during Extracellular Electron Transfer. *Angewandte Chemie International Edition 53*, 10988–10991.

(55) Okamoto, A., Hashimoto, K., Nealson, K. H., and Nakamura, R. (2013) Rate enhancement of bacterial extracellular electron transport involves bound flavin semiquinones. *Proc Natl Acad Sci U S A 110*, 7856–7861.

(56) Zhang, Y. T., Zhang, Y., and Peng, L. (2021) Electrochemical fluorescence microscopy reveals insignificant long-range extracellular electron transfer in *Shewanella oneidensis* anodic processes. *Electrochim Acta 398*, 1–7.

(57) Subramanian, P., Pirbadian, S., El-Naggar, M. Y., and Jensen, G. J. (2018) Ultrastructure of *Shewanella oneidensis* MR-1 nanowires revealed by electron cryotomography. *Proc Natl Acad Sci U S A 115*, E3246–E3255.

(58) Pirbadian, S., Chavez, M. S., and El-Naggar, M. Y. (2020) Spatiotemporal mapping of bacterial membrane potential responses to extracellular electron transfer. *Proc Natl Acad Sci U S A 117*, 20171–20179.

(59) Meyer, T. E., Tsapin, A. I., Vandenberghe, I., De Smet, L., Frishman, D., Nealson, K. H., Cusanovich, M. A., and Van Beeumen, J. J. (2004) Identification of 42 Possible Cytochrome C Genes in the *Shewanella oneidensis* Genome and Characterization of Six Soluble Cytochromes. *OMICS 8*, 57–77.

(60) Carmona-Martinez, A. A., Harnisch, F., Fitzgerald, L. A., Biffinger, J. C., Ringeisen, B. R., and Schröder, U. (2011) Cyclic voltammetric analysis of the electron transfer of *Shewanella oneidensis* MR-1 and nanofilament and cytochrome knock-out mutants. *Bioelectrochemistry 81*, 74–80.

(61) Marritt, S. J., Lowe, T. G., Bye, J., Mcmillan, D. G. G., Shi, L., Fredrickson, J., Zachara, J., Richardson, D. J., Cheesman, M. R., Jeuken, L. J. C., and Butt, J. N.

(2012) A functional description of CymA, an electron-transfer hub supporting anaerobic respiratory flexibility in *Shewanella*. *Biochemical Journal 444*, 465–474.

(62) McMillan, D. G. G., Marritt, S. J., Butt, J. N., and Jeuken, L. J. C. (2012) Menaquinone-7 Is Specific Cofactor in Tetraheme Quinol Dehydrogenase CymA. *J Biol Chem 287*, 14215–14225.

(63) Schwalb, C., Chapman, S. K., and Reid, G. A. (2003) The tetraheme cytochrome CymA is required for anaerobic respiration with dimethyl sulfoxide and nitrite in *Shewanella oneidensis*. *Biochemistry 42*, 9491–9497.

(64) Myers, C. R., and Myers, J. M. (1997) Cloning and Sequence of *cymA*, a Gene Encoding a Tetraheme Cytochrome *c* Required for Reduction of Iron(III), Fumarate, and Nitrate by *Shewanella putrefaciens* MR-1. *J Bacteriol 179*, 1143–1152.

(65) Myers, J. M., and Myers, C. R. (2000) Role of the tetraheme cytochrome CymA in anaerobic electron transport in cells of *Shewanella putrefaciens* MR-1 with normal levels of menaquinone. *J Bacteriol 182*, 67–75.

(66) Sun, W., Lin, Z., Yu, Q., Cheng, S., and Gao, H. (2021) Promoting Extracellular Electron Transfer of *Shewanella oneidensis* MR-1 by Optimizing the Periplasmic Cytochrome *c* Network. *Front Microbiol 12*, 1–13.

(67) Chen, Y., and Wang, F. (2015) Insights on nitrate respiration by *Shewanella*. *Front Mar Sci 1*, 1–9.

(68) Fonseca, B. M., Paquete, C. M., Neto, S. E., Pacheco, I., Soares, C. M., and Louro, R. O. (2013) Mind the gap: Cytochrome interactions reveal electron pathways across the periplasm of *Shewanella oneidensis* MR-1. *Biochemical Journal 449*, 101–108.

(69) Hartshorne, R. S., Jepson, B. N., Clarke, T. A., Field, S. J., Fredrickson, J., Zachara, J., Shi, L., Butt, J. N., and Richardson, D. J. (2007) Characterization of *Shewanella oneidensis* MtrC: A cell-surface decaheme cytochrome involved in respiratory electron transport to extracellular electron acceptors. *Journal of Biological Inorganic Chemistry 12*, 1083–1094.

(70) Ross, D. E., Brantley, S. L., and Tien, M. (2009) Kinetic characterization of OmcA and MtrC, terminal reductases involved in respiratory electron transfer for dissimilatory iron reduction in *Shewanella oneidensis* MR-1. *Appl Environ Microbiol 75*, 5218–5226.

(71) Firer-Sherwood, M., Pulcu, G. S., and Elliott, S. J. (2008) Electrochemical interrogations of the Mtr cytochromes from *Shewanella*: Opening a potential window. *Journal of Biological Inorganic Chemistry 13*, 849–854.

(72) Coursolle, D., Baron, D. B., Bond, D. R., and Gralnick, J. A. (2010) The Mtr respiratory pathway is essential for reducing flavins and electrodes in *Shewanella oneidensis*. *J Bacteriol 192*, 467–474.

(73) White, G. F., Shi, Z., Shi, L., Wang, Z., Dohnalkova, A. C., Marshall, M. J., Fredrickson, J. K., Zachara, J. M., Butt, J. N., Richardson, D. J., and Clarke, T. A. (2013) Rapid electron exchange between surface-exposed bacterial cytochromes and Fe(III) minerals. *Proc Natl Acad Sci U S A 110*, 6346–6351.

(74) Edwards, M. J., White, G. F., Butt, J. N., Richardson, D. J., and Clarke, T. A. (2020) The Crystal Structure of a Biological Insulated Transmembrane Molecular Wire. *Cell 181*, 665-673.e10.

(75) Edwards, M. J., White, G. F., Norman, M., Tome-Fernandez, A., Ainsworth, E., Shi, L., Fredrickson, J. K., Zachara, J. M., Butt, J. N., Richardson, D. J., and Clarke, T. A. (2015) Redox Linked Flavin Sites in Extracellular Decaheme Proteins Involved in Microbe-Mineral Electron Transfer. *Sci Rep 5*, 1–11.

(76) Babanova, S., Matanovic, I., Cornejo, J., Bretschger, O., Nealson, K., and Atanassov, P. (2017) Outer membrane cytochromes/flavin interactions in *Shewanella* spp.—A molecular perspective. *Biointerphases 12*, 1–10.

(77) Alves, M. N., Neto, S. E., Alves, A. S., Fonseca, B. M., Carrêlo, A., Pacheco, I., Paquete, C. M., Soares, C. M., and Louro, R. O. (2015) Characterization of the periplasmic redox network that sustains the versatile anaerobic metabolism of *Shewanella oneidensis* MR-1. *Front Microbiol 6*, 1–10.

(78) Ding, D., and Sun, X. (2018) Network-based methods for identifying key active proteins in the extracellular electron transfer process in *Shewanella oneidensis* MR-1. *Genes (Basel) 9*, 1–17.

(79) Sturm, G., Richter, K., Doetsch, A., Heide, H., Louro, R. O., and Gescher, J. (2015) A dynamic periplasmic electron transfer network enables respiratory flexibility beyond a thermodynamic regulatory regime. *ISME Journal 9*, 1802–1811.

(80) Delgado, V. P., Paquete, C. M., Sturm, G., and Gescher, J. (2019) Improvement of the electron transfer rate in Shewanella oneidensis MR-1 using a tailored periplasmic protein composition. *Bioelectrochemistry 129*, 18–25.

(81) Tefft, N. M., Ford, K., and TerAvest, M. A. (2022) NADH dehydrogenases drive inward electron transfer in *Shewanella oneidensis* MR-1. *Microb Biotechnol 00*, 1–9.

(82) Rowe, A. R., Rajeev, P., Jain, A., Pirbadian, S., Okamoto, A., Gralnick, J. A., El-Naggar, M. Y., and Nealson, K. H. (2018) Tracking electron uptake from a cathode into Shewanella cells: Implications for energy acquisition from solid-substrate electron donors. *mBio 9*.

(83) Lies, D. P., Hernandez, M. E., Kappler, A., Mielke, R. E., Gralnick, J. A., and Newman, D. K. (2005) *Shewanella oneidensis* MR-1 Uses Overlapping Pathways for Iron Reduction at a Distance and by Direct Contact under Conditions Relevant for Biofilms. *Appl Environ Microbiol 71*, 4414–4426.

(84) Von Canstein, H., Ogawa, J., Shimizu, S., and Lloyd, J. R. (2008) Secretion of flavins by *Shewanella* species and their role in extracellular electron transfer. *Appl Environ Microbiol 74*, 615–623.

(85) Covington, E. D., Gelbmann, C. B., Kotloski, N. J., and Gralnick, J. A. (2010) An essential role for UshA in processing of extracellular flavin electron shuttles by *Shewanella oneidensis*. *Mol Microbiol 78*, 519–532.

(86) Wu, C., Cheng, Y. Y., Li, B. B., Li, W. W., Li, D. B., and Yu, H. Q. (2013) Electron acceptor dependence of electron shuttle secretion and extracellular electron transfer by *Shewanella oneidensis* MR-1. *Bioresour Technol 136*, 711–714.

(87) Kees, E. D., Pendleton, A. R., Paquete, C. M., Arriola, M. B., Kane, A. L., Kotloski, N. J., Intile, P. J., and Gralnick, J. A. (2019) Secreted flavin cofactors for anaerobic respiration of fumarate and urocanate by Shewanella oneidensis: Cost and role. *Appl Environ Microbiol 85*.

(88) Grobbler, C., Virdis, B., Nouwens, A., Harnisch, F., Rabaey, K., and Bond, P. L. (2018) Effect of the anode potential on the physiology and proteome of *Shewanella oneidensis* MR-1. *Bioelectrochemistry 119*, 172–179.

(89) Jensen, H. M., TerAvest, M. A., Kokish, M. G., and Ajo-Franklin, C. M. (2016) CymA and Exogenous Flavins Improve Extracellular Electron Transfer and Couple It to Cell Growth in Mtr-Expressing *Escherichia coli*. *ACS Synth Biol 5*, 679–688.

(90) Shi, L., Rosso, K. M., Clarke, T. A., Richardson, D. J., Zachara, J. M., Fredrickson, J. K., Emerson, D., Gralnick, J. A., and Weiner, J. (2012) Molecular underpinnings of Fe(III) oxide reduction by *Shewanella oneidensis* MR-1. *Front Microbiol 3*, 1–10.

(91) Zhao, J., Li, F., Kong, S., Chen, T., Song, H., and Wang, Z. (2023) Elongated Riboflavin-Producing *Shewanella oneidensis* in a Hybrid Biofilm Boosts Extracellular Electron Transfer. *Advanced Science 10*, 1–11.

(92) Xiao, Y., Zhang, E., Zhang, J., Dai, Y., Yang, Z., Christensen, H. E. M., Ulstrup, J., and Zhao, F. (2017) Extracellular polymeric substances are transient media for microbial extracellular electron transfer. *Sci Adv 3*, 1–8.

(93) Norman, M. P., Edwards, M. J., White, G. F., Burton, J. A. J., Louro, R. O., Paquete, C. M., and Clarke, A. (2023) A Cysteine Pair Controls Flavin Reduction by Extracellular Cytochromes during Anoxic/Oxic Environmental Transitions. *mBio 14*, 1–12.

(94) Paquete, C. M., Fonseca, B. M., Cruz, D. R., Pereira, T. M., Pacheco, I., Soares, C. M., and Louro, R. O. (2014) Exploring the molecular mechanisms of electron shuttling across the microbe/metal space. *Front Microbiol 5*, 1–12.

(95) Liu, T., Luo, X., Wu, Y., Reinfelder, J. R., Yuan, X., Li, X., Chen, D., and Li, F. (2020) Extracellular electron shuttling mediated by soluble *c*-type cytochromes produced by *Shewanella oneidensis* MR-1. *Environ Sci Technol 54*, 10577–10587.

(96) Bao, H., Zheng, Z., Yang, B., Liu, D., Li, F., Zhang, X., Li, Z., and Lei, L. (2016) In situ monitoring of *Shewanella oneidensis* MR-1 biofilm growth on gold electrodes by using a Pt microelectrode. *Bioelectrochemistry 109*, 95–100.

(97) Arinda, T., Philipp, L. A., Rehnlund, D., Edel, M., Chodorski, J., Stöckl, M., Holtmann, D., Ulber, R., Gescher, J., and Sturm-Richter, K. (2019) Addition of riboflavin-coupled magnetic beads increases current production in bioelectrochemical systems via the increased formation of anode-biofilms. *Front Microbiol 10*, 1–8.

(98) Michelson, K., Alcalde, R. E., Sanford, R. A., Valocchi, A. J., and Werth, C. J. (2019) Diffusion-Based Recycling of Flavins Allows *Shewanella oneidensis* MR-1 to Yield Energy from Metal Reduction Across Physical Separations. *Environ Sci Technol 53*, 3480–3487.

(99) Ng, C. K., Xu, J., Cai, Z., Yang, L., Thompson, I. P., Huang, W. E., and Cao, B. (2020) Elevated intracellular cyclic-di-GMP level in *Shewanella oneidensis* increases expression of *c*-type cytochromes. *Microb Biotechnol 13*, 1904–1916.

(100) Thormann, K. M., Saville, R. M., Shukla, S., Pelletier, D. A., and Spormann, A. M. (2004) Initial phases of biofilm formation in *Shewanella oneidensis* MR-1. *J Bacteriol 186*, 8096–8104.

(101) Harris, H. W., El-Naggar, M. Y., and Nealson, K. H. (2012) *Shewanella oneidensis* MR-1 chemotaxis proteins and electron-transport chain components essential for congregation near insoluble electron acceptors, in *Biochemical Society Transactions*, pp 1167–1177.

(102) Yu, Y. Y., Chen, H. L., Yong, Y. C., Kim, D. H., and Song, H. (2011) Conductive artificial biofilm dramatically enhances bioelectricity production in *Shewanella*-inoculated microbial fuel cells. *Chemical Communications 47*, 12825–12827.

(103) Liang, Y., Gao, H., Chen, J., Dong, Y., Wu, L., He, Z., Liu, X., Qiu, G., and Zhou, J. (2010) Pellicle formation in *Shewanella oneidensis*. *BMC Microbiol 10*, 1–11.

(104) Thormann, K. M., Saville, R. M., Shukla, S., and Spormann, A. M. (2005) Induction of Rapid Detachment in *Shewanella oneidensis* MR-1 Biofilms. *J Bacteriol 187*, 1014–1021.

(105) Saville, R., Rakshe, S., Haagensen, J. A. J., Shukla, S., and Spormann, A. (2011) Energy-Dependent Stability of *Shewanella oneidensis* MR-1 Biofilms. *J Bacteriol 193*, 3257–3264.

(106) Saville, R. M., Dieckmann, N., and Spormann, A. M. (2010) Spatiotemporal activity of the *mshA* gene system in *Shewanella oneidensis* MR-1 biofilms. *FEMS Microbiol Lett 308*, 76–83.

(107) Theunissen, S., De Smet, L., Dansercoer, A., Motte, B., Coenye, T., Van Beeumen, J. J., Devreese, B., Savvides, S. N., and Vergauwen, B. (2009) The 285 kDa Bap/RTX hybrid cell surface protein (SO4317) of *Shewanella oneidensis* MR-1 is a key mediator of biofilm formation. *Res Microbiol 161*, 144–152.

(108) Kouzuma, A., Oba, H., Tajima, N., Hashimoto, K., and Watanabe, K. (2014) Electrochemical selection and characterization of a high current-generating *Shewanella oneidensis* mutant with altered cell-surface morphology and biofilm-related gene expression. *BMC Microbiol 14*, 1–11.

(109) Kouzuma, A., Meng, X. Y., Kimura, N., Hashimoto, K., and Watanabe, K. (2010) Disruption of the Putative Cell Surface Polysaccharide Biosynthesis Gene SO3177 in *Shewanella oneidensis* MR-1 Enhances Adhesion to Electrodes and Current Generation in Microbial Fuel Cells. *Appl Environ Microbiol 76*, 4151–4157.

(110) Matsumoto, A., Koga, R., Kanaly, R. A., Kouzuma, A., and Watanabe, K. (2021) Identification of a Diguanylate Cyclase That Facilitates Biofilm Formation on Electrodes by *Shewanella oneidensis* MR-1. *Appl Environ Microbiol 87*, 1–11.

(111) Nisbett, L. M., Binnenkade, L., Bacon, B., Hossain, S., Kotloski, N. J., Brutinel, E. D., Hartmann, R., Drescher, K., Arora, D. P., Muralidharan, S., Thormann, K. M., Gralnick, J. A., and Boon, E. M. (2019) NosP Signaling Modulates the NO/H-NOX-Mediated Multicomponent c-Di-GMP Metwork and Biofilm Formation in *Shewanella oneidensis*. *Biochemistry 58*, 4827–4841.

(112) Binnenkade, L., Kreienbaum, M., and Thormann, K. M. (2018) Characterization of ExeM, an extracellular nuclease of *Shewanella oneidensis* MR-1. *Front Microbiol 9*, 1–12.

(113) Kreienbaum, M., Dörrich, A. K., Brandt, D., Schmid, N. E., Leonhard, T., Hager, F., Brenzinger, S., Hahn, J., Glatter, T., Ruwe, M., Briegel, A., Kalinowski, J., and Thormann, K. M. (2020) Isolation and Characterization of *Shewanella* Phage Thanatos Infecting and Lysing *Shewanella oneidensis* and Promoting Nascent Biofilm Formation. *Front Microbiol 11*, 1–16.

(114) Gödeke, J., Heun, M., Bubendorfer, S., Paul, K., and Thormann, K. M. (2011) Roles of Two *Shewanella oneidensis* MR-1 Extracellular Endonucleases. *Appl Environ Microbiol 77*, 5342–5351.

(115) Choi, S., Kim, B., and Chang, I. S. (2018) Tracking of *Shewanella oneidensis* MR-1 biofilm formation of a microbial electrochemical system via differential pulse voltammetry. *Bioresour Technol 254*, 357–361.

(116) Silva, A. V, Edel, M., Gescher, J., and Paquete, C. M. (2020) Exploring the Effects of *bolA* in Biofilm Formation and Current Generation by *Shewanella oneidensis* MR-1. *Front Microbiol 11*, 1–7.

(117) Mukherjee, M., Zaiden, N., Teng, A., Hu, Y., and Cao, B. (2020, December 1) *Shewanella* biofilm development and engineering for environmental and bioenergy applications. *Curr Opin Chem Biol*. Elsevier Ltd.

(118) Kitayama, M., Koga, R., Kasai, T., Kouzuma, A., and Watanabe, K. (2017) Structures, Compositions, and Activities of Live *Shewanella* Biofilms Formed on Graphite Electrodes in Electrochemical Flow Cells. *Appl Environ Microbiol 83*, 1–11.

(119) Sanchez, D. V. P., Jacobs, D., Gregory, K., Huang, J., Hu, Y., Vidic, R., and Yun, M. (2015) Changes in carbon electrode morphology affect microbial fuel cell performance with *Shewanella oneidensis* MR-1. *Energies (Basel) 8*, 1817–1829.

(120) Yong, Y.-C., Yu, Y.-Y., Zhang, X., Song, H., Yong, Y. C., Yu, Y. Y., Song, H., and Zhang, X. (2014) Highly Active Bidirectional Electron Transfer by a Self-Assembled Electroactive Reduced-Graphene-Oxide-Hybridized Biofilm. *Angewandte Chemie International Edition 53*, 4480–4483.

(121) Zajdel, T. J., Baruch, M., Méhes, G., Stavrinidou, E., Berggren, M., Maharbiz, M. M., Simon, D. T., and Ajo-Franklin, C. M. (2018) PEDOT:PSS-based Multilayer Bacterial-Composite Films for Bioelectronics OPEN. *Nature Scientific Reports 8*, 1–12.

(122) Hsieh, M.-L., Hinton, D. M., and Waters, C. M. (2018) VpsR and cyclic di-GMP together drive transcription initiation to activate biofilm formation in Vibrio cholerae. *Nucleic Acids Res*.

(123) Hengge, R. (2009) Principles of c-di-GMP signalling in bacteria. *Nature Reviews 7*, 263–273.

(124) Srivastava, D., and Waters, C. M. (2012, September) A tangled web: Regulatory connections between quorum sensing and cyclic Di-GMP. *J Bacteriol*.

(125) Gorgel, M., Ulstrup, J. J., Bøggild, A., Jones, N. C., Hoffmann, S. V., Nissen, P., and Boesen, T. (2015) High-resolution structure of a type IV pilin from the metal-reducing bacterium *Shewanella oneidensis*. *BMC Struct Biol 15*, 1–17.

(126) Reguera, G., McCarthy, K. D., Mehta, T., Nicoll, J. S., Tuominen, M. T., and Lovley, D. R. (2005) Extracellular electron transfer via microbial nanowires. *Nature 435*, 1098–1101.

(127) Saffarini, D., Brockman, K., Beliaev, A. S., Bouhenni, R., and Shirodkar, S. (2015) *Shewanella oneidensis* and Extracellular Electron Transfer to Metal Oxides. *Bacteria-Metal Interactions*.

(128) Gorby, Y. A., Yanina, S., McLean, J. S., Rosso, K. M., Moyles, D., Dohnalkova, A., Beveridge, T. J., Chang, I. S., Kim, B. H., Kim, K. S., Culley, D. E., Reed, S. B., Romine, M. F., Saffarini, D. A., Hill, E. A., Shi, L., Elias, D. A., Kennedy, D. W., Pinchuk, G., Watanabe, K., Ishii, S., Logan, B., Nealson, K. H., and Fredrickson, J. K. (2006) Electrically conductive bacterial nanowires produced by *Shewanella oneidensis* strain MR-1 and other microorganisms. *Proc Natl Acad Sci U S A 103*, 11358–11363.

(129) Creasey, R. C. G., Mostert, A. B., Nguyen, T. A. H., Virdis, B., Freguia, S., and Laycock, B. (2018) Microbial nanowires – Electron transport and the role of synthetic analogues. *Acta Biomater 69*, 1–30.

(130) Lovley, D. R., and Malvankar, N. S. (2015) Seeing is believing: Novel imaging techniques help clarify microbial nanowire structure and function. *Environ Microbiol 17*, 2209–2215.

(131) Pirbadian, S., Barchinger, S. E., Leung, K. M., Byun, H. S., Jangir, Y., Bouhenni, R. A., Reed, S. B., Romine, M. F., Saffarini, D. A., Shi, L., Gorby, Y. A., Golbeck, J. H., and El-Naggar, M. Y. (2014) *Shewanella oneidensis* MR-1 nanowires are outer membrane and periplasmic extensions of the extracellular electron transport components. *Proc Natl Acad Sci U S A 111*, 12883–12888.

(132) Chong, G. W., Pirbadian, S., and El-Naggar, M. Y. (2019) Surface-induced formation and redox-dependent staining of outer membrane extensions in *Shewanella oneidensis* MR-1. *Front Energy Res 7*, 1–9.

(133) Barchinger, S. E., Pirbadian, S., Sambles, C., Baker, C. S., Leung, K. M., Burroughs, N. J., El-Naggar, M. Y., and Golbeck, J. H. (2016) Regulation of gene expression in *Shewanella oneidensis* MR-1 during electron acceptor limitation and bacterial nanowire formation. *Appl Environ Microbiol 82*, 5428–5443.

(134) El-Naggar, M. Y., Wanger, G., Leung, K. M., Yuzvinsky, T. D., Southam, G., Yang, J., Lau, W. M., Nealson, K. H., and Gorby, Y. A. (2010) Electrical transport along bacterial nanowires from *Shewanella oneidensis* MR-1. *Proc Natl Acad Sci U S A 107*, 18127–18131.

(135) Fredrickson, J. K., Romine, M. F., Beliaev, A. S., Auchtung, J. M., Driscoll, M. E., Gardner, T. S., Nealson, K. H., Osterman, A. L., Pinchuk, G., Reed, J. L., Rodionov, D. A., Rodrigues, J. L. M., Saffarini, D. A., Serres, M. H., Spormann, A. M., Zhulin, I. B., and Tiedje, J. M. (2008) Towards environmental systems biology of Shewanella. *Nat Rev Microbiol 6*, 592–603.

(136) Yu, H., Lu, Y., Lan, F., Wang, Y., Hu, C., Mao, L., Wu, D., Li, F., and Song, H. (2023) Engineering Outer Membrane Vesicles to Increase Extracellular Electron Transfer of *Shewanella oneidensis*. *ACS Synth Biol 12*, 1645–1656.

(137) Kouzuma, A., Hashimoto, K., and Watanabe, K. (2014) Influences of Aerobic Respiration on Current Generation by *Shewanella oneidensis* MR-1 in Single-Chamber Microbial Fuel Cells. *Bioscience, Biotechnology, and Biochemistry ISSN: 76*, 270–275.

(138) Delgado, V. P., Paquete, C. M., Sturm, G., and Gescher, J. (2019) Improvement of the electron transfer rate in *Shewanella oneidensis* MR-1 using a tailored periplasmic protein composition. *Bioelectrochemistry 129*, 18–25.

(139) Li, F., Li, Y. X., Cao, Y. X., Wang, L., Liu, C. G., Shi, L., and Song, H. (2018) Modular engineering to increase intracellular NAD(H/$^{+}$) promotes rate of extracellular electron transfer of *Shewanella oneidensis*. *Nat Commun 9*, 1–13.

(140) Ding, Q., Liu, Q., Zhang, Y., Li, F., and Song, H. (2023) Modular Engineering Strategy to Redirect Electron Flux into the Electron-Transfer Chain for Enhancing Extracellular Electron Transfer in *Shewanella oneidensis*. *ACS Synth Biol 12*, 471–481.

(141) Li, F., Tang, R., Zhang, B., Qiao, C., Yu, H., Liu, Q., Zhang, J., Shi, L., and Song, H. (2023) Systematic Full-Cycle Engineering Microbial Biofilms to Boost Electricity Production in *Shewanella oneidensis*. *Research 6*, 1–18.

(142) Heidelberg, J. F., Paulsen, I. T., Nelson, K. E., Gaidos, E. J., Nelson, W. C., Read, T. D., Eisen, J. A., Seshadri, R., Ward, N., Methe, B., Clayton, R. A., Meyer, T., Tsapin, A., Scott, J. H., Beanan, M., Brinkac, L., Daugherty, S., DeBoy, R. T., Dodson, R. J., Durkin, A. S., Haft, D. H., Kolonay, J. F., Madupu, R., Peterson, J. D., Umayam, L. A., White, O., Wolf, A. M., Vamathevan, J., Weidman, J., Impraim, M., Lee, K., Berry, K., Lee, C., Mueller, J., Khouri, H., Gill, J., Utterback, T. R., McDonald, L. A., Feldblyum, T. V., Smith, H. O., Venter, J. C., Nealson, K. H., and Fraser, C. M. (2002) Genome sequence of the dissimilatory metal ion-reducing bacterium *Shewanella oneidensis*. *Nat Biotechnol 20*, 1118–1123.

(143) West, E. A., Jain, A., and Gralnick, J. A. (2017) Engineering a Native Inducible Expression System in *Shewanella oneidensis* to Control Extracellular Electron Transfer. *ACS Synth Biol 6*, 1627–1634.

(144) Cheng, L., He, R.-L., Min, D., Li, W.-W., Liu, D.-F., and Yu, H.-Q. (2021) Engineering a Rhamnose-Inducible System to Enhance the Extracellular Electron Transfer Ability of *Shewanella* Genus for Improved Cr(VI) Reduction. *ACS Environmental Science & Technology 1*, 842–850.

(145) Yi, Y. C., and Ng, I. S. (2020) Establishment of toolkit and T7RNA polymerase/promoter system in *Shewanella oneidensis* MR-1. *J Taiwan Inst Chem Eng 109*, 8–14.

(146) Cao, Y., Song, M., Li, F., Li, C., Lin, X., Chen, Y., Chen, Y., Xu, J., Ding, Q., and Song, H. (2019) A Synthetic Plasmid Toolkit for *Shewanella oneidensis* MR-1. *Front Microbiol 10*, 1–12.

(147) Blomfield, I. C., Vaughn, V., Rest, R. F., and Eisenstein, B. I. (1991) Allelic exchange in *Escherichia coli* using the *Bacillus subtilis sacB* gene and a temperature-sensitive pSC101 replicon. *Mol Microbiol 5*, 1447–1457.

(148) Corts, A. D., Thomason, L. C., Gill, R. T., and Gralnick, J. A. (2019) Efficient and Precise Genome Editing in *Shewanella* with Recombineering and CRISPR/Cas9-Mediated Counter-Selection. *ACS Synth Biol 8*, 1877–1889.

(149) Cheng, L., Min, D., He, R. L., Cheng, Z. H., Liu, D. F., and Yu, H. Q. (2020) Developing a base-editing system to expand the carbon source utilization spectra of *Shewanella oneidensis* MR-1 for enhanced pollutant degradation. *Biotechnol Bioeng 117*, 2389–2400.

(150) Chen, Y., Cheng, M., Li, Y., Wang, L., Fang, L., Cao, Y., and Song, H. (2023) Highly efficient multiplex base editing: One-shot deactivation of eight genes in *Shewanella oneidensis* MR-1. *Synth Syst Biotechnol 8*, 1–10.

(151) Chen, Y., Cheng, M., Feng, X., Niu, X., Song, H., and Cao, Y. (2022) Genome Editing by CRISPR/Cas12 Recognizing AT-Rich PAMs in *Shewanella oneidensis* MR-1. *ACS Synth Biol 11*, 2947–2955.

(152) Chen, Y., Fang, L., Ying, X., Cheng, M., Wang, L., Sun, P., Zhang, Z., Shi, L., Cao, Y., and Song, H. (2022) Development of Whole Genome-Scale Base Editing Toolbox to Promote Efficiency of Extracellular Electron Transfer in *Shewanella oneidensis* MR-1. *Adv Biol 6*, 1–12.

(153) Li, J., Tang, Q., Li, Y., Fan, Y.-Y., Li, F.-H., Wu, J.-H., Min, D., Li, W.-W., Lam, P. K. S., and Yu, H.-Q. (2020) Rediverting Electron Flux with an Engineered CRISPR-ddAsCpf1 System to Enhance the Pollutant Degradation Capacity of *Shewanella oneidensis*. *Environ Sci Technol 54*, 3599–3608.

(154) Peters, J. M., Koo, B. M., Patino, R., Heussler, G. E., Hearne, C. C., Qu, J., Inclan, Y. F., Hawkins, J. S., Lu, C. H. S., Silvis, M. R., Harden, M. M., Osadnik, H., Peters, J. E., Engel, J. N., Dutton, R. J., Grossman, A. D., Gross, C. A., and Rosenberg, O. S. (2019) Enabling genetic analysis of diverse bacteria with Mobile-CRISPRi. *Nat Microbiol 4*, 244–250.

(155) Ford, K. C., Kaste, J. A. M., Shachar-Hill, Y., and TerAvest, M. A. (2022) Flux-Balance Analysis and Mobile CRISPRi-Guided Deletion of a Conditionally Essential Gene in *Shewanella oneidensis* MR-1. *ACS Synth Biol 11*, 3405–3413.

(156) Gong, Z., Yu, H., Zhang, J., Li, F., and Song, H. (2020, December 1) Microbial electro-fermentation for synthesis of chemicals and biofuels driven by bi-directional extracellular electron transfer. *Synth Syst Biotechnol*. KeAi Communications Co.

(157) Kracke, F., Lai, B., Yu, S., and Krömer, J. O. (2018, January 1) Balancing cellular redox metabolism in microbial electrosynthesis and electro fermentation – A chance for metabolic engineering. *Metab Eng*. Academic Press Inc.

(158) Ikeda, S., Takamatsu, Y., Tsuchiya, M., Suga, K., Tanaka, Y., Kouzuma, A., and Watanabe, K. (2021, July 1) *Shewanella oneidensis* MR-1 as a bacterial platform for electro-biotechnology. *Essays Biochem*. Portland Press Ltd.

(159) TerAvest, M. A., Zajdel, T. J., and Ajo-Franklin, C. M. (2014) The Mtr Pathway of *Shewanella oneidensis* MR-1 Couples Substrate Utilization to Current Production in *Escherichia coli*. *ChemElectroChem 1*, 1874–1879.

(160) Jensen, H. M., Albers, A. E., Malley, K. R., Londerd, Y. Y., Cohen, B. E., Helmsc, B. A., Weigele, P., Groves, J. T., and Ajo-Franklin, C. M. (2010) Engineering of a synthetic electron conduit in living cells. *Proc Natl Acad Sci U S A 107*, 19213–19218.

(161) Wang, J., Wu, M., Lu, G., and Si, Y. (2016) Biotransformation and biomethylation of arsenic by *Shewanella oneidensis* MR-1. *Chemosphere 145*, 329–335.

(162) Flynn, J. M., Ross, D. E., Hunt, K. A., Bond, D. R., and Gralnick, J. A. (2010) Enabling Unbalanced Fermentations by Using Engineered Electrode-Interfaced Bacteria. *mBio 1*, 1–8.

(163) Rosenbaum, M. A., and Henrich, A. W. (2014) Engineering microbial electrocatalysis for chemical and fuel production. *Curr Opin Biotechnol 29*, 93–98.

(164) Jeon, J.-M., Song, H.-S., Lee, D.-G., Won Hong, J., Gi Hong, Y., Moon, Y.-M., Kant Bhatia, S., Yoon, J.-J., Kim, W., and Yang, Y.-H. (2018) Butyrate-based *n*-butanol production from an engineered *Shewanella oneidensis* MR-1. *Bioprocess Biosyst Eng 41*, 1195–1204.

(165) Xiao, L., Liu, F., Lichtfouse, E., Zhang, P., Feng, D., and Li, F. (2020) Methane production by acetate dismutation stimulated by *Shewanella oneidensis* and carbon materials: An alternative to classical CO_2 reduction. *Chemical Engineering Journal 389*, 1–9.

(166) Yi, Y. C., and Ng, I. S. (2021) Redirection of metabolic flux in *Shewanella oneidensis* MR-1 by CRISPRi and modular design for 5-aminolevulinic acid production. *Bioresour Bioprocess 8*, 1–11.

(167) Fan, G., Dundas, C. M., Graham, A. J., Lynd, N. A., and Keitz, B. K. (2018) *Shewanella oneidensis* as a living electrode for controlled radical polymerization. *PNAS 115*, 4559–4564.

(168) Burgard, A. P., Pharkya, P., and Maranas, C. D. (2003) OptKnock: A Bilevel Programming Framework for Identifying Gene Knockout Strategies for Microbial Strain Optimization. *Biotechnol Bioeng 84*, 647–657.

(169) Pharkya, P., Burgard, A. P., and Maranas, C. D. (2003) Exploring the Overproduction of Amino Acids Using the Bilevel Optimization Framework OptKnock. *Biotechnol Bioeng 84*, 887–899.

(170) Antonovsky, N., Gleizer, S., and Milo, R. (2017) Engineering carbon fixation in *E. coli*: from heterologous RuBisCO expression to the Calvin–Benson–Bassham cycle. *Curr Opin Biotechnol 47*, 83–91.

(171) Gleizer, S., Ben-Nissan, R., Bar-On, Y. M., Antonovsky, N., Noor, E., Zohar, Y., Jona, G., Krieger, E., Shamshoum, M., Bar-Even, A., and Milo, R. (2019) Conversion of *Escherichia coli* to Generate All Biomass Carbon from CO_2. *Cell 179*, 1255–1263.

(172) Herz, E., Antonovsky, N., Bar-On, Y., Davidi, D., Gleizer, S., Prywes, N., Noda-Garcia, L., Lyn Frisch, K., Zohar, Y., Wernick, D. G., Savidor, A., Barenholz, U., and Milo, R. (2017) The genetic basis for the adaptation of *E. coli* to sugar synthesis from CO_2. *Nat Commun 8*, 1–10.

(173) Pinchuk, G. E., Hill, E. A., Geydebrekht, O. V., de Ingeniis, J., Zhang, X., Osterman, A., Scott, J. H., Reed, S. B., Romine, M. F., Konopka, A. E., Beliaev, A. S., Fredrickson, J. K., and Reed, J. L. (2010) Constraint-based model of *Shewanella oneidensis* MR-1 metabolism: A tool for data analysis and hypothesis generation. *PLoS Comput Biol 6*, 1–8.

Chapter 2: The electron transport chain of *Shewanella oneidensis* MR-1 can operate bidirectionally to enable microbial electrosynthesis

Kathryne C. Ford[1,2], Michaela A. TerAvest[1]

[1]Department of Biochemistry and Molecular Biology, Michigan State University, East Lansing, MI, 48824, USA

[2]Department of Microbiology and Molecular Genetics, Michigan State University, East Lansing, MI, 48824, USA

2.1 Abstract

Extracellular electron transfer (EET) by *S. oneidensis* can be used to drive intracellular biochemical reactions. Previous work used EET to generate 2,3-butanediol (2,3-BDO) via exogenous butanediol dehydrogenase reducing acetoin in an NADH dependent reaction. However, generating NADH via electron uptake from a cathode is energetically unfavorable, so NADH dehydrogenases couple the reaction to proton motive force. We therefore need to maintain the proton gradient across the membrane to sustain NADH production. This work explores accomplishing this task by bidirectional electron transfer, where electrons provided by the cathode go to both NADH formation and O_2 reduction by oxidases. We show that oxidases use trace dissolved oxygen in a microaerobic bioelectrical chemical systems (BES), and the translocation of protons across the membrane during O_2 reduction supports 2,3-butanediol generation. Additionally, at high levels of dissolved oxygen in an aerated system, cytotoxic reactive oxygen species form and result in cell death.

2.2 Introduction

As reliance on fossil fuels becomes increasingly unsustainable from an economic and environmental perspective, researchers work toward alternative energy sources. One solution is microbial electrosynthesis, which is the microbially catalyzed transfer of electrons from an electrode to cells to drive a biochemical reduction reaction[1–3].

Microbial electrosynthesis can be catalyzed by electroactive bacteria capable of interfacing with an electrode surface in a BES or by using the electrode to generate electron carriers, such as H_2 or formate, that can be taken up by bacteria[4–6]. When using electroactive bacteria, a potential is applied to the system to drive oxidation of an

electron donor (typically H_2O) at the anode, and the electrons liberated are taken up by bacteria at the cathode surface. These electrons are used for reduction of a feedstock, such as CO_2, to the desired product. When CO_2 is the reactant, microbial electrosynthesis becomes a carbon sink, acting as a carbon-neutral platform to produce biofuels, bioplastics, or specialty chemicals[7,8]. Because CO_2 is the ideal feedstock for microbial electrosynthesis, much of the existing research focused on bacterial strains or communities with the capacity for autotrophic growth. However, these microbes are inefficient due to slow growth rates and poor interaction with electrodes[9–11]. Recent advances in engineering autotrophy raise the possibility of expanding the applications of microbial electrosynthesis beyond the need for native autotrophy or mixed microbial populations[12–15]. Therefore, we have focused on a well-understood electroactive bacterial chassis, *Shewanella oneidensis* MR-1, and optimizing product generation[16,17].

S. oneidensis MR-1 is a metal-reducing bacterium with a well-characterized extracellular electron transfer pathway using MtrCAB[16–20]. The Mtr pathway allows *S. oneidensis* to respire anaerobically using extracellular, insoluble electron acceptors such as Fe(III) oxides, Mn(IV) oxides, and electrodes[21]. As with aerobic respiration, electrons are passed into the quinol pool (menaquinol and ubiquinol) by dehydrogenases in the electron transport chain that oxidizes metabolites such as lactate, formate, and NADH. For extracellular electron transfer, the reduced quinones (quinols) are oxidized by the inner membrane bound cytochrome CymA[22–25]. This protein acts as an electron hub, depositing electrons onto periplasmic electron carriers, such as fumarate reductase (FccA) and a small tetraheme cytochrome protein (CctA), to be shuttled onto terminal oxidoreductases. During respiration with an extracellular

electron acceptor such as an anode, electrons are transferred to the Mtr pathway, a three-protein complex that spans the outer membrane and extends into the extracellular space[26,27].

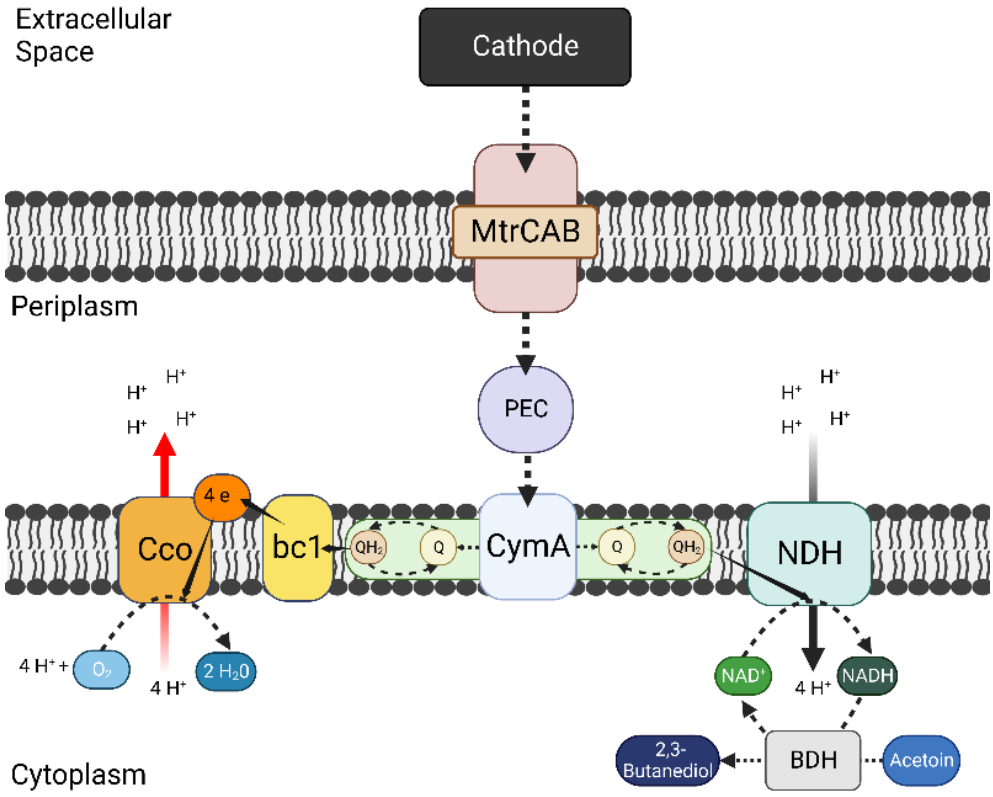

Figure 2.1 Overview of Bidirectional Electron Transfer to 2,3-BDO. *S. oneidensis* cells are incubated on a cathode poised at -500 $mV_{Ag/AgCl}$. Electrons are taken up by the cell via outer membrane MtrCAB pathway and passed to the inner membrane quinols via various periplasmic electron carriers (FccA, CctA) and CymA. Electrons from the quinol pool are used to reduce NAD^+ to NADH, catalyzed by NADH dehydrogenases (NDHs) coupling the reaction to proton movement across the inner membrane. The electrode produced NADH is used to reduce exogenous acetoin to 2,3-BDO via butanediol dehydrogenase (BDH).

Importantly, the Mtr pathway is reversible, allowing inward electron transfer from a cathode into the cell[2,26,28–32]. Electrons that are taken up via the Mtr pathway reduce respiratory quinones, and the cell can use the quinols as the electron donor for NAD^+ reduction by reversing NADH dehydrogenases. NADH can be used to drive a wide

variety of intracellular reduction reactions. As a proof-of-concept, we previously demonstrated that reducing power from the electrode can be used to drive the NADH-dependent reduction of acetoin to 2,3-BDO via the heterologous enzyme butanediol dehydrogenase (Bdh) (**Figure 2.1**). By measuring the accumulation of 2,3-BDO in the system, we can assess the rate and efficiency of electron uptake[28,33].

Inward electron transfer requires a continuous supply of electrons and an electron sink. In this system, acetoin is provided as the electron sink and electrons are supplied by a cathode poised at -0.5 $V_{Ag/AgCl}$. At this electrode potential, electron transfer from the cathode to the MtrCAB complex is thermodynamically favorable. All subsequent reactions in the pathway from electrode to menaquinol are also freely reversible. However, there is a significant energy barrier for electron transfer from menaquinol (-80 mV_{SHE}) to form NADH (-320 mV_{SHE}) due to the large difference in reduction potential. To overcome the energy barrier, the reaction is catalyzed by ion-coupled NADH dehydrogenases working in reverse. *S. oneidensis* uses both H^+-coupled and Na^+-coupled NADH dehydrogenases. In the forward direction, these enzymes couple NAD^+ reduction to the movement of ions down the electrochemical ($\Delta\psi$) and proton or sodium gradient (ΔpH or $\Delta[Na^+]$) known as proton or sodium motive force (PMF or SMF) across the inner membrane[34]. The movement of ions down these gradients into the cytoplasm provides the energy needed to power unfavorable chemical reactions; examples of this include formation of ATP via F_OF_1-ATP synthase or, as in this case, NAD^+ reduction by NADH dehydrogenases. In nature, reverse NADH dehydrogenase activity is a means to prevent the potentially lethal overreduction of the quinol pool by generating NADH[25,32,34–36].

To enable electron uptake from the electrode, *S. oneidensis* cells are incubated in a BES in the absence of an organic substrate or native terminal electron acceptor. Under these conditions, the cells do not generate PMF via NADH dehydrogenases (Nuo or Nqr) or succinate dehydrogenase (Sdh) because no substrate for these complexes is available[34,35]. Similarly, the absence of a terminal electron acceptor prevents forward electron transport chain flux. Because the reduction of NAD^+ to NADH requires the free energy provided by PMF, continuous PMF regeneration is necessary for the sustained production of 2,3-BDO. This concept is supported by the prior observation that addition of CCCP (carbonyl cyanide m-chlorophenyl hydrazone), an ionophore that dissipates PMF, results in the cessation of 2,3-BDO production[33]. This result underscores an important consideration for microbial electrosynthesis design; how the cell will maintain PMF to continuously drive the reduction reaction forward. To maintain PMF in previous experiments, we introduced proteorhodopsin (PR). PR is a light-driven proton pump that moves protons against the proton gradient into the periplasm, sustaining PMF. Active PR and illumination resulted in an increase of both 2,3-BDO production and cathodic current[28]. However, relying on PR as a source of PMF is not a viable solution for scale-up due to well-known issues with light penetration in industrial photobioreactors, and the additional energy cost associated with continuous illumination[28]. Understanding this, we sought to utilize bidirectional electron transfer so electrons from the electrode are used for generating both NADH and PMF.

In bidirectional electron transfer, electrons taken up by the cell go towards both the generation of NADH and the reduction of a terminal electron acceptor, e.g., oxygen. This coupling of electron uptake to oxygen reduction by terminal oxidases for PMF

generation was first described in *S. oneidensis* by Rowe et al.[32]. They found that under carbon-starvation and aerobic conditions, *S. oneidensis* on a cathode generated "non-growth-linked energy" in the form of PMF via terminal oxidase activity. Evidence indicated that PMF was used for production of ATP and reduced cytoplasmic electron carriers ($FMNH_2$, NAD(P)H). However, it is still unknown whether this process could continuously generate reducing power for use in MES as there was no sink for NADH. By implementing the Bdh-based system, we sought to determine if bidirectional electron transfer could sustain PMF generation to drive 2,3-BDO generation.

2.3 Results and Discussion

2.3.1 Eliminating electrode-independent 2,3-BDO Production

We previously demonstrated that the combination of an electrode and active PR led to higher levels of 2,3-BDO production than without either of these components. Before exploring the possibility of using bidirectional electron transfer instead of PR to drive PMF generation, we reexamined 2,3-BDO production in wild-type (WT) *S. oneidensis* MR-1 with and without active PR. Importantly, this experiment was done using an updated version of the previously described experiment protocol. In previous experiments, 35-50% of 2,3-BDO production was independent of the electrode, likely generated using NADH from organic carbon oxidation. To address the high background, we altered the protocol to promote residual organic carbon in the presence of an electron acceptor (anode) to reduce the availability of alternative sources of NADH. Briefly, in the updated protocol *S. oneidensis* is pre-grown in minimal medium (M5) with 20 mM lactate aerobically (or anaerobically with 40 mM fumarate as described later) for 18 hours, followed by inoculation into the BES under aerobic and anodic conditions

(+0.2 $V_{Ag/AgCl}$). After six hours, N_2 sparging is started to switch the cells from using oxygen to the anode as the electron acceptor. In the current study, this anaerobic, anodic phase continued for 40 hours (versus 18 hours in the previous protocol) before the potential is switched to cathodic (-0.5 $V_{Ag/AgCl}$). After this modification, we observed elimination of electrode-independent butanediol production (**Figure 2.2**, No Potential).

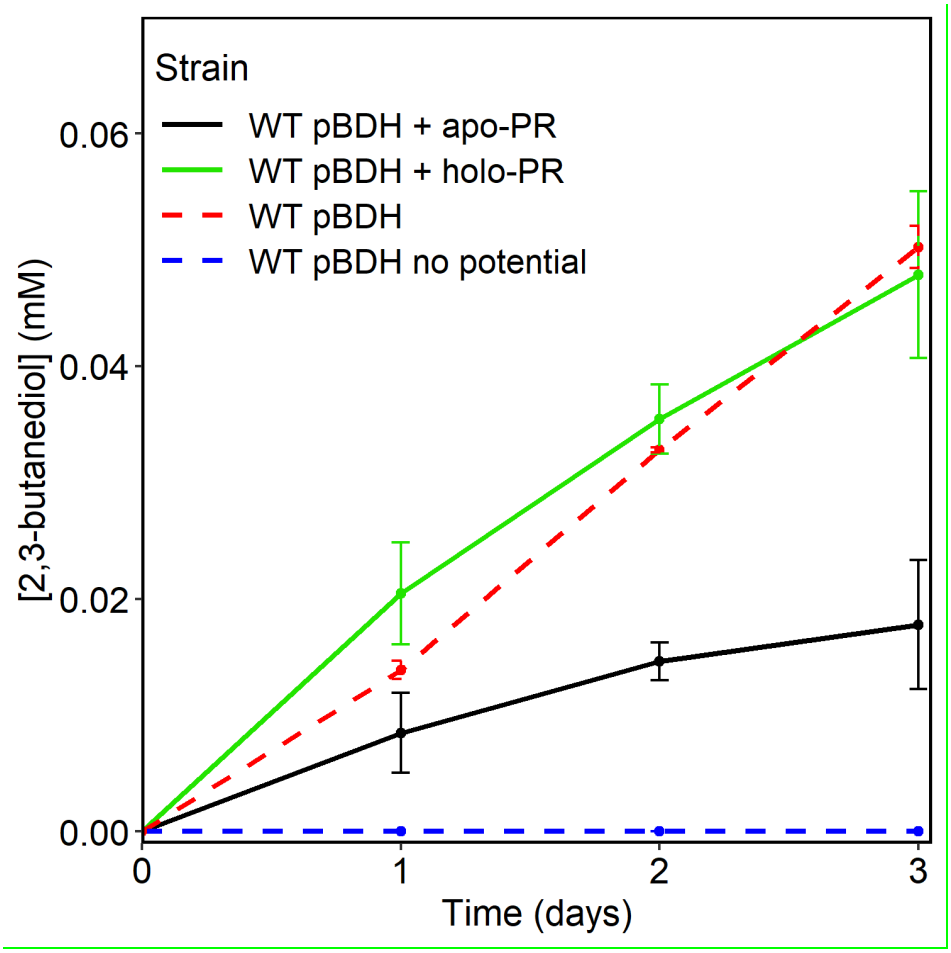

Figure 2.2 All 2,3-Butanediol Production is Electrode Dependent. Measurement of 2,3-butanediol in BES experiment with modified protocol. WT cells with pBDH or pBDH-PR with (holo-) or without (apo-) retinal as a cofactor, were pre-grown aerobically, washed, and inoculated into anodic BES. After 40 hours potential was switched to cathodic, and acetoin was added to a final concentration of 1 mM (T=0). Samples were collected for HPLC analysis every 24 hours. Lines and error bars represent averages and standard error (n=3).

We tested the amended protocol using a strain expressing PR, with and without the essential cofactor all-*trans*-retinal. Cells with active PR (holo-PR) produced more 2,3-BDO than those with inactive PR (apo-PR). Interestingly, cells with active PR produced approximately the same amount of 2,3-BDO as cells not expressing PR, while cells with inactive PR showed a decrease in 2,3-BDO production (**Figure 2.2**). This finding suggests that while PMF generation by PR supports an increase in 2,3-BDO production, the metabolic burden or membrane occupancy constraints of expressing PR outweigh the benefits. Moreover, this result suggests that there is an unaccounted-for source of PMF in the absence of PR. Another source of PMF appears more likely than the possibility that PMF is unnecessary, based on experimental evidence and thermodynamic calculations. Our prior work demonstrated that 2,3-BDO production is halted when PMF is dissipated by CCCP[33]. Additionally, electron transfer from quinols to form NADH cannot occur at an appreciable rate without the energy gained from proton translocation across the membrane. To sustain the NADH dehydrogenase-catalyzed reaction, which utilizes PMF, there must be a mechanism to replenish the proton gradient. We considered formate dehydrogenase and F_oF_1 ATP synthase as possible PMF sources, but found them unlikely due to the lack of a formate or ATP source. Therefore, we speculated that trace amounts of oxygen entering the BES could be sufficient to enable bidirectional electron transfer.

2.3.2 Bidirectional Electron Transfer to Oxygen and NAD^+

We investigated the possibility of bidirectional electron transfer as the unknown source of PMF because this reaction could be powered by the electrode, and the substrate (O_2) is readily accessible. Although the working chamber was continuously

degassed by N_2 bubbling (99.999% N_2), we suspected that the environment was microaerobic. The BESs may not be completely airtight due to the use of neoprene tubing and plastic connectors, and the possibility of oxygen diffusion from the anode through the ion exchange membrane (**Figure S2.1**). Additionally, the N_2 tank used can contain up to 1 ppm O_2 contamination, per the product specifications (Airgas). To ascertain if oxygen was present, we inserted an optical dissolved oxygen (DO) probe into the BES and conducted an experiment as normal. The DO in the working chamber was at ~100% saturation before inoculation, decreased to ~60% saturation upon cell addition, and dropped to ~1% upon N_2 bubbling (**Figure 2.3A**). This single experiment produced 0.046 mM 2,3-BDO over 3 days, which is consistent with previous experiments (**Figure 2.3C**).

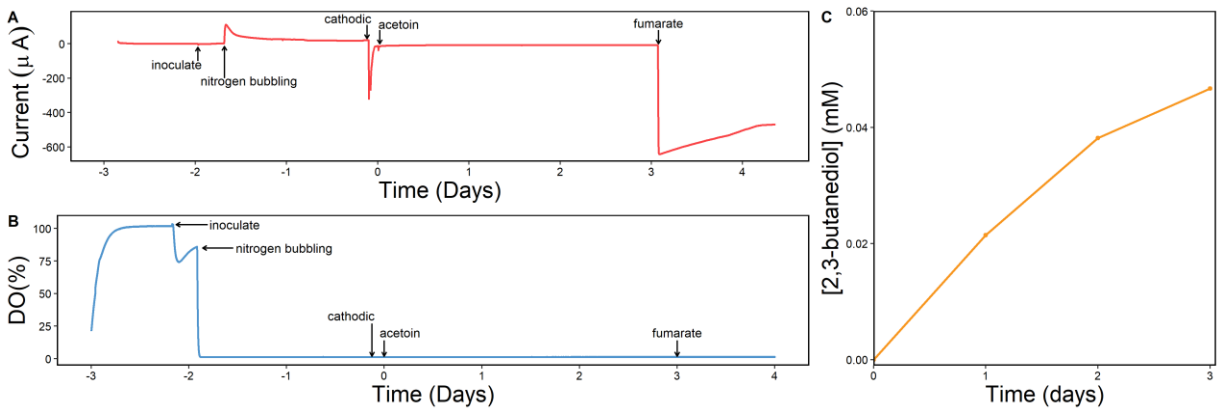

Figure 2.3 Presence of Oxygen in BES. Time course of the experiment from setup (Day -3) to final timepoint (Day 4), showing the current (A) and dissolved oxygen (B). Samples collected daily from Day 0 to Day 3 to quantify 2,3-BDO production (C) (n=1).

Production of one 2,3-BDO molecule from acetoin requires oxidation of one NADH, which in turn depletes four H^+ from available PMF via Nuo. One molecule of oxygen (O_2) allows translocation of four H^+ across the membrane if it is reduced by either of the proton-pumping terminal oxidases, Cco and Cox[37–39]. Therefore, the reduction of one O_2 molecule can sustain production of one molecule of 2,3-BDO from

the perspective of PMF balance. The 1% saturation DO concentration observed is equivalent to 0.073 mg/L (30°C, 856` elevation), or ~2 µM of oxygen available throughout the experiment[40]. Considering this concentration, there is more than enough oxygen available to support 0.046 mM 2,3-BDO production over 72 hours (0.638 µM 2,3-BDO/hour) as the sole source of PMF.

To verify the contribution of terminal oxidases in generating PMF during electron uptake, we compared current and 2,3-BDO production between WT MR-1 and a strain lacking all 3 terminal oxidases (Δ*cyd*Δ*cco*Δ*cox*, here named Δ*oxidase*)[32]. This strain cannot use O_2 as a terminal electron acceptor meaning that even with trace amounts of oxygen, the mutant cells would not be able to use it.[41] This mutant cannot grow in aerobic conditions, so further comparisons were performed using anaerobic pre-growth of all strains. To ensure consistency, we compared anaerobic growth of WT versus Δ*oxidase* cells in M5 minimal medium (20 mM lactate, 40 mM fumarate). We observed similar growth rates (**Figure S2.2**), so for MES experiments, these strains were pre-grown anaerobically. WT cells pre-grown in an anoxic environment produced 0.047 ± 0.002 mM butanediol, consistent with previous work, and exhibited similar current profiles and magnitudes (**Figure 2.4**). Conversely, the Δ*oxidase* strain produced minimal butanediol, with only a small amount accumulating by day 6, and less than half the current of WT cells. This result highlights that the cells were unable to sustain electrode-dependent acetoin reduction in the absence of aerobic terminal oxidases.

To confirm that the observed phenotype was due to the loss of PMF from proton-pumping oxidase activity, the Δ*oxidase* strain was functionally complemented by PR expression. If 2,3-BDO production is rescued by PR, it indicates that the loss of 2,3-

BDO generation in Δ*oxidase* is caused by a loss of PMF as opposed to off target effects, such as changes in gene regulation. When PR was expressed in Δ*oxidase*, we observed a restoration of 2,3-BDO production and partial rescue of current (**Figure 2.4**). In this instance, electron transfer to form NADH but not O_2 is restored, and as one O_2 is required to produce one 2,3-BDO molecule, a 50% rescue of current is consistent with our model. Taken together, these results support the hypothesis that PMF is a limiting resource, and the proton pumping activity of oxidases in this microaerobic environment is essential to continuous electron transfer to form NADH.

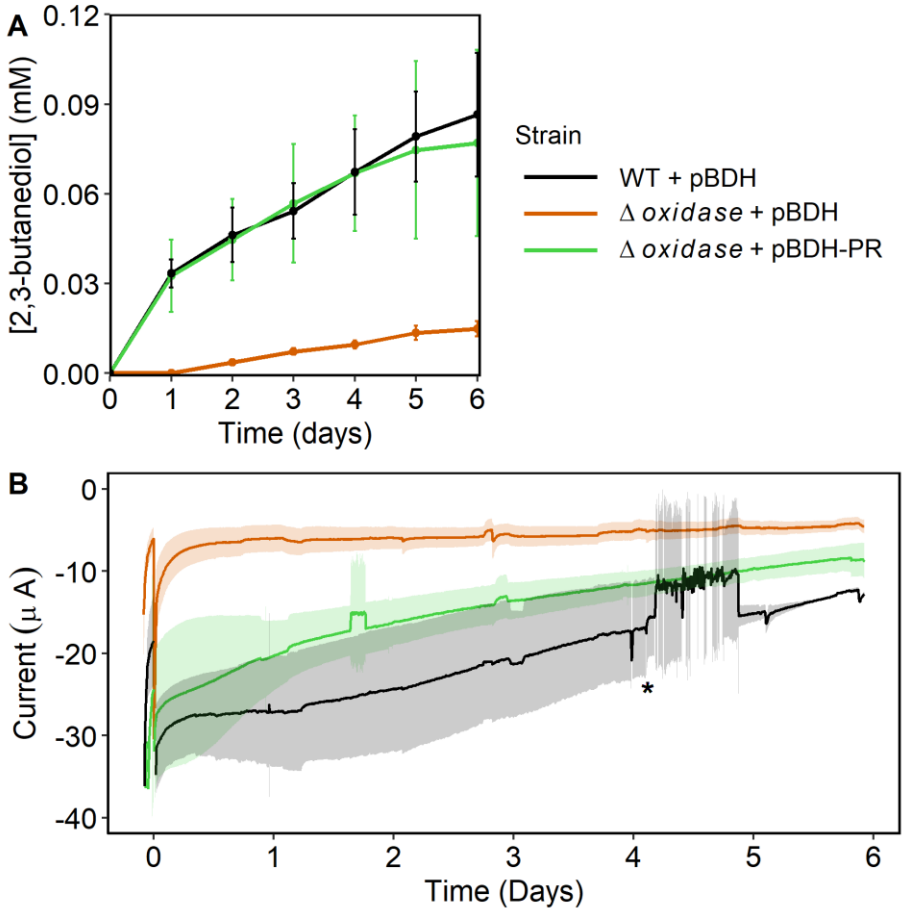

Figure 2.4 2,3-BDO and Current Production in Microaerobic BES. (A) 2,3-Butanediol accumulation in BES with WT pBDH, Δ*oxidase* pBDH, and Δ*oxidase* pBDH-PR with nitrogen bubbling. (B) Cathodic current from BES. Noisy current marked by (*) was due to stirring issues with one of the BES replicates. Points (A) and lines (B) represent averages with standard error bars, n=3.

2.3.3 Reactive Oxygen Species Formation

We next investigated whether increasing DO in the BES, and by extension oxidase activity, would result in an increase in 2,3-BDO. To do this, BESs were not sparged with N_2 to allow passive aeration. DO measurements indicated a highly oxygenated environment (300 μM) in the BES (**Figure S2.3**). This condition resulted in a severe decrease in 2,3-BDO production relative to the N_2-bubbling microaerobic condition (**Figure 2.5**). Current was greatly inflated by O_2 intrusion (data not shown).

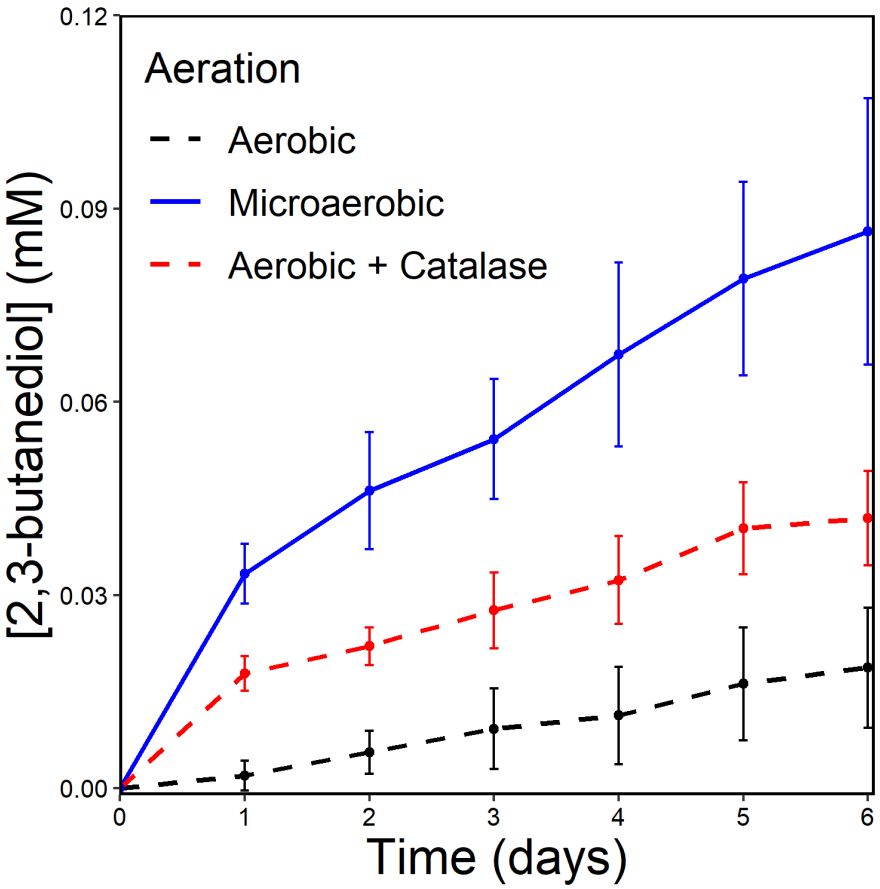

Figure 2.5 2,3-BDO Production in Aerobic and Microaerobic BES. (A) 2,3-Butanediol accumulation in BES with WT pBDH with N_2 bubbling (Microaerobic), and passive aeration (Aerobic) with or without the addition of 0.3 U/mL catalase. Points represent averages with standard error bars, n=3.

The failure of increased DO to translate to an increase in 2,3-BDO accumulation could be attributed to three factors: decreased *mtrCAB* expression, formation of reactive oxygen species (ROS), or a shift in electron flow to favor oxygen reduction over NADH generation. In the presence of oxygen, *S. oneidensis* MR-1 decreases expression of anaerobic respiration pathways such as Mtr in favor of aerobic respiration and a decrease in Mtr expression will likely result in a decrease in inward ET[42]. However, the cells are not actively growing under the experimental conditions, and it is improbable that a significant shift in the proteome occurred under the carbon starvation conditions of the experiment. Similarly, while loss of all electron flux in favor of oxygen reduction is possible, the small amount of 2,3-BDO produced during passive aeration suggests there are still electrons going towards NADH formation. Additionally, it has been shown that bidirectional electron transfer to NAD^+ and oxygen occurs under active aeration; if all electrons were being lost to oxygen, the effect would likely have been more pronounced under those conditions[32]. Further research done to optimize DO concentration should explore this possibility.

To assess the possibility of ROS formation, we measured hydrogen peroxide (H_2O_2) in the BESs. In the presence of oxygen and a strong reductant, such as a cathode or reduced flavin, O_2 can be reduced to form H_2O_2[42–45]. H_2O_2 accumulation in the BESs may result in cell death and a decrease in the ability to produce 2,3-BDO. H_2O_2 can also react directly with 2,3-BDO, possibly leading to reduced accumulation because of abiotic degradation[46,47]. To investigate if ROS accumulated in the passive aerobic condition, experiments with WT pBDH were performed with and without N_2 bubbling, with and without potential, and samples were taken for colony forming unit

(CFU) and H_2O_2 measurements. When the potential was swapped from anodic to cathodic, we observed an immediate drop in CFUs/mL and generation of H_2O_2 in BES with passive aeration, while the microaerobic BES maintained the same levels of both (**Figure 2.6**). There was no detectable peroxide formation in the no potential controls (data not shown). This result demonstrates that the formation of H_2O_2 is dependent on the presence of oxygen and a cathode. The formation of H_2O_2 was correlated with ~2.5 $\log_{10}$ cell death in the first 3 hours.

We next explored whether addition of catalase (an H_2O_2 degrading enzyme) could reduce H_2O_2 accumulation. This approach has the potential to harness the benefits of oxygen inclusion, such as PMF generation, while minimizing the production of harmful by-products[42]. Aerobic BESs were run with the addition of 0.3 U/mL catalase added immediately before the potential was switched to -0.5 $V_{Ag/AgCl}$. Aerobic BESs with catalase did not result in the same rapid decrease in CFUs/mL is increase in H_2O_2 as those without, as well as a less prominent spike in peroxide formation (**Figure 2.6**). Catalase addition also resulted in a partial rescue of 2,3-BDO production (**Figure 2.5**). These results show that one of the challenges with oxygen inclusion in a BES is the cytotoxic formation of H_2O_2, resulting in cell death and decrease in product yield. Future experimentation with aerated BES should focus on optimizing DO concentration to maximize reverse electron flux to oxygen reduction relative to forward electron flux to NAD^+; having high oxidase activity to generate PMF without losing electron flow to NADH formation.

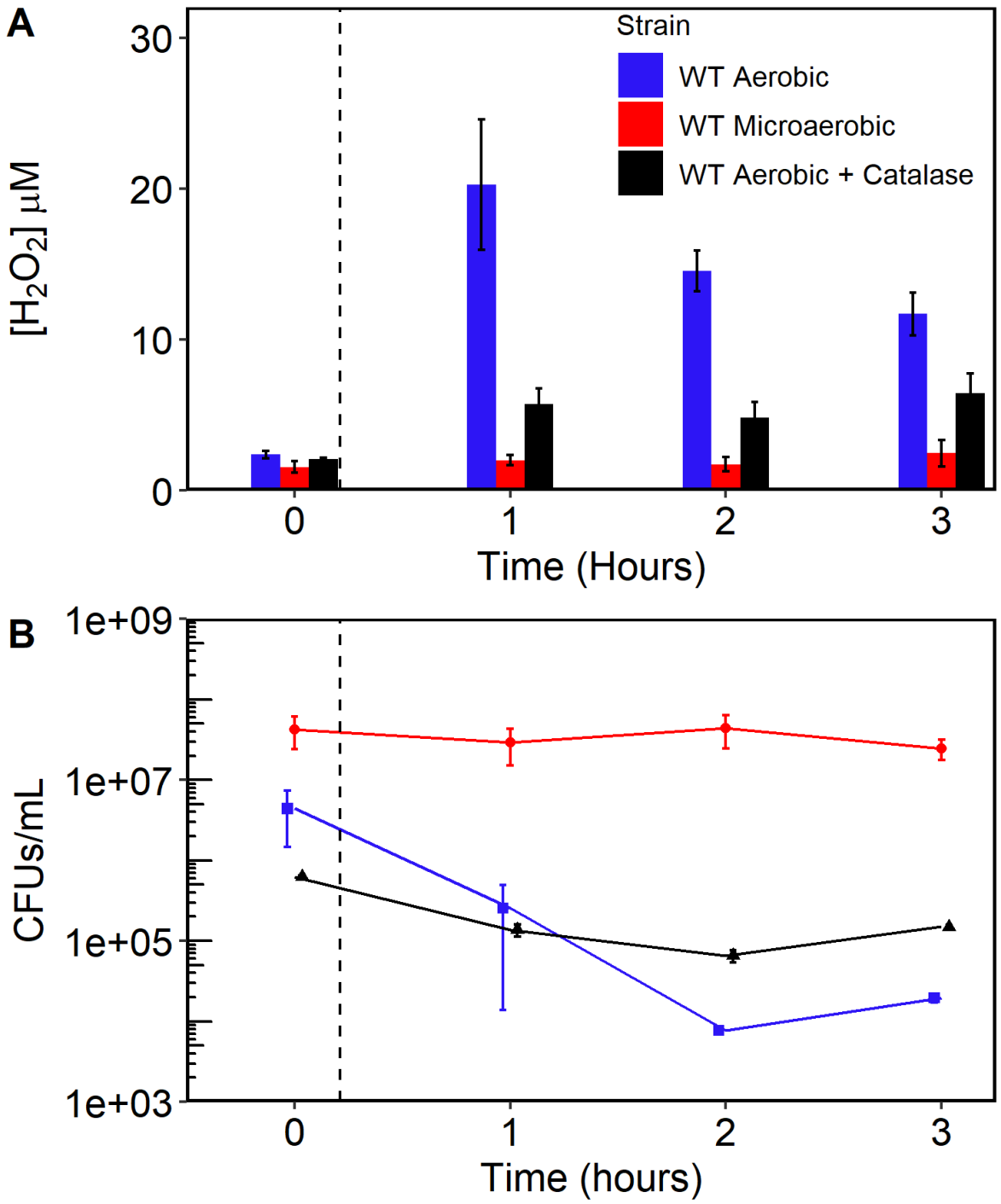

Figure 2.6 CFUs and [H_2O_2] in Aerobic and Microaerobic BES. (A) CFUs/mL and (B) [H_2O_2] µM in bulk medium of working chamber. Dashed line represents the potential change from 0.2 $V_{Ag/AgCl}$ to -0.5 $V_{Ag/AgCl}$. Points represent averages of n=3 with standard error bars. Lines are included in CFU/mL data to guide the eye. CFUs/mL at inoculation (~46 hrs. prior to T=0) for all conditions were ~1.8×10^8.

2.4 Conclusion

Effective microbial electrosynthesis requires attention to detail in both BES design and bacterial physiology. In the system discussed here, understanding the thermodynamic factors involved in driving inward electron transfer is crucial. The reversible nature of the electron transport pathways, which enables cells to use electrodes as electron acceptors and donors, depends on the reduction potential of each step[22,48–52]. Electron transfer reactions from electrode to quinol pool are freely reversible, but the final transfer from menaquinol to NADH formation has a much larger shift in potential between donor (-80 mV) and acceptor (-330 mV). This barrier is overcome by NADH dehydrogenases catalyzing the reaction and coupling the reduction to PMF utilization. In this work, we show that during electron transfer from an electrode to NADH, PMF can be regenerated by bidirectional electron transfer. Importantly, *S. oneidensis'* native aerobic terminal oxidases (Cco, Cox, Cyd) can sustain PMF via oxygen reduction without fully redirecting the flow of electrons away from NADH. This ability was best demonstrated in microaerobic conditions, where the DO concentration struck the balance between electron flow to oxygen and NAD^+. Higher levels of oxygen had the off-target effect of generating H_2O_2 that resulted in cell death. While the conditions tested here were limited to microaerobic and passively aerobic, future work should focus on fine tuning the DO in BES. This could be done through a combination of oxygen scavengers, gas mixing/modulating inflow, inclusion of other ROS neutralizing enzymes such as superoxide dismutase, or selective deletion of native oxidases as they have varying oxygen affinities and proton pumping efficiencies. The goal should be to balance the redox state of the quinone pool to maximize the flow of electrons 'uphill' to

NAD^+ relative to the energetically favorable reduction of oxygen. Taken together, this work shows the strong influence even trace oxygen has on the energetics of inward electron transport.

2.5 Materials and Methods

Table 2.1 Strains and Plasmids Used

Strain or Plasmid	Description	Source
S. oneidensis		
MR-1	Wild type *S. oneidensis*	Meyers and Nealson, 1988
Δ*oxidase*	Mutant with gene deletion of *cco, cyd, cox, (SO2361–SO2364, SO3285–SO3286, SO4606–SO4609)*	Rowe et al. 2018
Plasmids		
pBDH	pBBR1MCS2 bearing butanediol dehydrogenase gene from *Enterobacter cloacae*, kan^R	Tefft and TerAvest, 2019
pBDH-PR	pBBR1MCS2 bearing butanediol dehydrogenase from *Enterobacter cloacae* and proteorhodopsin (uncultured marine gamma proteobacterium EBAC31A08), kan^R	Tefft and TerAvest, 2019

Strains and Plasmids

Strains and plasmids used are listed in Table 2.1. *S. oneidensis* MR-1 strains were grown at 30 °C and shaking at 275 rpm for aerobic growth, and no shaking for anaerobic growth (~5% H_2, balanced with N_2). For BES experiments, MR-1 was pre-grown aerobically in 5 mL of lysogeny broth (LB) supplemented with 50 μg/mL kanamycin for strains with pBBR1-BDH, for inoculating minimal medium. For pre-growth, cells were grown in M5 minimal medium containing: 1.29 mM K_2HPO_4, 1.65 mM KH_2PO_4, 7.87 mM NaCl, 1.70 mM NH_4SO_4, 475 μM $MgSO_4 \cdot 7\ H_2O$, 10 mM HEPES, 0.01% (w/v) casamino acids, 1× Wolfe's vitamin solution, and 1× Wolfe's mineral solution, then the pH adjusted to 7.2 with 5 M NaOH. After autoclaving, D,L-lactate was

added to a final concentration of 20 mM. During anaerobic pre-growth, fumarate was added to a final concentration of 40 mM and 400 mL of medium was used per repeat. During bioelectrochemical experiments, the M5 medium recipe was amended to 100 mM HEPES, 0.2 µM riboflavin, and no D,L-lactate, fumarate, or casamino acids.

Growth Curves

For anaerobic growth experiments, cells were pre-grown in 5 mL LB supplemented with 40 mM fumarate and 20 mM D,L-lactate. Cells from the overnight culture were washed with M5 medium and resuspended to an OD_{600} of 0.05 in 2 mL M5 medium in a 24-well plate. OD_{600} was measured every 15 minutes for 35 hours in an anaerobic plate reader (BioTek, HTX). This protocol was repeated 3 times for replication.

Bioelectrochemical System Experiments

BES experiments were conducted in custom made two-chamber bioreactors kept at 30 °C as described in previous work (Tefft and TerAvest 2019)[28], and a similar set up to work described in (Tefft et al. 2022)[29]. The working chamber was filled with 144 mL amended M5 medium, with 0.2 µM riboflavin being added an hour before inoculation, and the counter chamber contained ~150 mL of 1x PBS. For experiments run with PR, green LED lights were attached to the reactors. Bioreactors were autoclaved for 45 minutes, then connected to a potentiostat (VMP, BioLogic USA) and current data was collected every 1 s for the course of the experiment. After the initial setup, the working electrode poised at an anodic potential of +0.2 $V_{Ag/AgCl}$ for ~16 hours. For aerobic pre-growth experiments, cells were grown in two 50-mL cultures of M5 in 250-mL flasks for each bioreactor (6 total for 3 replicates) for 18 hours. For anaerobic pre-growth experiments, cells were grown in 400-mL cultures of M5 in 1-L flasks for each bioreactor

(3 total for 3 replicates) for 18 hours. For experiments with PR, 400 µL 20 mM all-*trans*-retinal was added after 17 hours of growth as the essential cofactor for PR. Cultures were transferred to a 50-mL conical tube and centrifuged at 8000 rpm (Thermo Scientific ST8R; Rotor: 75005709) for 5 minutes. Pellets were washed twice in 30 mL M5 (100 mM HEPES, no carbon) and then resuspended in M5 (100 mM HEPES, no carbon), to a final OD_{600} of 3.6 in 10 mL. Then, 9 mL of this normalized resuspension was inoculated into the working chamber of the bioreactor using a sterile 10 mL syringe with an 18 g needle. Six hours after inoculation, N_2 gas (99.999%, AirGas) was bubbled into reactors through a 0.2 µM filter, and a bubbler attached to a 0.2 µM filter connected to the gas outlet. For 40 hours after N_2 bubbling, reactors were maintained at an anodic potential of +0.2 $V_{Ag/AgCl}$, before being changed to a cathodic potential of -0.5 $V_{Ag/AgCl}$. After three hours at cathodic potential, 17 mL of a sterile, de-gassed 10 mM acetoin solution was added to a final concentration of 1 mM in the bioreactor (Final volume in working chamber = 170 mL). The bioreactors were sampled (2 mL) immediately after acetoin addition for OD_{600} and HPLC analysis every 24 hours for 144 hours.

DO Measurements

DO measurements shown in **Figure 3** were collected using a Hamilton VisiFerm DO sensor and ArcAir Software. The probe was calibrated before each experiment as described in the manual. The probe was inserted into the BES prior to autoclaving and secured with a rubber gasket. DO measurements were recorded every 5 s during the experiment. To ensure that the inclusion of the DO probe did not interfere with oxygen intrusion into the system, we also utilized a smaller fiber optic DO probe and collected data every 30 s using a NeoFox Fluorimeter and Software (Ocean Insight). The probe

consists of a patch made from 5% mixture of polymer (poly(2,2,2-trifluoroethyl methacrylate), Scientific Polymer Products Inc.) and 5 mM porphyrin (Pt(II) meso-tetra(pentafluorophenyl)porphine, Frontier Scientific) dissolved in a 50/50 mixture of 1,4-dioxane and 1,2-dichloroethane (Sigma Aldrich). This patch is deposited onto the end of a fiber optic probe[53]. Results from this probe corroborated observations made with the Hamilton Probe (**Figure S2.3A**). Data from passively aerobic BES (**Figure S3B**) was collected using the smaller fiber optic probe.

CFU Plating

During BES experiments, samples were taken every ~24 hours starting at inoculation, with additional time points in the three hours following potential change from anodic to cathodic. These samples were used for CFU plating, H_2O_2 measurements, and HPLC analysis. Samples were serially diluted in a 96-well plate and 10 µL of each of 8 dilutions (10^0-10^{-7}) was plated on LB + Kan. Dilutions with between ~10^1-10^2 CFUs were counted and back calculated to determine CFUs/mL in bulk solution. Mean and standard error were calculated for biological replicates (n=3).

H_2O_2 Measurements

At each sampled time point, H_2O_2 formation was measured using the Pierce™ Quantitative Peroxide Assay Kit (ThermoFisher, Cat: 23280) according to the kit instructions. In brief, 20 µL of sample was mixed with 200 µL of reagent mixture in a 96-well plate, and absorbance was read at 595 nm. Sample values were compared to a standard curve with background subtraction of cell-only controls in 1xPBS to exclude any interference from cell OD_{600}. Mean and standard error were calculated for biological replicates (n=3).

HPLC analysis

HPLC analysis was performed as previously described (Tefft and TerAvest, 2019) with the amendments described in (Tefft et al., 2022)[28,29]. Sample analysis was performed on a Shimadzu 20A HPLC, using an Aminex HPX-87H (BioRad, Hercules, CA) column with a Microguard Cation H^+ guard column (BioRad, Hercules, CA) at 65 °C with a 0.5 ml/min flow rate. 2,3-butanediol concentration in samples was calculated by comparing sample value to an external standard curve.

Data analysis

Analysis of HPLC data, DO %, OD, current data, and growth curve data was done using RStudio using the following packages: ggplot2, dplyr, ggpubr, plyr, data.table, stringr, and growthcurver[54–60].

2.6 Author Contributions

K.C.F. and M.T. conceptualized the project. K.C.F. lead the investigation and data visualization under the supervision of M.T. K.C.F. wrote the original draft of the manuscript, with review and edits by M.T.

2.7 Acknowledgements

The authors would like to thank Nathan Frantz (Michigan State University - Department of Chemistry) and Dr. Denis A. Proshlyakov (Michigan State University - Department of Physiology) for their assistance with DO measurements. This research was supported by the National Science Foundation Graduate Research Fellowship Grant No. (DGE-1848739) to K.C.F., and a National Science Foundation CAREER Award (1750785) and 2018 Beckman Young Investigator Award to M.T.

REFERENCES

(1) Rabaey, K., and Rozendal, R. A. (2010) Microbial electrosynthesis — revisiting the electrical route for microbial production. *Nat Rev Microbiol 8*, 706–716.

(2) Karthikeyan, R., Singh, R., and Bose, A. (2019) Microbial electron uptake in microbial electrosynthesis: a mini-review. *J Ind Microbiol Biotechnol 46*, 1419–1426.

(3) Choi, O., and Sang, B. I. (2016) Extracellular electron transfer from cathode to microbes: Application for biofuel production. *Biotechnol Biofuels 9*, 1–14.

(4) Hirose, A., Kouzuma, A., and Watanabe, K. (2021) Hydrogen-dependent current generation and energy conservation by Shewanella oneidensis MR-1 in bioelectrochemical systems. *J Biosci Bioeng 131*, 27–32.

(5) Joshi, K., Kane, A. L., Kotloski, N. J., Gralnick, J. A., and Bond, D. R. (2019) Preventing Hydrogen Disposal Increases Electrode Utilization Efficiency by *Shewanella oneidensis*. *Front Energy Res 7*, 95.

(6) Xiong, J., Chan, D., Guo, X., Chang, F., Chen, M., Wang, Q., Song, X., and Wu, C. (2020) Hydrogen production driven by formate oxidation in *Shewanella oneidensis* MR-1. *Appl Microbiol Biotechnol 104*, 5579–5591.

(7) Prévoteau, A., Carvajal-Arroyo, J. M., Ganigué, R., and Rabaey, K. (2020, April 1) Microbial electrosynthesis from CO_2: forever a promise? *Curr Opin Biotechnol*. Elsevier Ltd.

(8) Gong, Z., Yu, H., Zhang, J., Li, F., and Song, H. (2020) Microbial electro-fermentation for synthesis of chemicals and biofuels driven by bi-directional extracellular electron transfer. *Synth Syst Biotechnol 5*, 304–313.

(9) Bajracharya, S., Ter Heijne, A., Dominguez Benetton, X., Vanbroekhoven, K., Buisman, C. J. N., Strik, D. P. B. T. B., and Pant, D. (2015) Carbon dioxide reduction by mixed and pure cultures in microbial electrosynthesis using an assembly of graphite felt and stainless steel as a cathode. *Bioresour Technol 195*, 14–24.

(10) Harnisch, F., Holtmann, D., Batlle-Vilanova, P., Berger, C., Enzmann, F., Geppert, F., Gescher, J., Halan, B., Kerzenmacher, S., Korth, B., Krieg, T., Liu, D., Lütz, S., Madjarov, J., Puig, S., Rabaey, K., Rosa, L. F. M., Rosenbaum, M. A., Rosenthal, K., Schippers, A., Schmid, A., Schmitz, L. M., Schmitz, S., Simonte, F., Sleutels, T. H. J. A., Sturm, G., Sturm-Richter, K., Tanne, C. K., ter Heijne, A., Trschörtner, J., Uhlig, R., and Vidakovic-Koch, T. (2019) Bioelectrosynthesis.

(11) Hengsbach, J. N., Sabel-Becker, B., Ulber, R., and Holtmann, D. (2022, June 1) Microbial electrosynthesis of methane and acetate—comparison of pure and mixed cultures. *Appl Microbiol Biotechnol*. Springer Science and Business Media Deutschland GmbH.

(12) Gleizer, S., Ben-Nissan, R., Bar-On, Y. M., Antonovsky, N., Noor, E., Zohar, Y., Jona, G., Krieger, E., Shamshoum, M., Bar-Even, A., and Milo, R. (2019) Conversion of *Escherichia coli* to Generate All Biomass Carbon from CO_2. *Cell 179*, 1255–1263.

(13) Herz, E., Antonovsky, N., Bar-On, Y., Davidi, D., Gleizer, S., Prywes, N., Noda-Garcia, L., Lyn Frisch, K., Zohar, Y., Wernick, D. G., Savidor, A., Barenholz, U., and Milo, R. (2017) The genetic basis for the adaptation of *E. coli* to sugar synthesis from CO_2. *Nat Commun 8*, 1–10.

(14) Antonovsky, N., Gleizer, S., Noor, E., Zohar, Y., Herz, E., Barenholz, U., Zelcbuch, L., Amram, S., Wides, A., Tepper, N., Davidi, D., Bar-On, Y., Bareia, T., Wernick, D. G., Shani, I., Malitsky, S., Jona, G., Bar-Even, A., and Milo, R. (2016) Sugar Synthesis from CO_2 in *Escherichia coli*. *Cell 166*, 115–125.

(15) Flamholz, A. I., Dugan, E., Blikstad, C., Gleizer, S., Ben-nissan, R., Amram, S., Antonovsky, N., Ravishankar, S., and Noor, E. (2020) Functional reconstitution of a bacterial CO_2 concentrating mechanism in *Escherichia coli*. *Elife 2*, 1–30.

(16) Coursolle, D., and Gralnick, J. A. (2010) Modularity of the Mtr respiratory pathway of *Shewanella oneidensis* strain MR-1. *Mol Microbiol 77*, 995–1008.

(17) Coursolle, D., and Gralnick, J. A. (2012) Reconstruction of extracellular respiratory pathways for iron(III) reduction in *Shewanella oneidensis* strain MR-1. *Front Microbiol 3*, 56.

(18) Nealson, K. H., and Rowe, A. R. (2016) Electromicrobiology: realities, grand challenges, goals and predictions. *Microb Biotechnol 9*, 595.

(19) Ikeda, S., Takamatsu, Y., Tsuchiya, M., Suga, K., Tanaka, Y., Kouzuma, A., and Watanabe, K. (2021) *Shewanella oneidensis* MR-1 as a bacterial platform for electro-biotechnology. *Essays Biochem 65*, 355–364.

(20) Mitchell, A. C., Peterson, L., Reardon, C. L., Reed, S. B., Culley, D. E., Romine, M. R., and Geesey, G. G. (2012) Role of outer membrane c-type cytochromes MtrC and OmcA in *Shewanella oneidensis* MR-1 cell production, accumulation, and detachment during respiration on hematite. *Geobiology 10*, 355–370.

(21) Fredrickson, J. K., Romine, M. F., Beliaev, A. S., Auchtung, J. M., Driscoll, M. E., Gardner, T. S., Nealson, K. H., Osterman, A. L., Pinchuk, G., Reed, J. L., Rodionov, D. A., Rodrigues, J. L. M., Saffarini, D. A., Serres, M. H., Spormann, A. M., Zhulin, I. B., and Tiedje, J. M. (2008) Towards environmental systems biology of *Shewanella*. *Nat Rev Microbiol 6*, 592–603.

(22) Marritt, S. J., Lowe, T. G., Bye, J., McMillan, D. G. G., Shi, L., Fredrickson, J., Zachara, J., Richardson, D. J., Cheesman, M. R., Jeuken, L. J. C., and Butt, J. N. (2012) A functional description of CymA, an electron-transfer hub supporting anaerobic respiratory flexibility in *Shewanella*. *Biochemical Journal 444*, 465–474.

(23) Sturm, G., Richter, K., Doetsch, A., Heide, H., Louro, R. O., and Gescher, J. (2015) A dynamic periplasmic electron transfer network enables respiratory flexibility beyond a thermodynamic regulatory regime. *ISME Journal 9*, 1802–1811.

(24) McMillan, D. G. G., Marritt, S. J., Butt, J. N., and Jeuken, L. J. C. (2012) Menaquinone-7 is specific cofactor in tetraheme quinol dehydrogenase CymA. *Journal of Biological Chemistry 287*, 14215–14225.

(25) Ross, D. E., Flynn, J. M., Baron, D. B., Gralnick, J. A., and Bond, D. R. (2011) Towards electrosynthesis in *Shewanella*: Energetics of reversing the Mtr pathway for reductive metabolism. *PLoS One 6*, 1–9.

(26) Rowe, A. R., Salimijazi, F., Trutschel, L., Sackett, J., Adesina, O., Anzai, I., Kugelmass, L. H., Baym, M. H., and Barstow, B. (2021) Identification of a pathway for electron uptake in *Shewanella oneidensis*. *Commun Biol 4*, 1–10.

(27) Edwards, M. J., White, G. F., Lockwood, C. W., Lawes, M. C., Martel, A., Harris, G., Scott, D. J., Richardson, D. J., Butt, J. N., and Clarke, T. A. (2018) Structural modeling of an outer membrane electron conduit from a metal-reducing bacterium suggests electron transfer via periplasmic redox partners. *Journal of Biological Chemistry 293*.

(28) Tefft, N. M., and TerAvest, M. A. (2019) Reversing an Extracellular Electron Transfer Pathway for Electrode-Driven Acetoin Reduction. *ACS Synth Biol 8*, 1590–1600.

(29) Tefft, N. M., Ford, K., and TerAvest, M. A. (2022) NADH dehydrogenases drive inward electron transfer in *Shewanella oneidensis* MR-1. *Microb Biotechnol 00*, 1–9.

(30) Rabaey, K., Read, S. T., Clauwaert, P., Freguia, S., Bond, P. L., Blackall, L. L., and Keller, J. (2008) Cathodic oxygen reduction catalyzed by bacteria in microbial fuel cells. *ISME Journal 2*, 519–527.

(31) Rosenbaum, M., Aulenta, F., Villano, M., and Angenent, L. T. (2011) Cathodes as electron donors for microbial metabolism: Which extracellular electron transfer mechanisms are involved? *Bioresour Technol 102*, 324–333.

(32) Rowe, A. R., Rajeev, P., Jain, A., Pirbadian, S., Okamoto, A., Gralnick, J. A., El-Naggar, M. Y., and Nealson, K. H. (2018) Tracking electron uptake from a cathode into *Shewanella* cells: Implications for energy acquisition from solid-substrate electron donors. *mBio 9*.

(33) Tefft, N. M., Ford, K., and TerAvest, M. A. (2022) NADH dehydrogenases drive inward electron transfer in Shewanella oneidensis MR-1. *Microb Biotechnol 00*, 1–9.

(34) Duhl, K. L., Tefft, N. M., and TerAvest, M. A. (2018) *Shewanella oneidensis* MR-1 utilizes both sodium- and proton-pumping NADH dehydrogenases during aerobic growth. *Appl Environ Microbiol 84*, 1–12.

(35) Duhl, K. L., and TerAvest, M. A. (2019) *Shewanella oneidensis* NADH Dehydrogenase Mutants Exhibit an Amino Acid Synthesis Defect. *Front Energy Res 7*, 1–12.

(36) Madsen, C. S., and TerAvest, M. A. (2019) NADH dehydrogenases Nuo and Nqr1 contribute to extracellular electron transfer by *Shewanella oneidensis* MR-1 in bioelectrochemical systems. *Sci Rep 9*.

(37) Chen, H., Luo, Q., Yin, J., Gao, T., and Gao, H. (2015) Evidence for the requirement of CydX in function but not assembly of the cytochrome *bd* oxidase in *Shewanella oneidensis*. *Biochim Biophys Acta Gen Subj 1850*, 318–328.

(38) Yin, J., Meng, Q., Fu, H., and Gao, H. (2016) Reduced expression of cytochrome oxidases largely explains cAMP inhibition of aerobic growth in *Shewanella oneidensis*. *Sci Rep 6*, 1–11.

(39) Le Laz, S., Kpebe, A., Bauzan, M., Lignon, S., Rousset, M., and Brugna, M. (2014) A biochemical approach to study the role of the terminal oxidases in aerobic respiration *Shewanella oneidensis* MR-1. *PLoS One 9*, 86343.

(40) Mortimer, C. H. (1956) The oxygen content of air-saturated fresh waters, and aids in calculating percentage saturation. *SIL Communications, 1953-1996 6*, 1–20.

(41) Zhou, G., Yin, J., Chen, H., Hua, Y., Sun, L., and Gao, H. (2013) Combined effect of loss of the *caa*$_3$ oxidase and Crp regulation drives *Shewanella* to thrive in redox-stratified environments. *ISME Journal 7*, 1752–1763.

(42) Norman, M. P., Edwards, M. J., White, G. F., Burton, J. A. J., Louro, R. O., Paquete, C. M., and Clarke, A. (2023) A Cysteine Pair Controls Flavin Reduction by Extracellular Cytochromes during Anoxic/Oxic Environmental Transitions. *mBio 14*, 1–12.

(43) Burek, B. O., Bormann, S., Hollmann, F., Bloh, J. Z., and Holtmann, D. (2019) Hydrogen peroxide driven biocatalysis. *Green Chemistry 21*, 3232–3249.

(44) Massey Vincent. (1994) Activation of Molecular Oxygen by Flavins and Flavoproteins. *Journal of Biological Chemistry 269*, 22459–22462.

(45) Roncel, M., Navarro, J. A., Rosa, F. F. D. la, and Rosa, M. A. D. la. (1984) Flavin-Mediated Production of Hydrogen Peroxide in Photoelectrochemical Cells. *Photochem Photobiol 40*, 395–398.

(46) Zhou, Z. Y., Zhang, H. T., and Shi, Y. (2004) Theoretical study of the interactions between 1,3-butanediol and hydrogen peroxide. *Journal of Physical Chemistry A 108*, 6520–6526.

(47) Sato, K., Aoki, M., Takagi, J., and Noyori, R. (1998) Organic solvent- and halide-free oxidation of alcohols with aqueous hydrogen peroxide. *Chemtracts 11*, 629–631.

(48) Hartshorne, R. S., Reardon, C. L., Ross, D., Nuester, J., Clarke, T. A., Gates, A. J., Mills, P. C., Fredrickson, J. K., Zachara, J. M., Shi, L., Beliaev, A. S., Marshall, M. J., Tien, M., Brantley, S., Butt, J. N., and Richardson, D. J. (2009) Characterization of an electron conduit between bacteria and the extracellular environment. *Proceedings of the National Academy of Sciences 106*, 22169–22174.

(49) Harada, E., Kumagai, J., Ozawa, K., Imabayashi, S., Tsapin, A. S., Nealson, K. H., Meyer, T. E., Cusanovich, M. A., and Akutsu, H. (2002) A directional electron transfer regulator based on heme-chain architecture in the small tetraheme cytochrome *c* from *Shewanella oneidensis*. *FEBS Lett 532*, 333–337.

(50) Pessanha, M., Rothery, E. L., Miles, C. S., Reid, G. A., Chapman, S. K., Louro, R. O., Turner, D. L., Salgueiro, C. A., and Xavier, A. V. (2009) Tuning of functional heme reduction potentials in *Shewanella* fumarate reductases. *Biochim Biophys Acta Bioenerg 1787*, 113–120.

(51) White, G. F., Shi, Z., Shi, L., Wang, Z., Dohnalkova, A. C., Marshall, M. J., Fredrickson, J. K., Zachara, J. M., Butt, J. N., Richardson, D. J., and Clarke, T. A. (2013) Rapid electron exchange between surface-exposed bacterial cytochromes and Fe(III) minerals. *Proc Natl Acad Sci U S A 110*, 6346–6351.

(52) Firer-Sherwood, M., Pulcu, G. S., and Elliott, S. J. (2008) Electrochemical interrogations of the Mtr cytochromes from *Shewanella*: Opening a potential window. *Journal of Biological Inorganic Chemistry 13*, 849–854.

(53) Frantz, N. L., Brakoniecki, G., Chen, D., and Proshlyakov, D. A. (2021) Assessment of the maximal activity of complex IV in the inner mitochondrial membrane by tandem electrochemistry and respirometry. *Anal Chem 93*, 1360–1368.

(54) Wickham, H. (2016) ggplot2: Elegant Graphics for Data Analysis. Springer-Verlag New York. ISBN 978-3-319-24277-4, https://ggplot2.tidyverse.org.

(55) Wickham, H., François, R., and Henry, L. (2020) dplyr: A Grammar of Data Manipulation. https://dplyr.tidyverse.org, https://github.com/tidyverse/dplyr.

(56) Kassambara, A. (2023) ggpubr:“ggplot2” based publication ready plots. *https://CRAN.R-project.org/package=ggpubr 438*.

(57) Wickham, H., and Wickham, M. H. (2011) The Split-Apply-Combine Strategy for Data Analysis. *J Stat Softw 40*, 1–29.

(58) Dowle, M., Srinivasan, A., Gorecki, J., Chirico, M., Stetsenko, P., Short, T., Lianoglou, S., Antonyan, E., Bonsch, M., and Parsonage, H. (2019) data.table: Extension of “data.frame.” *https://CRAN.R-project.org/package=data.table 596*.

(59) Wickham, H. (2022) stringr: Simple, Consistent Wrappers for Common String Operations. *http://stringr. tidyverse. org, https://github. com/tidyverse/stringr*.

(60) Sprouffske, K., and Wagner, A. (2016) Growthcurver: an R package for obtaining interpretable metrics from microbial growth curves. *BMC Bioinformatics 17*, 1–4.

APPENDIX A: Supplementary Figures for Chapter 2

Figure S2.1 Bioelectrochemical System Design. Setup of our 2-chamber BES during an experiment with cells expressing PR, hence the inclusion of the green lights. Chambers are sealed with blue stoppers and N_2 is bubbled in from a neoprene tube attached to a 0.2 µm filter (foreground).

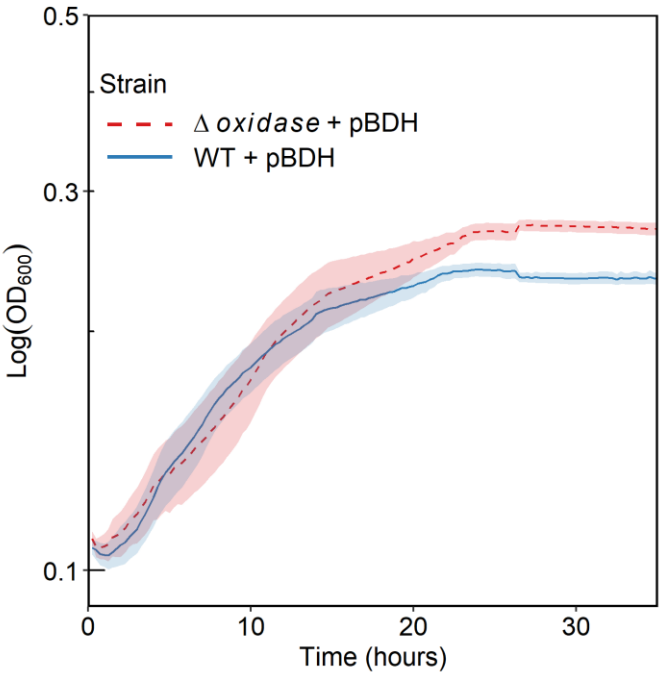

Figure S2.2 Growth curves of WT and Δ*oxidase*. Each strain was struck on LB + 20 mM D,L-lactate + 40 mM fumarate + Kan plates and incubated anaerobically at 30°C. Three single colonies were used to start 5 mL anaerobic overnight cultures in LB + 20 mM D,L-lactate + 40 mM fumarate + Kan. Overnight cultures were spun down and pellets resuspended in M5 + 20 mM D,L-lactate + 40 mM fumarate + Kan to an OD_{600} of 1.0. These samples were used to inoculate 2 mL of M5 + 20 mM D,L-lactate + 40 mM fumarate + Kan in a 24-well plate at an initial OD_{600} of 0.05. OD_{600} was measured every 15 minutes for 35 hours. Lines and shaded region represent the mean and standard error, respectively, for n=3 replication.

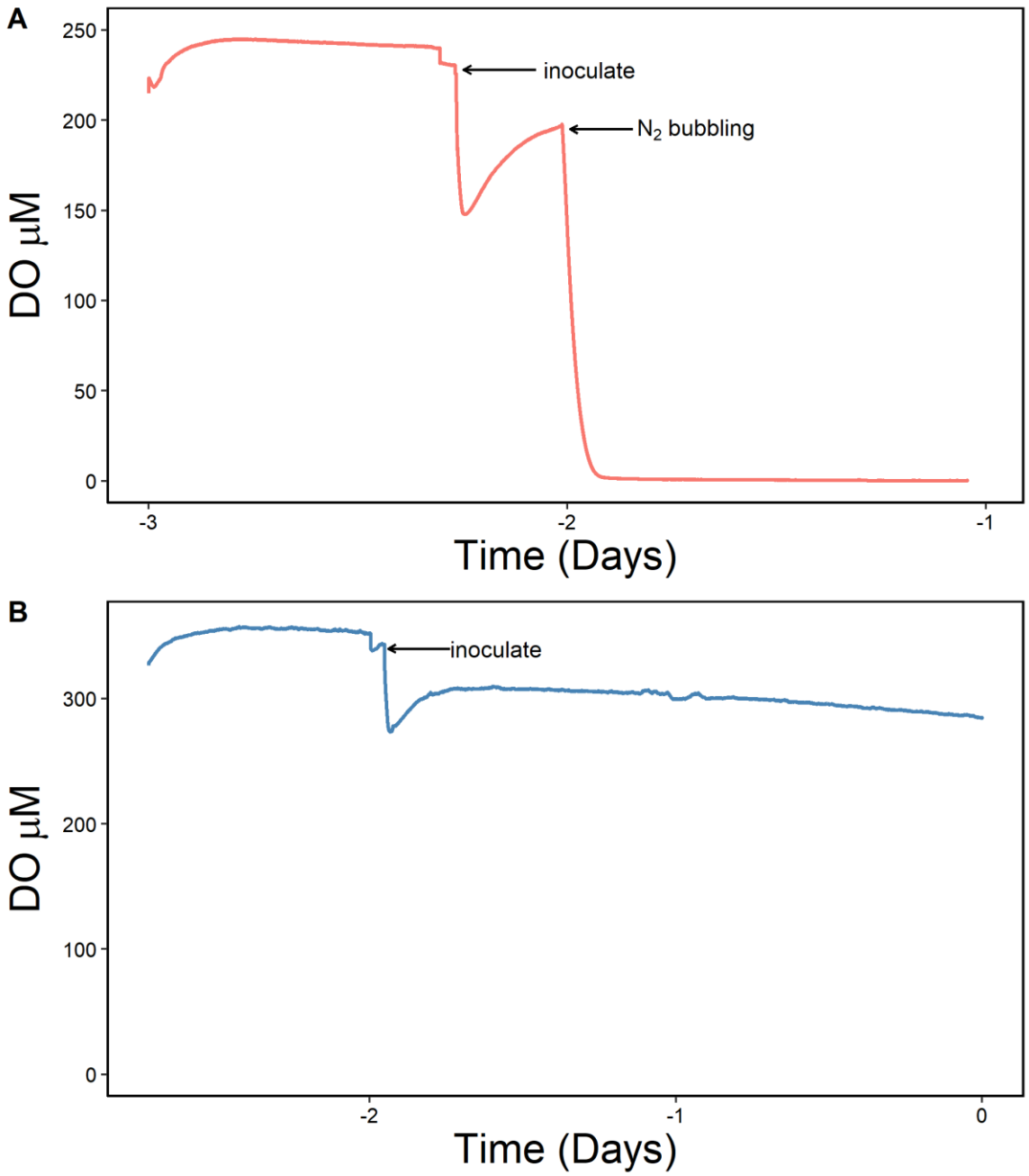

Figure S2.3 Dissolved Oxygen in Microaerobic and Passively Aerobic BES. Measurements of DO in BES under N_2 bubbling (A) and passive aeration (B) with the small fiber optic probe. T=0 corresponds to addition of acetoin. DO concentration for N_2 bubbled reactors ~0.5-1.0 µM O_2, and ~300 µM O_2 after inoculation.

Chapter 3: Flexibility of Inward Electron Transfer Pathway in *Shewanella oneidensis* MR-1

Kathryne C. Ford[1,2], Michaela A. TerAvest[1]

[1]Department of Biochemistry and Molecular Biology, Michigan State University, East Lansing, MI, 48824, USA

[2]Department of Microbiology and Molecular Genetics, Michigan State University, East Lansing, MI, 48824, USA

3.1 Abstract

The extracellular electron transport chain of *S. oneidensis* has been well characterized in the context of current generation on an anode. However, work to understand electron uptake from the cathode has largely relied on current data as opposed to biological outputs. To employ this organism as a biocatalyst for microbial electrosynthesis, we must have a clear picture of the path of electrons into the cell to ensure high coulombic efficiency and mitigate undesirable off-target reactions. We aim to do this by assessing the contribution of well-known electron transport pathway components to cathode-driven NADH production. In this work, we confirm that MtrCAB is essential for this, while CymA is important but can be slightly compensated for by other quinol-linked proteins. Additionally, we show that endogenous flavins are important for electron uptake, but their absence cannot be complemented by exogenous flavins. Finally, the hydrogenase HyaB plays an important role during cell survival during stationary phase on the electrode.

3.2 Introduction

As a model exoelectrogenic bacterium, *Shewanella oneidensis* MR-1 has been extensively studied as a chassis for microbial electrosynthesis (MES). MES is a process by which microorganisms act as biocatalysts on a cathode to drive synthesis of valuable chemical products. MES systems have expanded their potential applications to include production of valuable chemicals like cancer therapeutics, as well as serving as a tool for biosensors and bioremediation[1–11]. As such, there are many different approaches for optimization of these platforms. One such push is the development of new tools for genetic engineering.

S. oneidensis MR-1 is a genetically tractable organism, with a thoroughly characterized genome and proteome[12–15], making it a good target for rapid development of new tools for gene deletions, knockdowns, and precise regulation of gene expression from vectors[16–21]. Being able to rapidly generate different genetic modifications, and studying their resulting phenotypes, has been instrumental in growing our understanding of *S. oneidensis* physiology. In the context of MES, these genetic tools are employed to optimize electrons transfer between *S. oneidensis* and electrodes. To make such improvements, two major fields of research have investigated biofilm development and flavin export. Compared to another well-known exoelectrogen, *Geobacter* spp., *S. oneidensis* forms thinner, less conductive biofilms. Biofilms are essential for facilitating direct electron transfer to the electrode and creating an enclosed environment within which electron transfer mediators like flavins can be recycled. To this end, bioengineering work has aimed to increase biofilm thickness, conductivity, and surface area coverage[22–30]. These efforts have met with moderate success, with some of the greatest gains resulting from increased electrode coverage and improved conductivity of biofilm Exopolymeric substances (EPS)[26,29,31,32].

Excreted flavins play a role in shuttling electrons between the cell surface and the extracellular electron acceptor in *S. oneidensis*[33–36]. They also associate with outer membrane cytochromes (OMCs), such as MtrC and OmcA, to form flavocytochrome complexes[37]. The contribution of flavin-mediated electron transport has been debated in the context of long range versus short range transfer, as well as inward versus outward tranfer[38,39]. Genetic engineering allows exploration of these intricate relationships though gene overexpression or deletions. Increasing flavin export consistently increases

current generation[40]. There is also evidence that under cathodic conditions, flavins only aid electron transfer in the presence of OMCs[41].

Relying solely on electrical output as a benchmark for improved biotic reactions with the electrode may overlook other important factors. Assessing the impact of different genetic modifications on electron uptake should consider additional quantifiable outputs, depending on the research goal. Solely focusing on increasing electrical output may not always provide accurate insights into bacterial physiology. Electrochemistry experiments are influenced by electrode material, medium components, oxygen intrusion, and abiotic interactions with free flavins. This is further complicated when looking at differences between anodic and cathodic interactions. One way to address this is by calculating the coulombic efficiency. This is a measure of how effectively electrons are used in a specific reaction; ideally you want 100% efficiency where all the electrons are going solely to the desired reaction, or at least can be accounted for[42]. While this calculation has been done extensively with *S. oneidensis* on an anode, it has been less common for electron uptake with a cathode. There are a range of potential off target reactions during inward electron transfer. Therefore, we suggest that evaluation of genetic modifications for their impact on electron exchange should incorporate additional measurable outcomes, namely metabolite generation. One way this has already been implemented is by adding fumarate to BES to measure its reduction to succinate by FccA[10,43–46]. This measurement has been used to characterize the EET abilities of *S. oneidensis* mutants on cathodes and anodes. However, a caveat to this practice is that FccA is in the periplasm and can accept electrons directly from MtrA, therefore using fumarate as the metabolite may obscure the contribution of downstream

players like CymA. When examining the role of flavins, this is further complicated by the requirement of flavin mononucleotide (FMN) as a cofactor for FccA[35].

To address this problem, we have utilized a butanediol dehydrogenase (Bdh) based assay[9,10]. Within this system, electrons taken up by *S. oneidensis* enter the inner membrane to generate a pool of reduced menaquinol. NADH dehydrogenases use the menaquinols as redox partners to generate NADH from available NAD^+ by coupling the reaction to proton motive force (PMF). NADH can be used as a redox partner for many metabolic reactions and is therefore an important intermediate for MES. In our experimental design, *S. oneidensis* expresses Bdh from a vector (pBDH) to convert exogenous acetoin to 2,3-butanediol through an NADH dependent reduction reaction. Because *S. oneidensis* does not naturally metabolize acetoin and 2,3-butanediol is stable under these conditions, we can measure the production of 2,3-butanediol as a proxy for NADH generation. We believe that this system provides a more accurate reflection of the influence that genetic modifications have on inward electron transfer in the context of MES, rather than solely relying on comparative current data. It allows for quick and straightforward quantification of product output. This system was employed to examine the role of prominent electron transport pathway components to examine their roles in inward electron transport.

3.3 Results and Discussion

3.3.1 Inward Electron Transport uses Mtr and CymA

Traditionally, the electron transport pathway of *S. oneidensis* is described as electrons being passed from CymA to MtrCAB via periplasmic carriers, where they are then deposited onto extracellular electron acceptors though direct contact or mediated

by flavins. Recent developments have shown that not only is electron transfer more of a network than a pathway, but that it may be different when electrons are being taken into the cell than compared to when electrons are transported outward. We employed the Bdh system to investigate the major components of the electron transfer pathway in the organism *S. oneidensis* MR-1.

We first examined the contribution of MtrA to electrode-dependent NADH generation during electron uptake to acetoin in a bioelectrochemical system (BES). MtrA is the decaheme cytochrome present in the periplasmic portion of the Mtr complex[47–49]. Of the single Mtr complex knockouts, MtrA consistently shows the strongest phenotype, and is poorly compensated for by homologs compared to MtrB and MtrC[43,50]. Loss of MtrA results in a severe loss of current on an anode, and a 97% decrease in current during fumarate reduction on a cathode, so we expect to see a similar decrease[43,51]. Additionally, determining the contribution of Mtr also sheds light on the role of hydrogen-mediated electron transport. Hydrogen formation is possible at the cathodic potential used in our experiments (-0.5 v $V_{Ag/AgCl}$) and could potentially act as a bypass of the Mtr pathway. MR-1 contains two hydrogenases, one of which (Hya) could potentially oxidize electrode-produced hydrogen H_2 and transfer electrons into the quinol pool. Testing a Δ*mtrA* pBDH strain will aid in determining the flux of electrons through Mtr vs. hydrogen mediated electron transfer. In line with previous studies that looked at cathodic current in this knockout, we saw a ~95% decrease in 2,3-butanediol generation relative to WT (**Figure 3.1**). This supports the hypothesis that inward electron transport to form NADH relies on the Mtr pathway. Additionally, because this strain contained active hydrogenases, this result implies that hydrogen-mediated

electron transport does not compensate for the role of Mtr. A possible explanation for the limited accumulation of 2,3-butanediol by day 3 could be linked to cell death on the cathode creating a source of organic carbon for NADH formation.

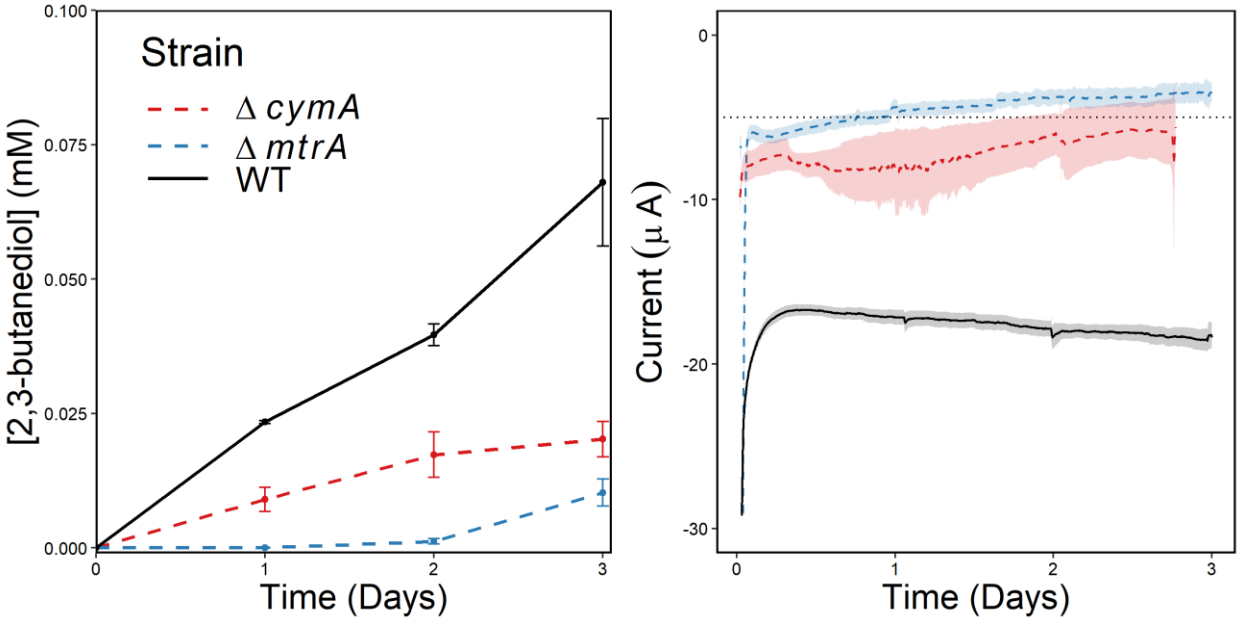

Figure 3.1 Inward Electron Transfer to Acetoin Reduction. Measurement of 2,3-butanediol accumulation and current generation in BES experiments with either WT, Δ*mtrA,* or Δ*cymA*. Cells were pre-grown in minimal medium aerobically, washed, and inoculated into anodic BES. 40 hours later, potential was changed to cathodic and acetoin was added to a final concentration of 1 mM (T=0) and samples were collected every 24 hours for HPLC analysis. Dotted line representative of abiotic current. Lines and error bars represent mean and standard error, respectively (n=3). All figures showing "WT" are the same set of experiments.

The other major component of the electron transport pathway is CymA, an inner membrane tetraheme protein cytochrome *c* responsible for connecting electron carriers to the quinol pool. Consistent with the findings of Ross et al., we observed a significant reduction in both current and 2,3-butanediol production in the Δ*cymA* pBDH strain (~70%)[43]. This suggests that there is an alternative pathway for electrons to enter the quinol pool from MtrA. Recent work has shown the potential for such a pathway; a CymA-independent periplasmic electron transport pathway[51,52]. This alternative pathway

could account for the remaining fraction of electrode-dependent 2,3-butanediol production. This could be an uncharacterized feature of FccA or CctA or be the result of some yet unidentified shuttling protein as has been previously suggested[51–53]. Alternatively, Xiao et al. suggested a role for other quinol-linked oxidases like TorC or PsrC, compensating for a loss of CymA[52]. Relative to our results, the loss of CymA could relegate the cell to using these slower pathways.

3.2.2 Flavins Have Complex Contributions to Electron Transport

The ratio of indirect to direct electron transfer (with and without soluble redox shuttles, respectively) is an important consideration for the efficiency of electron transfer. Flavins such as riboflavin (RF), flavin mononucleotide (FMN), and flavin adenine dinucleotide (FAD) are known to play a major role in electron transfer to the electrode suRFace[33,34,37,40,54,55]. In MR-1, FAD is transported across the inner membrane via Bfe, and cleaved in the periplasm by UshA to FMN and AMP. The FMN diffuses out of the cell, where a fraction of the extracellular FMN gradually hydrolyzes to form RF[40]. Extracellular RF has been shown to contribute to 70-95% of electron transfer in MR-1[33,34,36,56]. Therefore, to probe the effects of flavins during inward electron transfer, we tested inward electron transfer capability in a strain incapable of exporting flavins to produce RF (Δ*bfe*). The Δ*bfe* strain showed a significant decrease in BDO production of ~72%, which aligns almost exactly with the work by Marsili et al. for flavin impact during outward ET (**Figure 3.2**). We then aimed to compensate for this phenotype through the addition of exogenous RF at 1 μM. Surprisingly, while the addition of exogenous flavins resulted in a slight increase in current (**Figure 3.2**) it did not result in an increase in BDO production. The increase in current is likely be due to

abiotic interactions of photo-oxidized flavins at the electrode surface. Importantly, this did not result in increased BDO production. To determine whether the increased current was caused by abiotic reactions, sterile reactors were set up as normal with or without the addition of RF (0.2 µM). They demonstrated a similar pattern, with a slight increase in current in the reactors with RF versus those without (**Figure S3.1**).

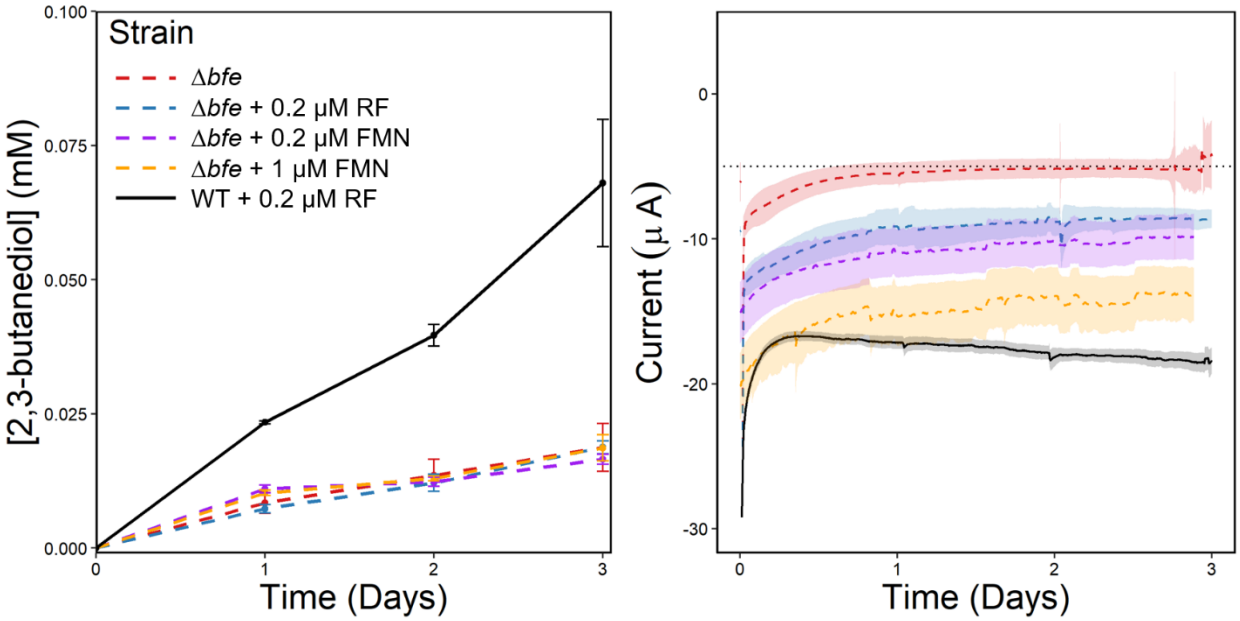

Figure 3.2 Endogenous flavins contribute to inward electron transfer. Measurement of 2,3-butanediol accumulation and current generation in BES experiments with either WT with exogenous RF or Δ*bfe* with exogenous RF or FMN. Cells were pre-grown in minimal medium aerobically, washed, and inoculated into anodic BES. 40 hours later, potential was changed to cathodic and acetoin was added to a final concentration of 1 mM (T=0) and samples were collected every 24 hours for HPLC analysis. Dashed line representative of abiotic current. Lines and error bars represent mean and standard error, respectively (n=3).

We also tested electron uptake with 2 different concentrations of FMN (0.2 µM and 1 µM), because FMN associates with OMCs and increases conductivity. Similarly to results with RF, we saw a slight increase in current compared to Δ*bfe* with no flavin addition, but no increase in BDO production. Overall, addition of exogenous RF and FMN did not improve inward electron transfer in cells that lacked Bfe. Flavins also play

a regulatory role and increase expression of cytochromes and biofilm components[29,57]. Because cells are not actively growing in the BES, the observed phenotype could be due to regulatory changes occurring during the pre-growth in the absence of extracellular flavins. To address this, experiments with Δ*bfe* were repeated with either 0.2 µM RF or FMN added to the pre-growth medium and BES. This also failed to restore 2,3-butanediol accumulation to WT levels (data not shown). However, *S. oneidensis* cells undergo regulatory changes upon electrode attachment and during different stages of biofilm formation; cells are in stationary phase under our conditions, there may still be a regulatory role for flavins at these later time points and should be further explored[57–60].

Understanding the impact flavins have on inward electron transfer is particularly vital as there is much debate regarding their mechanism of action and importance under different conditions. Initial research proposed that a majority of electron exchange is mediated by free flavins in extracellular space[33,34]. Later evidence suggested that flavins are more important as cofactors associated with OMCs[37,57,61]. Additionally, flavins can stimulate transcriptional changes that impact the cytochrome profile, biofilm formation, and EPS conductivity, further obfuscating their influence[41,58,59,62]. Our work aims to clarify this uncertainty by directly characterizing the contribution of flavins to cathode-driven NADH production, as it does not rely solely on current data and is less susceptible to abiotic influence. To accomplish this goal, BES were inoculated with Δ*bfe*, with and without supplemental flavins (RF or FMN). Bfe transports FAD from the cytoplasm to the periplasm to then be cleaved by UshA to FMN and AMP. Deletion of this transporter prevents the excretion of flavins to both the periplasm and the extracellular space. This strain has a proportional decrease in both 2,3-butanediol

production and cathodic current (~60%*) compared to WT. While this doesn't suggest a specific mechanism, it does demonstrate that flavins aid electron transfer. Interestingly, addition of exogenous RF or FMN does not rescue the Δ*bfe* phenotype for 2,3-butanediol production but does result in an increase in cathodic current. This was somewhat surprising, because it suggests that free flavins do not contribute to inward electron transfer to form NADH under these conditions. Additionally, if flavin's main role is as cofactors for OMCs, they either cannot associate with OMCs that are already anchored in the membrane or have a stronger influence in a different capacity such as gene regulation or biofilm formation. We investigated the latter by pre-growing Δ*bfe* with either RF or FMN as well as supplementing the media in the BES but saw similar results. As FccA is a known periplasmic carrier that uses FMN as a cofactor, we tested a strain with a knockout of *fccA* to determine if this was the source of this observed phenotype, but observed results comparable to WT. Future work should investigate this phenomenon to determine why exogenous flavins appear unable to fulfill the role of endogenous flavins for inward electron transfer to NAD^+. Also of note, the current in the Δ*bfe* BES increased with either RF or FMN in the medium. This result exemplifies why relying solely on current data may obscure our understanding of biological versus abiotic processes.

During electron transfer, periplasmic *c*-type cytochromes facilitate the movement of electrons between CymA and MtrA, such as the small tetraheme cytochrome CctA and the fumarate reductase FccA. FccA uses FMN as an essential cofactor, which is unavailable in the Δ*bfe* strain[35]. To confirm that the phenotype of the Δ*bfe* strain was due to flavin availability and not an off-target effect of an inactive FccA, we tested the

effect of a *fccA* deletion on 2,3-butanediol production. There was no significant difference in current or BDO production for Δ*fccA* compared to WT (**Figure 3.3**). There is evidence that FccA and CctA are functionally redundant, so the loss of FccA is likely compensated by CctA or other periplasmic electron carriers[63–65].This result confirms that the phenotype seen in the flavin experiments is not attributable to FccA lacking its cofactor.

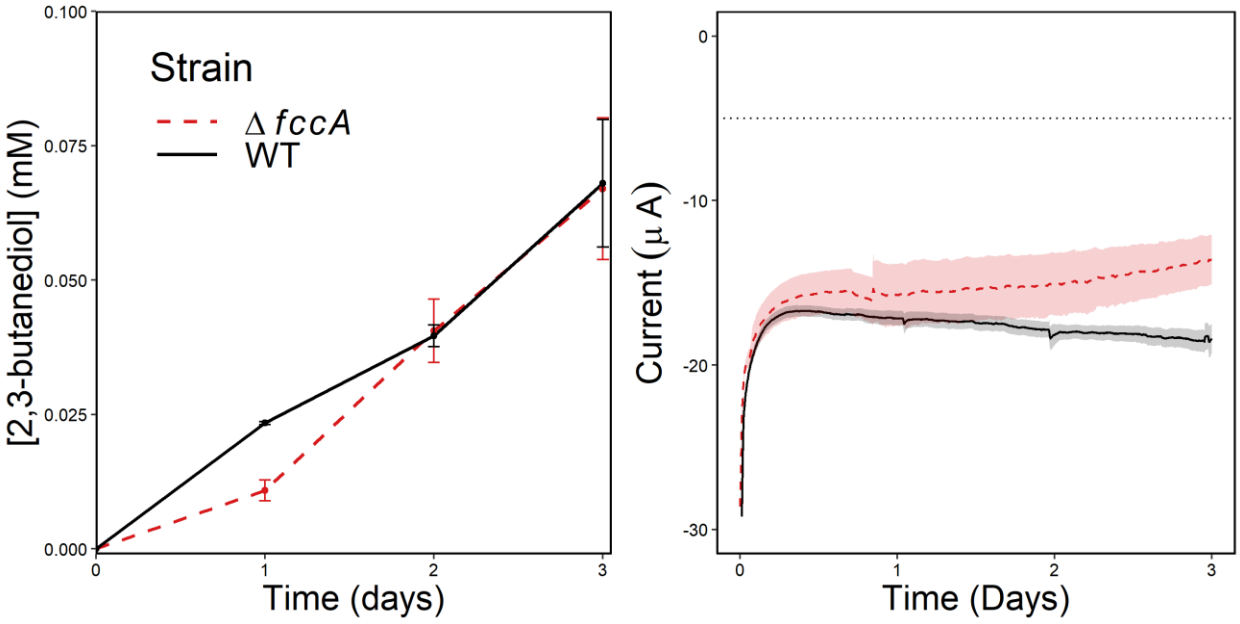

Figure 3.3 FccA is dispensable for Inward Electron Transfer. Measurement of 2,3-butanediol accumulation and current generation in BES experiments with either WT or Δ*fccA*. Cells were pre-grown in minimal media aerobically, washed, and inoculated into anodic BES. 40 hours later, potential was changed to cathodic and acetoin was added to a final concentration of 1 mM (T=0) and samples were collected every 24 hours for HPLC analysis. Dashed line representative of abiotic current. Lines and error bars represent mean and standard error, respectively (n=3).

3.3.3 Hydrogenases Enhance Cell Survival on Anode

In previously published work using this system, we noted that deletion of the two hydrogenases (Δ*hyaBhydA*) resulted in an increase in BDO accumulation[9]. This increase was attributed to hydrogen generation acting as an electron sink, siphoning off

electrons that would otherwise have gone to form NADH. However, the experimental protocol has since been modified by extending the anodic phase prior to acetoin addition. This delay was done for the purpose of removing residual organic carbon to prevent electrode-independent NADH formation. When Δ*hyaBhydA* was used with this new protocol, we observed a decrease in both current and BDO accumulation relative to WT (**Figure 3.4A,B**). Single hydrogenase deletion mutants (Δ*hyaB,* Δ*hydA*) indicated that this phenotype is largely attributable to HyaB; Δ*hyaB* showed the same 2,3-butanediol production as the double knockout, while Δ*hydA* behaved like WT. However, both single knockouts had current increase compared to Δ*hyaBhydA*.

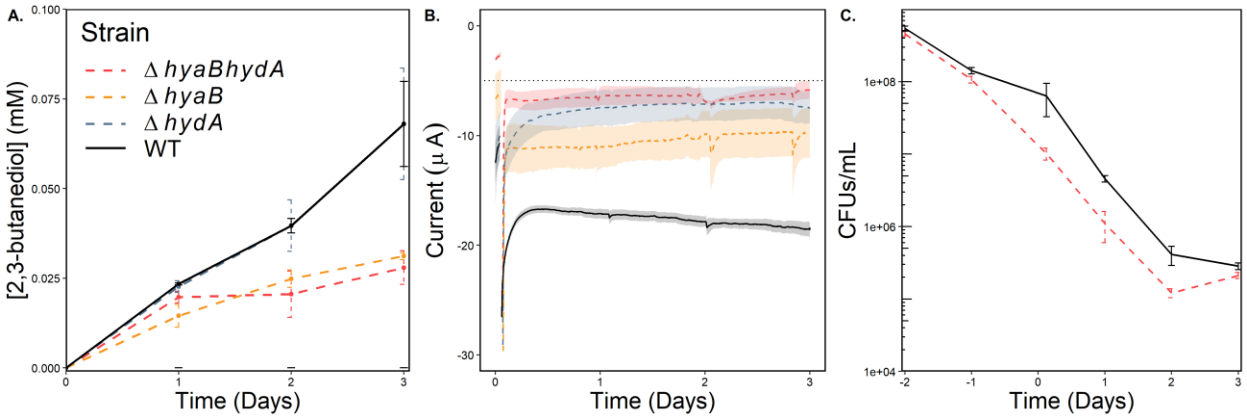

Figure 3.4 Hydrogenases Contribute to Cell Survival. Measurement of 2,3-butanediol accumulation (A) and current generation in BES experiments with either WT, Δ*hyaBhydA,* Δ*hydA* or Δ*hyaB* (B). Cells were pre-grown in minimal medium aerobically, washed, inoculated into anodic BES. 40 hours after inoculation, acetoin was added to a final concentration of 1 mM (T=0) and samples were collected every 24 hours for HPLC analysis. WT and Δ*hyaBhydA* BES samples were plated for CFUs every 24 hours starting at inoculation (T=-2) (C). Dotted line in (B) representative of abiotic current. Lines and error bars represent mean and standard error, respectively (n=3).

HyaB is predicted to be a bidirectional hydrogenase, capable of either generating or oxidizing H_2, while HydA only generates H_2[66–68]. Therefore, one potential explanation for this observation is that hydrogen mediates electron transfer between the cathode and the inner membrane quinols. However, as previously stated, most (~95%) of the

electrons being transported rely on the Mtr complex, making it unlikely that hydrogen is a major contributor to electron shuttling. A hypothesis that we find more likely is that the hydrogenases, primarily HyaB, act as a release valve to prevent overreduction of the redox pool in the cell. This is supported by Joshi et al. who showed greater survival of cells during stationary phase when hydrogenases were present[68]. To test this, WT and Δ*hyaBhydA* BES experiments were performed again and samples were taken every 24 hours starting from inoculation and plated for CFUs (**Figure 3.4C**). Overall, the CFUs/mL in the bulk medium decreased over time for both strains, which is not surprising as cells become attached to the electrode over time. However, while the CFUs/mL for the two strains were similar for the first 24 hours, by 48 hours Δ*hyaBhydA* decreased by a $\log_{10}$ more than WT. This finding is similar to the pattern of survival seen by Joshi et al. for cells during stationary phase. Therefore, we can attribute the decrease in 2,3-butanediol production to cell death during the first 48 hours of the experiment. This result also coincides with the time before acetoin addition (T=0) being extended compared to earlier iterations.

3.4 Conclusions

MES is a technology that often utilizes the extracellular electron transfer capabilities of exoelectrogenic microorganisms to produce a variety of industrial chemicals, including biofuels and bioplastics. Recent developments in this field have focused on optimizing microbes in the system. In *S. oneidensis*, this approach has included streamlining the cytochrome network, increasing cell attachment to electrodes, and overproduction of electron shuttles[40,61,69]. A variety of creative strategies have greatly increased the electrical output in these systems. However, the increase in

current may not always translate to increased biotic activity. This inconsistency is a problem for research dedicated to the generation of industrially relevant products powered by electricity from a cathode. Our solution to this is the use of a Bdh-based system in which we can measure 2,3-butanediol accumulation as a proxy for NADH generation (**Figure 3.5**). For the purposes of optimizing inward electron transfer to NAD^+ via genetic manipulation, this system allows for accurate more assessment of efficiency than just current.

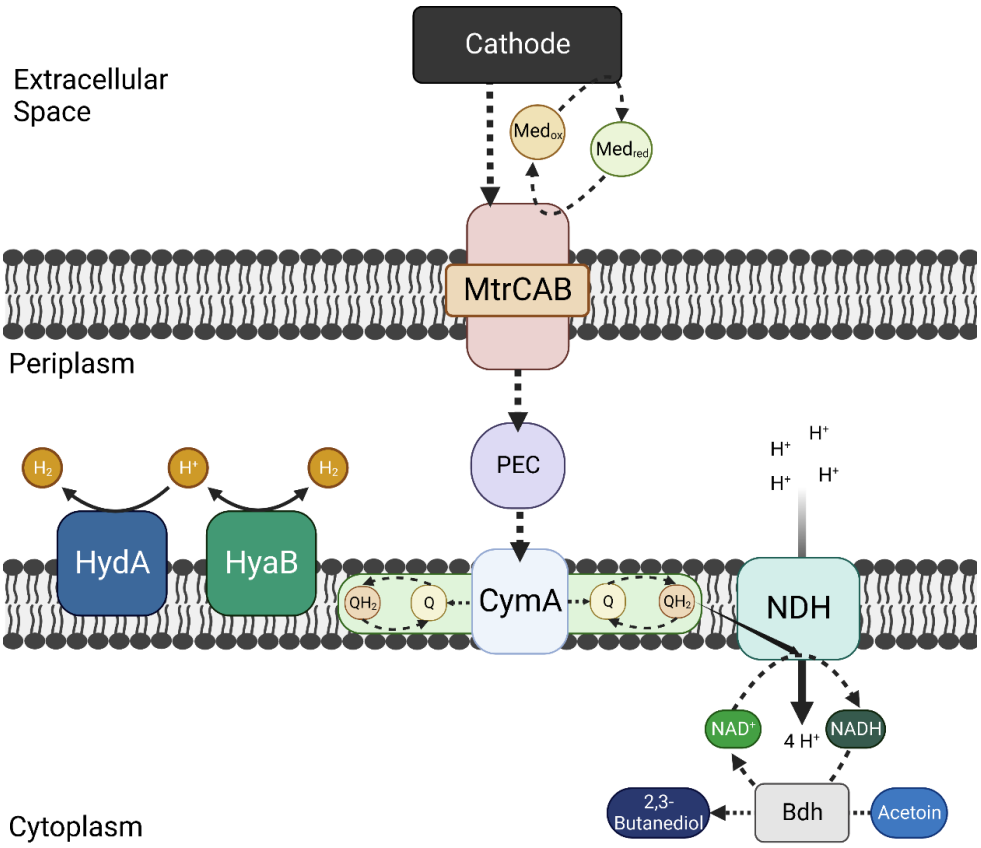

Figure 3.5 Inward Electron Transfer Path to Acetoin in *S. oneidensis.* During inward electron transfer to form NADH for acetoin reduction to 2,3-butanediol, electrons are taken up from a cathode via MtrCAB. Periplasmic electron carriers (PECs) shuttle electrons to CymA, or other quinol-linked reductases to a lesser extent. Endogenous exported flavins aid in inward electron transfer via mediation as free flavins, as OMC cofactors, or in a regulatory capacity. HyaB aids in cell survival during stationary phase on the electrode.

3.5 Materials and Methods

Table 3.1 Strains and Plasmids Used

Strain or Plasmid	Description	Source
S. oneidensis		
MR-1	Wild type *S. oneidensis*	Myers and Nealson, 1988[70]
Δ*mtrA*	Mutant with gene deletion of SO_1777	Rowe et al. 2018[71]
Δ*cymA*	Mutant with gene deletion of SO_4591	This work
Δ*bfe*	Mutant with gene deletion of SO_0702	Kotloski and Gralnick, 2013[33]
Δ*fccA*	Mutant with gene deletion of SO_0970	Gao et al., 2010[72]
Δ*hydA*	Mutant with gene deletion of SO_ 3920	This work
Δ*hyaB*	Mutant with gene deletion of SO_2098	This work
Δ*hyaBhydA*	Mutant with gene deletion of SO_3920 and SO_2098	Tefft and TerAvest, 2019[9]
Plasmids		
pBDH	pBBR1MCS2 bearing butanediol dehydrogenase gene from *Enterobacter cloacae*, kan^R	Tefft and TerAvest, 2019[9]

Strains and Plasmids

Strains and plasmids used are listed in Table 1. *S. oneidensis* MR-1 strains were grown at 30 °C and shaking at 275 rpm for aerobic growth. For bioelectrochemical system experiments, MR-1 was pre-grown aerobically in 5 mL of lysogeny broth (LB) supplemented with 50 μg/mL kanamycin for strains with pBBR1-BDH, for inoculating minimal medium. For pre-growth, cells were grown in M5 minimal medium containing: 1.29 mM K_2HPO_4, 1.65 mM KH_2PO_4, 7.87 mM NaCl, 1.70 mM NH_4SO_4, 475 μM $MgSO_4 \cdot 7\ H_2O$, 10 mM HEPES, 0.01% (w/v) casamino acids, 1× Wolfe's vitamin

solution, and 1× Wolfe's mineral solution, then the pH adjusted to 7.2 with 5 M NaOH. After autoclaving, D,L-lactate was added to a final concentration of 20 mM. During bioelectrochemical experiments, M5 medium recipe was amended to 100 mM HEPES, 0.2 µM riboflavin, and no D,L-lactate, or casamino acids.

Bioelectrochemical System Experiments

Bioelectrochemical system experiments were conducted in custom made two-chamber bioreactors kept at 30 °C as described in previous work (Tefft and TerAvest 2019)[9], and a similar set up to work described in (Tefft et al. 2022)[10]. The working chamber was filled with 144 mL amended M5 media, with 0.2 µM riboflavin being added an hour before inoculation, and the counter chamber contained ~150 mL of 1x PBS. Bioreactors were autoclaved for 45 minutes, then hooked up to a potentiostat (VMP, BioLogic USA) and current data was collected every 1 s for the course of the experiment. After the initial setup, the working electrode poised at an anodic potential of +0.2 $V_{Ag/AgCl}$ for ~16 hours. For aerobic pre-growth experiments, cells were grown in two 50-mL cultures of M5 in 250-mL flasks for each bioreactor (6 total for 3 replicates) for 18 hours. Cultures were transferred to a 50-mL conical tube and centrifuged at 8000 rpm (Thermo Scientific ST8R; Rotor: 75005709) for 5 minutes. Pellets were washed twice in 30 mL M5 (100 mM HEPES, no carbon) and then resuspended in M5 (100 mM HEPES, no carbon), to a final OD_{600} of 3.6 in 10 mL. Then, 9 mL of this normalized resuspension was inoculated into the working chamber of the bioreactor using a sterile 10 mL syringe with an 18 g needle. 6 hours after inoculation, N_2 gas (99.999%, AirGas) was bubbled into reactors through a 0.2 µM filter, and a bubbler attached to a 0.2 µM filter connected to the gas outlet. For 40 hours after N_2 bubbling, reactors were maintained at an anodic

potential of +0.2 $V_{Ag/AgCl}$, before being changed to a cathodic potential of -0.5 $V_{Ag/AgCl}$. After 3 hours at cathodic potential, 17 mL of a sterile, de-gassed 10 mM acetoin solution was added to a final concentration of 1 mM in the bioreactor (Final volume in working chamber = 170 mL). The bioreactors were sampled (2 mL) immediately after acetoin addition for OD_{600} and HPLC analysis every 24 hours after that for 72 hours.

CFU Plating

During BES experiments, samples were taken every ~24 hours starting at inoculation, with additional time points in the three hours following potential swap from anodic to cathodic. These samples were used for CFU plating, H_2O_2 measurements, and HPLC analysis. Samples were serially diluted in a 96-well plate and 10 µL of each of 8 dilutions (10^0-10^{-7}) was plated on LB + Kan. Dilutions with between ~10^1-10^2 CFUs were counted and back calculated to determine CFUs/mL in bulk solution. Mean and standard error were calculated for biological replicates (n=3).

HPLC analysis

HPLC analysis was performed as previously described (Tefft and TerAvest, 2019) with the amendments described in (Tefft et al., 2022)[9,10]. Sample analysis was performed on a Shimadzu 20A HPLC, using an Aminex HPX-87H (BioRad, Hercules, CA) column with a Microguard Cation H^+ guard column (BioRad, Hercules, CA) at 65 °C with a 0.5 ml/min flow rate. 2,3-butanediol concentration in samples was calculated by comparing sample value to an external standard curve.

Data analysis

Analysis of HPLC data, DO %, OD, current data, and growth curve data was done using RStudio using the following packages: ggplot2, dplyr, ggpubr, plyr, data.table, stringr, , and growthcurver[73–79].

3.6 Author Contributions

K.C.F. and M.T. conceptualized the project. K.C.F. lead the investigation and data visualization under the supervision of M.T. K.C.F. wrote the original draft of the manuscript, with review and edits by M.T.

3.7 Acknowledgements

This research was supported by the National Science Foundation Graduate Research Fellowship Grant No. (DGE-1848739) to K.C.F., and a National Science Foundation CAREER Award (1750785) and 2018 Beckman Young Investigator Award to M.T.

REFERENCES

(1) Yi, Y. C., and Ng, I. S. (2021) Redirection of metabolic flux in *Shewanella oneidensis* MR-1 by CRISPRi and modular design for 5-aminolevulinic acid production. *Bioresour Bioprocess 8*, 1–11.

(2) Wang, J., Wu, M., Lu, G., and Si, Y. (2016) Biotransformation and biomethylation of arsenic by *Shewanella oneidensis* MR-1. *Chemosphere 145*, 329–335.

(3) Webster, D. P., TerAvest, M. A., Doud, D. F. R., Chakravorty, A., Holmes, E. C., Radens, C. M., Sureka, S., Gralnick, J. A., and Angenent, L. T. (2014) An arsenic-specific biosensor with genetically engineered *Shewanella oneidensis* in a bioelectrochemical system. *Biosens Bioelectron 62*, 320–324.

(4) Ikeda, S., Takamatsu, Y., Tsuchiya, M., Suga, K., Tanaka, Y., Kouzuma, A., and Watanabe, K. (2021, July 1) *Shewanella oneidensis* MR-1 as a bacterial platform for electro-biotechnology. *Essays Biochem*. Portland Press Ltd.

(5) Sani, R. K., Sevinc Sengor, S., Magnuson, T., Beyenal, H., Ahmed, B., Renslow, R. S., Nuñez, J. R., Cao, B., Majors, P. D., and Fredrickson, J. K. (2017) Modeling Substrate Utilization, Metabolite Production, and Uranium Immobilization in *Shewanella oneidensis* Biofilms. *Front Environ Sci 5*, 1–15.

(6) Bursac, T., Gralnick, J. A., and Gescher, J. (2017) Acetoin production via unbalanced fermentation in *Shewanella oneidensis*. *Biotechnol Bioeng 114*, 1283–1289.

(7) Rosenbaum, M. A., and Henrich, A. W. (2014) Engineering microbial electrocatalysis for chemical and fuel production. *Curr Opin Biotechnol 29*, 93–98.

(8) Jeon, J. M., Park, H., Seo, H. M., Kim, J. H., Bhatia, S. K., Sathiyanarayanan, G., Song, H. S., Park, S. H., Choi, K. Y., Sang, B. I., and Yang, Y. H. (2015) Isobutanol production from an engineered *Shewanella oneidensis* MR-1. *Bioprocess Biosyst Eng 38*, 2147–2154.

(9) Tefft, N. M., and TerAvest, M. A. (2019) Reversing an Extracellular Electron Transfer Pathway for Electrode-Driven Acetoin Reduction. *ACS Synth Biol 8*, 1590–1600.

(10) Tefft, N. M., Ford, K., and TerAvest, M. A. (2022) NADH dehydrogenases drive inward electron transfer in *Shewanella oneidensis* MR-1. *Microb Biotechnol 00*, 1–9.

(11) Fan, G., Dundas, C. M., Graham, A. J., Lynd, N. A., and Keitz, B. K. (2018) *Shewanella oneidensis* as a living electrode for controlled radical polymerization. *PNAS 115*, 4559–4564.

(12) Pinchuk, G. E., Hill, E. A., Geydebrekht, O. V., de Ingeniis, J., Zhang, X., Osterman, A., Scott, J. H., Reed, S. B., Romine, M. F., Konopka, A. E., Beliaev, A. S., Fredrickson, J. K., and Reed, J. L. (2010) Constraint-based model of *Shewanella*

oneidensis MR-1 metabolism: A tool for data analysis and hypothesis generation. *PLoS Comput Biol 6*, 1–8.

(13) Ong, W. K., Vu, T. T., Lovendahl, K. N., Llull, J. M., Serres, M. H., Romine, M. F., and Reed, J. L. (2014) Comparisons of *Shewanella* strains based on genome annotations, modeling, and experiments. *BMC Syst Biol 8*.

(14) Rodionov, D. A., Yang, C., Li, X., Rodionova, I. A., Wang, Y., Obraztsova, A. Y., Zagnitko, O. P., Overbeek, R., Romine, M. F., Reed, S., Fredrickson, J. K., Nealson, K. H., and Osterman, A. L. (2010) Genomic encyclopedia of sugar utilization pathways in the *Shewanella*genus. *BMC Genomics 11*, 1–19.

(15) Pinchuk, G. E., Rodionov, D. A., Yang, C., Li, X., Osterman, A. L., Dervyn, E., Geydebrekht, O. V., Reed, S. B., Romine, M. F., Collart, F. R., Scott, J. H., Fredrickson, J. K., and Beliaev, A. S. (2009) Genomic reconstruction of *Shewanella oneidensis* MR-1 metabolism reveals a previously uncharacterized machinery for lactate utilization. *Proc Natl Acad Sci U S A 106*, 2874–2879.

(16) Chen, Y., Niu, X., Cheng, M., Wang, L., Sun, P., Song, H., and Cao, Y. (2022) CRISPR/dCas9-RpoD-Mediated Simultaneous Transcriptional Activation and Repression in *Shewanella oneidensis* MR-1. *ACS Synth Biol 11*, 2184–2192.

(17) Corts, A. D., Thomason, L. C., Gill, R. T., and Gralnick, J. A. (2019) Efficient and Precise Genome Editing in *Shewanella* with Recombineering and CRISPR/Cas9-Mediated Counter-Selection. *ACS Synth Biol 8*, 1877–1889.

(18) Cao, Y., Li, X., Li, F., and Song, H. (2017) CRISPRi-sRNA: Transcriptional-Translational Regulation of Extracellular Electron Transfer in *Shewanella oneidensis*. *ACS Synth Biol 6*, 1679–1690.

(19) Li, J., Tang, Q., Li, Y., Fan, Y.-Y., Li, F.-H., Wu, J.-H., Min, D., Li, W.-W., Lam, P. K. S., and Yu, H.-Q. (2020) Rediverting Electron Flux with an Engineered CRISPR-ddAsCpf1 System to Enhance the Pollutant Degradation Capacity of *Shewanella oneidensis*. *Environ Sci Technol 54*, 3599–3608.

(20) Ford, K. C., Kaste, J. A. M., Shachar-Hill, Y., and TerAvest, M. A. (2022) Flux-Balance Analysis and Mobile CRISPRi-Guided Deletion of a Conditionally Essential Gene in *Shewanella oneidensis* MR-1. *ACS Synth Biol 11*, 3405–3413.

(21) Chen, Y., Cheng, M., Feng, X., Niu, X., Song, H., and Cao, Y. (2022) Genome Editing by CRISPR/Cas12 Recognizing AT-Rich PAMs in *Shewanella oneidensis* MR-1. *ACS Synth Biol 11*, 2947–2955.

(22) Yu, Y. Y., Chen, H. L., Yong, Y. C., Kim, D. H., and Song, H. (2011) Conductive artificial biofilm dramatically enhances bioelectricity production in *Shewanella*-inoculated microbial fuel cells. *Chemical Communications 47*, 12825–12827.

(23) Liu, T., Yu, Y.-Y., Deng, X.-P., Ng, C. K., Cao, B., Wang, J.-Y., Rice, S. A., Kjelleberg, S., and Song, H. (2015) Enhanced *Shewanella* Biofilm Promotes Bioelectricity Generation. *Biotechnol Bioeng 112*, 2051–2059.

(24) Matsumoto, A., Koga, R., Kanaly, R. A., Kouzuma, A., and Watanabe, K. (2021) Identification of a Diguanylate Cyclase That Facilitates Biofilm Formation on Electrodes by *Shewanella oneidensis* MR-1. *Appl Environ Microbiol 87*, 1–11.

(25) Gödeke, J., Heun, M., Bubendorfer, S., Paul, K., and Thormann, K. M. (2011) Roles of Two *Shewanella oneidensis* MR-1 Extracellular Endonucleases. *Appl Environ Microbiol 77*, 5342–5351.

(26) Ng, C. K., Xu, J., Cai, Z., Yang, L., Thompson, I. P., Huang, W. E., and Cao, B. (2020) Elevated intracellular cyclic-di-GMP level in *Shewanella oneidensis* increases expression of *c*-type cytochromes. *Microb Biotechnol 13*, 1904–1916.

(27) Silva, A. V, Edel, M., Gescher, J., and Paquete, C. M. (2020) Exploring the Effects of *bolA* in Biofilm Formation and Current Generation by *Shewanella oneidensis* MR-1. *Front Microbiol 11*, 1–7.

(28) Mukherjee, M., Zaiden, N., Teng, A., Hu, Y., and Cao, B. (2020, December 1) *Shewanella* biofilm development and engineering for environmental and bioenergy applications. *Curr Opin Chem Biol*. Elsevier Ltd.

(29) Zhao, J., Li, F., Kong, S., Chen, T., Song, H., and Wang, Z. (2023) Elongated Riboflavin-Producing *Shewanella oneidensis* in a Hybrid Biofilm Boosts Extracellular Electron Transfer. *Advanced Science 10*, 1–11.

(30) Zhou, G., Yuan, J., and Gao, H. (2015) Regulation of biofilm formation by BpfA, BpfD, and BpfG in *Shewanella oneidensis*. *Front Microbiol 6*, 1–11.

(31) Kouzuma, A., Meng, X. Y., Kimura, N., Hashimoto, K., and Watanabe, K. (2010) Disruption of the Putative Cell Surface Polysaccharide Biosynthesis Gene SO3177 in *Shewanella oneidensis* MR-1 Enhances Adhesion to Electrodes and Current Generation in Microbial Fuel Cells. *Appl Environ Microbiol 76*, 4151–4157.

(32) Kitayama, M., Koga, R., Kasai, T., Kouzuma, A., and Watanabe, K. (2017) Structures, Compositions, and Activities of Live *Shewanella* Biofilms Formed on Graphite Electrodes in Electrochemical Flow Cells. *Appl Environ Microbiol 83*, 1–11.

(33) Kotloski, N. J., and Gralnick, J. A. (2013) Flavin electron shuttles dominate extracellular electron transfer by Shewanella oneidensis. *mBio 4*, 553–565.

(34) Brutinel, E. D., and Gralnick, J. A. (2012) Shuttling happens: Soluble flavin mediators of extracellular electron transfer in Shewanella. *Appl Microbiol Biotechnol 93*, 41–48.

(35) Covington, E. D., Gelbmann, C. B., Kotloski, N. J., and Gralnick, J. A. (2010) An essential role for UshA in processing of extracellular flavin electron shuttles by *Shewanella oneidensis*. *Mol Microbiol 78*, 519–532.

(36) Marsili, E., Baron, D. B., Shikhare, I. D., Coursolle, D., Gralnick, J. A., and Bond, D. R. (2008) *Shewanella* secretes flavins that mediate extracellular electron transfer. *Proc Natl Acad Sci U S A 105*, 3968–3973.

(37) Xu, S., Jangir, Y., and El-Naggar, M. Y. (2016) Disentangling the roles of free and cytochrome-bound flavins in extracellular electron transport from *Shewanella oneidensis* MR-1. *Electrochim Acta 198*, 49–55.

(38) Lies, D. P., Hernandez, M. E., Kappler, A., Mielke, R. E., Gralnick, J. A., and Newman, D. K. (2005) *Shewanella oneidensis* MR-1 Uses Overlapping Pathways for Iron Reduction at a Distance and by Direct Contact under Conditions Relevant for Biofilms. *Appl Environ Microbiol 71*, 4414–4426.

(39) Yi, Y., Zhao, T., Zang, Y., Xie, B., and Liu, H. (2021) Different mechanisms for riboflavin to improve the outward and inward extracellular electron transfer of *Shewanella loihica*. *Electrochem commun 124*, 1–7.

(40) Yang, Y., Ding, Y., Hu, Y., Cao, B., Rice, S. A., Kjelleberg, S., and Song, H. (2015) Enhancing Bidirectional Electron Transfer of *Shewanella oneidensis* by a Synthetic Flavin Pathway. *ACS Synth Biol 4*, 815–823.

(41) Okamoto, A., Hashimoto, K., and Nealson, K. H. (2014) Flavin Redox Bifurcation as a Mechanism for Controlling the Direction of Electron Flow during Extracellular Electron Transfer. *Angewandte Chemie International Edition 53*, 10988–10991.

(42) TerAvest, M. A., and Angenent, L. T. (2014) Oxidizing Electrode Potentials Decrease Current Production and Coulombic Efficiency through Cytochrome *c* Inactivation in *Shewanella oneidensis* MR-1. *ChemElectroChem 1*, 2000–2006.

(43) Ross, D. E., Flynn, J. M., Baron, D. B., Gralnick, J. A., and Bond, D. R. (2011) Towards electrosynthesis in *Shewanella*: Energetics of reversing the Mtr pathway for reductive metabolism. *PLoS One 6*, 1–9.

(44) Zhang, P., Liu, J., Qu, Y., and Feng, Y. (2017) Enhanced *Shewanella oneidensis* MR-1 anode performance by adding fumarate in microbial fuel cell. *Chemical Engineering Journal 328*, 697–702.

(45) Myers, C. R., and Myers, J. M. (1997) Cloning and Sequence of *cymA*, a Gene Encoding a Tetraheme Cytochrome *c* Required for Reduction of Iron(III), Fumarate, and Nitrate by *Shewanella putrefaciens* MR-1. *J Bacteriol 179*, 1143–1152.

(46) Kees, E. D., Pendleton, A. R., Paquete, C. M., Arriola, M. B., Kane, A. L., Kotloski, N. J., Intile, P. J., and Gralnick, J. A. (2019) Secreted Flavin Cofactors for Anaerobic

Respiration of Fumarate and Urocanate by *Shewanella oneidensis*: Cost and Role. *Appl Environ Microbiol 85*, 1–12.

(47) Edwards, M. J., White, G. F., Butt, J. N., Richardson, D. J., and Clarke, T. A. (2020) The Crystal Structure of a Biological Insulated Transmembrane Molecular Wire. *Cell 181*, 665–673.

(48) Hartshorne, R. S., Jepson, B. N., Clarke, T. A., Field, S. J., Fredrickson, J., Zachara, J., Shi, L., Butt, J. N., and Richardson, D. J. (2007) Characterization of *Shewanella oneidensis* MtrC: A cell-surface decaheme cytochrome involved in respiratory electron transport to extracellular electron acceptors. *Journal of Biological Inorganic Chemistry 12*, 1083–1094.

(49) Ross, D. E., Brantley, S. L., and Tien, M. (2009) Kinetic characterization of OmcA and MtrC, terminal reductases involved in respiratory electron transfer for dissimilatory iron reduction in *Shewanella oneidensis* MR-1. *Appl Environ Microbiol 75*, 5218–5226.

(50) Coursolle, D., and Gralnick, J. A. (2010) Modularity of the Mtr respiratory pathway of *Shewanella oneidensis* strain MR-1. *Mol Microbiol 77*, 995–1008.

(51) Rowe, A. R., Salimijazi, F., Trutschel, L., Sackett, J., Adesina, O., Anzai, I., Kugelmass, L. H., Baym, M. H., and Barstow, B. (2021) Identification of a pathway for electron uptake in *Shewanella oneidensis*. *Commun Biol 4*, 1–10.

(52) Xiao, X., Li, C. X., Peng, J. R., Fan, Y. Y., and Li, W. W. (2023) Dynamic roles of inner membrane electron-transfer hub of *Shewanella oneidensis* MR-1 in response to extracellular reduction kinetics. *Chemical Engineering Journal 451*.

(53) Flynn, J. M., Ross, D. E., Hunt, K. A., Bond, D. R., and Gralnick, J. A. (2010) Enabling Unbalanced Fermentations by Using Engineered Electrode-Interfaced Bacteria. *mBio 1*, 1–8.

(54) TerAvest, M. A., Rosenbaum, M. A., Kotloski, N. J., Gralnick, J. A., and Angenent, L. T. (2014) Oxygen allows *Shewanella oneidensis* MR-1 to overcome mediator washout in a continuously fed bioelectrochemical system. *Biotechnol Bioeng 111*, 692–699.

(55) Jensen, H. M., TerAvest, M. A., Kokish, M. G., and Ajo-Franklin, C. M. (2016) CymA and Exogenous Flavins Improve Extracellular Electron Transfer and Couple It to Cell Growth in Mtr-Expressing *Escherichia coli*. *ACS Synth Biol 5*, 679–688.

(56) Von Canstein, H., Ogawa, J., Shimizu, S., and Lloyd, J. R. (2008) Secretion of flavins by *Shewanella* species and their role in extracellular electron transfer. *Appl Environ Microbiol 74*, 615–623.

(57) Edel, M., Sturm, G., Sturm-Richter, K., Wagner, M., Ducassou, J. N., Couté, Y., Horn, H., and Gescher, J. (2021) Extracellular riboflavin induces anaerobic biofilm formation in *Shewanella oneidensis*. *Biotechnol Biofuels 14*, 1–14.

(58) Bao, H., Zheng, Z., Yang, B., Liu, D., Li, F., Zhang, X., Li, Z., and Lei, L. (2016) In situ monitoring of *Shewanella oneidensis* MR-1 biofilm growth on gold electrodes by using a Pt microelectrode. *Bioelectrochemistry 109*, 95–100.

(59) Choi, S., Kim, B., and Chang, I. S. (2018) Tracking of *Shewanella oneidensis* MR-1 biofilm formation of a microbial electrochemical system via differential pulse voltammetry. *Bioresour Technol 254*, 357–361.

(60) Kees, E. D., Levar, C. E., Miller, S. P., Bond, D. R., Gralnick, J. A., and Dean, A. M. (2021) Survival of the first rather than the fittest in a *Shewanella* electrode biofilm. *Commun Biol 4*, 1–9.

(61) Zhang, Y. T., Zhang, Y., and Peng, L. (2021) Electrochemical fluorescence microscopy reveals insignificant long-range extracellular electron transfer in *Shewanella oneidensis* anodic processes. *Electrochim Acta 398*, 1–7.

(62) Xiao, Y., Zhang, E., Zhang, J., Dai, Y., Yang, Z., Christensen, H. E. M., Ulstrup, J., and Zhao, F. (2017) Extracellular polymeric substances are transient media for microbial extracellular electron transfer. *Sci Adv 3*, 1–8.

(63) Sturm, G., Richter, K., Doetsch, A., Heide, H., Louro, R. O., and Gescher, J. (2015) A dynamic periplasmic electron transfer network enables respiratory flexibility beyond a thermodynamic regulatory regime. *ISME Journal 9*, 1802–1811.

(64) Fonseca, B. M., Paquete, C. M., Neto, S. E., Pacheco, I., Soares, C. M., and Louro, R. O. (2013) Mind the gap: Cytochrome interactions reveal electron pathways across the periplasm of *Shewanella oneidensis* MR-1. *Biochemical Journal 449*, 101–108.

(65) Delgado, V. P., Paquete, C. M., Sturm, G., and Gescher, J. (2019) Improvement of the electron transfer rate in *Shewanella oneidensis* MR-1 using a tailored periplasmic protein composition. *Bioelectrochemistry 129*, 18–25.

(66) Meshulam-Simon, G., Behrens, S., Choo, A. D., and Spormann, A. M. (2007) Hydrogen metabolism in *Shewanella oneidensis* MR-1. *Appl Environ Microbiol 73*, 1153–1165.

(67) Shi, L., Belchik, S. M., Plymale, A. E., Heald, S., Dohnalkova, A. C., Sybirna, K., Bottin, H., Squier, T. C., Zachara, J. M., and Fredrickson, J. K. (2011) Purification and characterization of the [NiFe]-Hydrogenase of *Shewanella oneidensis* MR-1. *Appl Environ Microbiol 77*, 5584–5590.

(68) Joshi, K., Kane, A. L., Kotloski, N. J., Gralnick, J. A., and Bond, D. R. (2019) Preventing Hydrogen Disposal Increases Electrode Utilization Efficiency by *Shewanella oneidensis*. *Front Energy Res 7*, 95.

(69) Sun, W., Lin, Z., Yu, Q., Cheng, S., and Gao, H. (2021) Promoting Extracellular Electron Transfer of *Shewanella oneidensis* MR-1 by Optimizing the Periplasmic Cytochrome *c* Network. *Front Microbiol 12*, 1–13.

(70) Myers, C. R., and Nealson, K. H. (1988) Bacterial manganese reduction and growth with manganese oxide as the sole electron acceptor. *Science Science 240*, 1319–1321.

(71) Rowe, A. R., Rajeev, P., Jain, A., Pirbadian, S., Okamoto, A., Gralnick, J. A., El-Naggar, M. Y., and Nealson, K. H. (2018) Tracking electron uptake from a cathode into *Shewanella* cells: Implications for energy acquisition from solid-substrate electron donors. *mBio 9*.

(72) Gao, H., Barua, S., Liang, Y., Wu, L., Dong, Y., Reed, S., Chen, J., Culley, D., Kennedy, D., Yang, Y., He, Z., Nealson, K. H., Fredrickson, J. K., Tiedje, J. M., Romine, M. F., and Zhou, J. (2010) Impacts of *Shewanella oneidensis c*-type cytochromes on aerobic and anaerobic respiration. *Microb Biotechnol 3*, 455–466.

(73) Wickham, H. (2016) ggplot2: Elegant Graphics for Data Analysis. Springer-Verlag New York. ISBN 978-3-319-24277-4, https://ggplot2.tidyverse.org.

(74) Wickham, H., François, R., and Henry, L. (2020) dplyr: A Grammar of Data Manipulation. https://dplyr.tidyverse.org, https://github.com/tidyverse/dplyr.

(75) Kassambara, A. (2023) ggpubr:“ggplot2” based publication ready plots. *https://CRAN.R-project.org/package=ggpubr 438*.

(76) Wickham, H., and Wickham, M. H. (2011) The Split-Apply-Combine Strategy for Data Analysis. *J Stat Softw 40*, 1–29.

(77) Dowle, M., Srinivasan, A., Gorecki, J., Chirico, M., Stetsenko, P., Short, T., Lianoglou, S., Antonyan, E., Bonsch, M., and Parsonage, H. (2019) data.table: Extension of “data.frame.” *https://CRAN.R-project.org/package=data.table 596*.

(78) Wickham, H. (2022) stringr: Simple, Consistent Wrappers for Common String Operations. *http://stringr. tidyverse. org, https://github. com/tidyverse/stringr*.

(79) Sprouffske, K., and Wagner, A. (2016) Growthcurver: an R package for obtaining interpretable metrics from microbial growth curves. *BMC Bioinformatics 17*, 1–4.

APPENDIX B: Supplementary Figures for Chapter 3

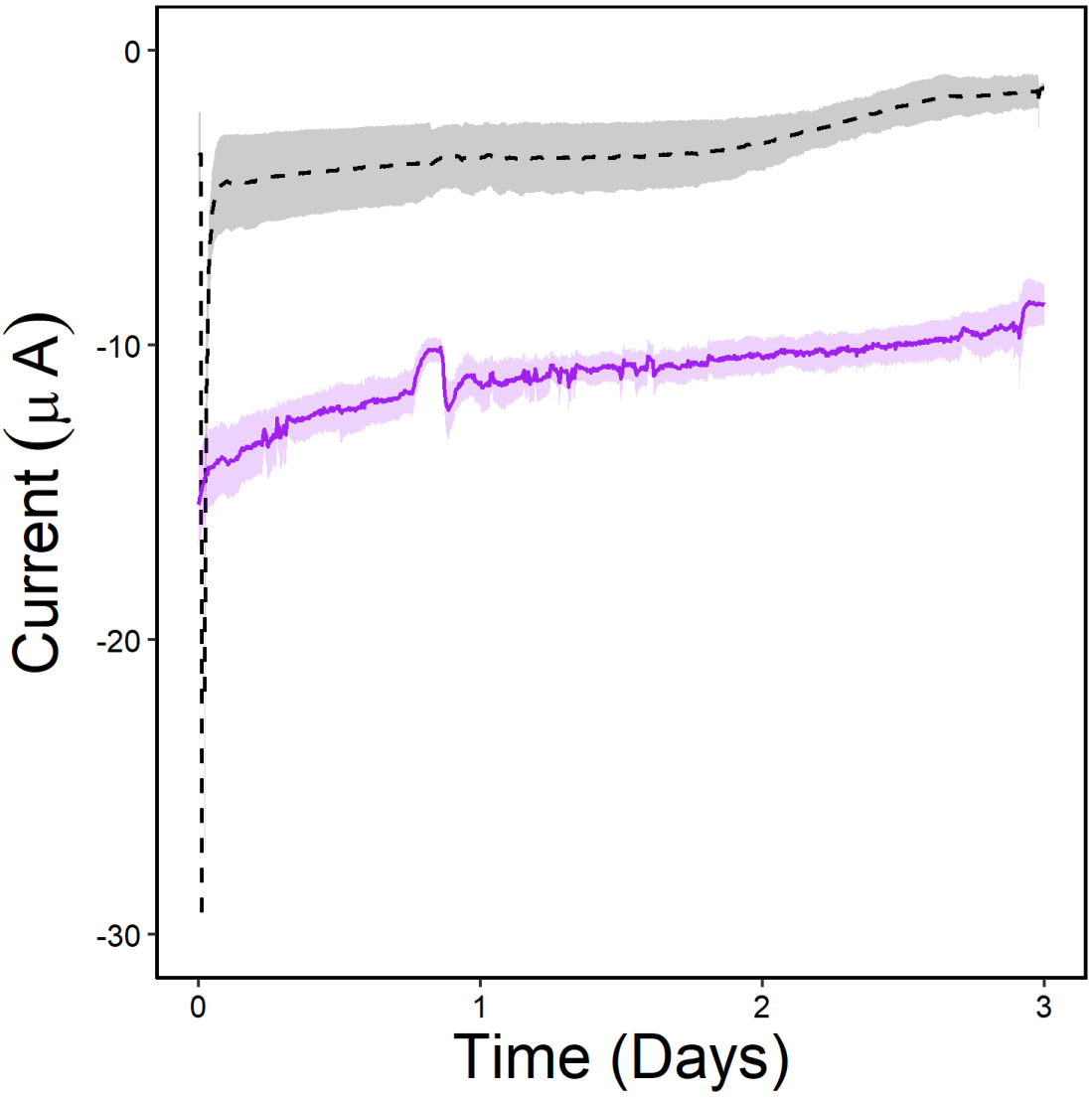

Figure S3.1 Abiotic current with and without exogenous flavins. Current generation in abiotic BES experiments with (purple) or without (black) the addition of 1 μM RF. Lines and error bars represent mean and standard error, respectively (n=3).

Chapter 4: Flux Balance Analysis and Mobile CRISPRi guided deletion of a conditionally essential gene in *Shewanella oneidensis* MR-1

Kathryne C. Ford[1,2], Joshua A.M. Kaste[1,3], Yair Shachar-Hill[3], Michaela A. TerAvest[1]*

[1]Department of Biochemistry and Molecular Biology, Michigan State University, East Lansing, MI, 48824, USA

[2]Department of Microbiology and Molecular Genetics, Michigan State University, East Lansing, MI, 48824, USA

[3]Department of Plant Biology, Michigan State University, East Lansing, MI, 48824, USA

This chapter is adapted from a publication in ASC Synthetic Biology

4.1 Abstract

Carbon neutral production of valuable bioproducts is critical to sustainable development but remains limited by the slow engineering of photosynthetic organisms. Improving existing synthetic biology tools to engineer model organisms to fix carbon dioxide is one route to overcoming the limitations of photosynthetic organisms. In this work, we describe a pipeline that enabled deletion of a conditionally essential gene from the *Shewanella oneidensis* MR-1 genome. *S. oneidensis* is a simple bacterial host that could be used for electricity-driven conversion of carbon dioxide in the future with further genetic engineering. We used Flux Balance Analysis (FBA) to model carbon and energy flows in central metabolism and assess the effects of single and double gene deletions. We modeled the growth of deletion strains under several alternative conditions to identify substrates that restore viability to an otherwise lethal gene knockout. These predictions were tested *in vivo* using a Mobile-CRISPRi gene knockdown system. The information learned from FBA and knockdown experiments informed our strategy for gene deletion, allowing us to successfully delete an 'expected essential' gene, *gpmA*. FBA predicted, knockdown experiments supported, and deletion confirmed that the 'essential' gene *gpmA* is not needed for survival, dependent on the medium used. Removal of *gpmA* is a first step towards driving electrode powered CO_2 fixation via RuBisCO. This work demonstrates the potential for broadening the scope of genetic engineering in *S. oneidensis* as a synthetic biology chassis. By combining computational analysis with a CRISPRi knockdown system in this way, one can systematically assess the impact of conditionally essential genes and use this knowledge to generate mutations previously thought unachievable.

4.2 Introduction

Mounting challenges associated with anthropogenic carbon emissions have led researchers to investigate microbial engineering solutions to capture carbon dioxide (CO_2). Additionally, bacterial products made from fixed CO_2 represent a carbon-neutral platform for generation of biofuels and chemicals. To achieve these goals, researchers employ an ever-expanding list of genetic engineering techniques to rewire microbial central carbon metabolism. These include broad approaches such as expression vectors and inhibitors, to specific genetic modifications like gene deletions and site-directed mutagenesis[1,2]. The latter can be an arduous task, depending on the organism and target site. Synthetic biology workhorse organisms like *Escherichia coli* and *Saccharomyces cerevisiae* have been studied extensively in the context of rewiring central carbon metabolism for the purposes of carbon capture and bioproduction[3–12]. As such, they come with a substantial genetic toolkit and mutant libraries (e.g., the Keio Collection)[13,14] that allow quick and easy genome modifications. A prominent example relevant to this work is the development of a complete CO_2 fixation pathway in *E. coli*[15–17]*.* In their work, Antonovsky et al. utilized a combination of Flux Balance Analysis (FBA), phage transduction of mutations in the Keio Collection, heterologous protein expression, and laboratory evolution to develop a CO_2-fixing strain. This highlights the fact that even in well-understood bacterial species, bioengineering is typically much harder *in vivo* than on paper. When applying these strategies to non-model organisms with a less extensive investigative history, it can be more difficult to create the desired mutations. Here, we combined flux-balance analysis (FBA) and a CRISPRi gene knockdown system as a pipeline for troubleshooting difficult mutations and enabling

deletion of conditionally essential genes. Specifically, this was done in the electroactive bacteria *Shewanella oneidensis* MR-1 for the deletion of the gene *gpmA*. Creation of this mutant demonstrates the capacity of this approach to expand the scope of feasible genetic alterations.

S. oneidensis MR-1 is a γ-proteobacterium commonly used in biotechnology research due to its genetic tractability and diverse metabolism[18]. It is a Gram-negative, facultative anaerobe that contains an extracellular electron transfer pathway (the Mtr pathway) that enables it to use extracellular metal oxides and electrodes as electron acceptors for respiration[19–21]. The Mtr pathway can also be reversed, expanding the potential for catalyzing electrode-driven carbon reduction[22–24]. A major benefit of using an electrode as an electron donor during bioproduction is the ability to use renewable energy, such as wind or solar, to power the reduction of CO_2, eliminating the need for exogenous chemical electron donors[25,26]. Another benefit of using *S. oneidensis* is that previous research has demonstrated that *S. oneidensis'* central carbon metabolism can be altered to grow on carbon substrates it cannot natively use, such as glucose[27–29]. *S. oneidensis*' preferred carbon source is D,L-lactate, which is converted to pyruvate via lactate dehydrogenases (Ldh, Dld, Lld)[30–32]. In wild-type (WT) *S. oneidensis*, this pyruvate is used both to generate reducing power and ATP via oxidation by the TCA cycle and for gluconeogenesis and other biomass-building processes. A key reaction that connects these processes is catalyzed by the enzyme phosphoglycerate mutase (Gpm)[33] (**Figure 4.1**).

In this work, we sought to separate energy production and biomass synthesis in *S. oneidensis* as a first step toward rewiring it for carbon fixation through deletion of

gpmA. This would enable future repurposing of the existing gluconeogenesis machinery into a carbon-fixing Calvin-Benson Cycle (CBC), as was previously done in a Δ*gpmAM* mutant of *E. coli*[15–17]. However, before any carbon fixing pathway could be constructed, there were significant challenges associated with *gpmA* deletion in *S. oneidensis* MR-1. Deutschbauer et al. previously classified *gpmA* as 'essential' based on Flux Balance Analysis (FBA) and a lack of transposon insertion mutants in *gpmA* when the library was generated in LB medium[34,35]. However, Gpm (*gpmAM*) is not essential in *E. coli*, and *E. coli* Δ*gpmAM* mutants can grow in LB or minimal medium when two carbon sources are provided, one entering metabolism 'above' the Gpm reaction and one entering 'below.' This led us to hypothesize that *gpmA* was only conditionally essential in *S. oneidensis*. However, initial attempts to create a knockout using a common sucrose counter selection protocol were unsuccessful[21,36]. To overcome this pitfall, we adapted existing technologies to enable systematic modeling and testing of different growth media. Because the target gene participates in carbon metabolism, we hypothesized that this pipeline would reveal optimized conditions that allow the survival of *gpmA* mutants. We used FBA to predict conditions that would enable an *S. oneidensis* Δ*gpmA* strain to grow and implemented a CRISPRi gene knockdown system for characterization of *gpmA* in *S. oneidensis*[37,38]. In combination, *in silico* modeling and systematic testing of phenotypic responses of gene knockdown in different media enabled deletion of a gene thought to be essential.

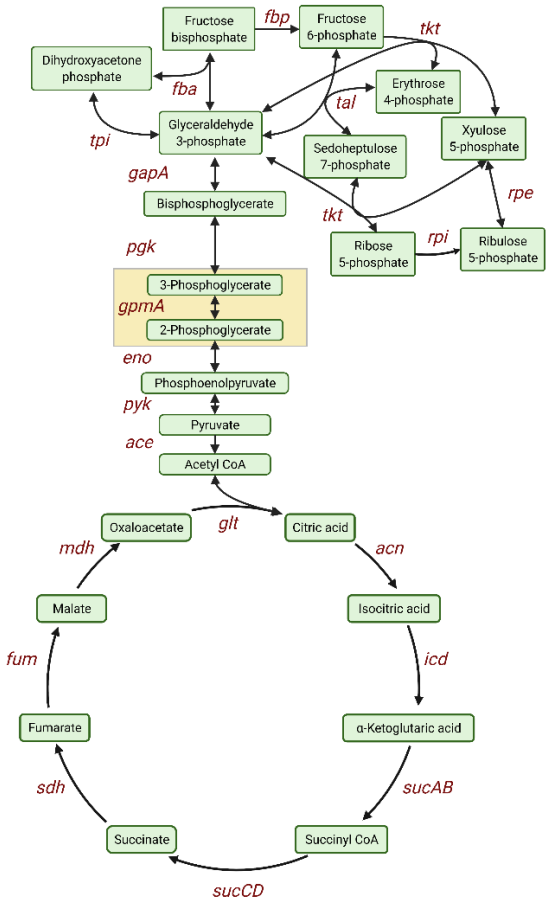

Figure 4.1 Central carbon metabolism of *S. oneidensis* MR-1. Metabolites are shown in green boxes, and the genes encoding the proteins which catalyze enzymatic reactions (black arrows) are shown in red. This schematic comprises components of glycolysis, the pentose phosphate pathway, and the TCA cycle. The targeted reaction catalyzed by the product of *gpmA* is in the yellow box. Gene names listed in red are as annotated in NCBI for *S. oneidensis* genome (NCBI:txid211586).

4.3 Results

We initially attempted to delete *gpmA* from the *S. oneidensis* genome using a homologous recombination method that is widely used for this organism[21,36,39–41]. Briefly, sequences homologous to regions upstream and downstream of *gpmA* were cloned into a non-replicating vector containing an antibiotic selection gene and *sacB*, then conjugated into *S. oneidensis* where it inserted into the genome at the *gpmA* locus to create primary integrants. A second homologous recombination event was enabled

by growth without antibiotic, and we selected for cells that had resolved the vector out of the genome by plating on 10% sucrose. The resulting colonies were screened for *gpmA* deletion or reversion to WT. Initial efforts were not successful, and all colonies (~300) screened after plasmid resolution were WT revertants. However, because *gpmA* could be deleted from *E. coli* and the mutant grew well when provided with separate energy and sugar backbone sources, we explored whether a two-substrate strategy would enable *gpmA* deletion in *S. oneidensis.*

We used FBA to model the maximum theoretical specific growth rate (i.e., the growth potential [h^{-1}]) of a WT strain and a Δ*gpmA* strain under a range of single- and double-carbon source conditions. To do this, we used FBA optimization functions built into the COBRA Toolbox[42] and applied them to an existing model of *S. oneidensis* metabolism[43]. Based on previous work[15,16], we hypothesized that a Δ*gpmA* strain would require two carbon sources, with one entering metabolism 'above' and one entering 'below' the *gpmA* deletion (**Figure 4.1**). We chose nucleosides (adenosine, inosine, and uridine) as three 'upper' carbon sources and lactate as the model 'lower' carbon source to model a strain grown in M5 Minimal Medium[44]. These carbon sources were chosen because they are known substrates for *S. oneidensis*[39,45,46], which does not typically grow using sugars such as glucose, but is capable of robust growth on nucleosides[47–51]. As expected, we observed that a WT strain had a non-zero predicted growth potential in all the tested conditions, including single substrates (**Table 4.1**). In contrast, FBA analysis of the Δ*gpmA* strain showed zero growth potential when provided only lactate. Notably, the Δ*gpmA* strain showed non-zero growth potential only when supplemented with a carbon source entering 'above' *gpmA*, alone or in addition to lactate.

Table 4.1 Calculated growth potential of *S. oneidensis* MR-1 WT and Δ*gpmA* strains with different substrates Flux balance analysis was used to determine the effect of *gpmA* deletion on the growth potential of *S. oneidensis*. The predicted specific growth rate was calculated for WT and Δ*gpmA* cells grown in M5 medium with fixed uptake rates for either solely lactate, adenosine, inosine, uridine, or in combination.

Strain	Carbon	Growth Potential (h^{-1})
WT	Lactate	0.533
	Adenosine	0.543
	Lactate + Adenosine	1.093
	Inosine	0.547
	Lactate + Inosine	1.103
	Uridine	0.549
	Lactate + Uridine	1.105
Δ*gpmA*	Lactate	0
	Adenosine	0.526
	Lactate + Adenosine	1.079
	Inosine	0.530
	Lactate + Inosine	1.089
	Uridine	0.534
	Lactate + Uridine	1.092

We next used a CRISPRi-based gene knockdown method to experimentally evaluate the predictions of the FBA. In this system, a catalytically inactive dCas9 protein and a small guide RNA (sgRNA) targeting the gene of interest are chromosomally expressed under an isopropyl ß-D-1-thiogalactopyranoside (IPTG)-inducible promoter. The 20 bp tag on the sgRNA binds immediately downstream of the start codon on the gene of interest, and the dCas9 then binds to the sgRNA to prevent transcription[37,38]. Strains of *S. oneidensis* expressing the inducible dCas9 and gene-targeting sgRNA were pre-grown in Lysogeny Broth (LB), then plated on LB + 10 mM IPTG. We constructed three strains with this system, with sgRNA targeting either *gpmA, rpoC* (essential gene control), or no target (negative control). During growth on LB with

inducer, the strain with a *gpmA*-targeting sgRNA showed a severe growth defect compared to growth on LB without IPTG, similar to a strain with a *rpoC*-targeting sgRNA (**Figure 4.2**). In contrast, when the growth medium was supplemented with uridine and lactate, the *gpmA* knockdown strain survived similarly to the non-targeting sgRNA control, although it took longer for colonies to develop (24 hours) compared to WT (16 hours) (**Figure 4.3**).

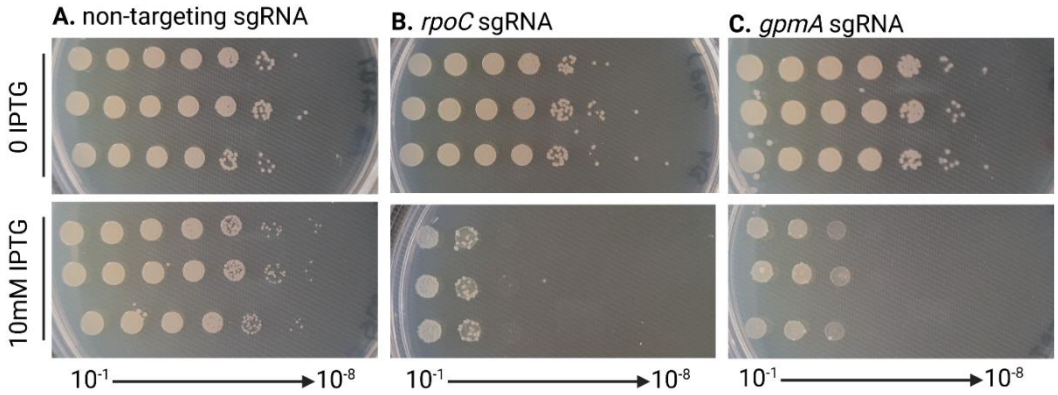

Figure 4.2 CRISPRi gene knockdown in *S. oneidensis* MR-1. Strains of *S. oneidensis* MR-1 were constructed to chromosomally express dCas9 and sgRNA targeting (A) nothing (non-essential gene control), (B) *rpoC* (essential gene control), or (C) *gpmA*. Both the dCas9 and sgRNA are under ITPG induction. Strains were pre-grown in LB + selection at 30^{o}C. 3ul of serial ten-fold dilutions of a 1.0 OD_{600} cell suspension were plated on LB +/- inducer (10 mM IPTG) as described in Materials and Methods. Each panel shows replicate (n=3) plating of each strain.

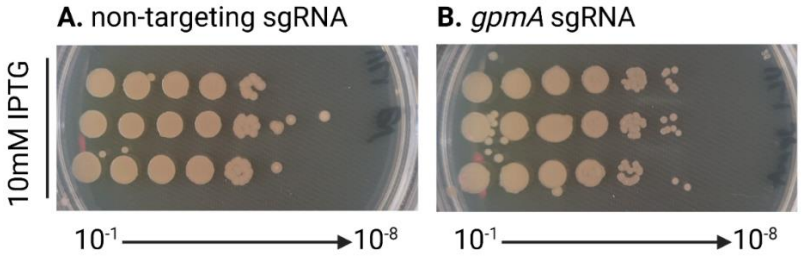

Figure 4.3 CRISPRi knockdown of genes in *S. oneidensis* MR-1 with supplemented media. Previously constructed strains of MR-1, with sgRNA targeting either nothing (A) or *gpmA* (B), were pre-grown as before. This time, strains were plated on LB + 10mM IPTG supplemented with 10mM uridine and 20mM lactate. The growth rate of the *gpmA* knockdown was restored to WT-levels under these conditions. Each panel shows replicate (n=3) plating of each strain.

Based on FBA and knockdown results suggesting that *gpmA* is non-essential when an upper carbon source and a lower carbon source are provided simultaneously, we repeated the gene deletion protocol and included 10 mM uridine and 20 mM lactate in the LB. In this iteration, a Δ*gpmA* strain was obtained (**Figure 4.4A**). Of the 50 colonies screened, 23 of them were Δ*gpmA,* 13 were WT revertants, and 14 failed to resolve out the vector. We grew the resulting Δ*gpmA* strain and WT cells in LB in a 96-well plate at 30°C with shaking and observed that the mutant had a severe growth defect (WT = 0.17 h^{-1}, Δ*gpmA* = 0.08 h^{-1}).

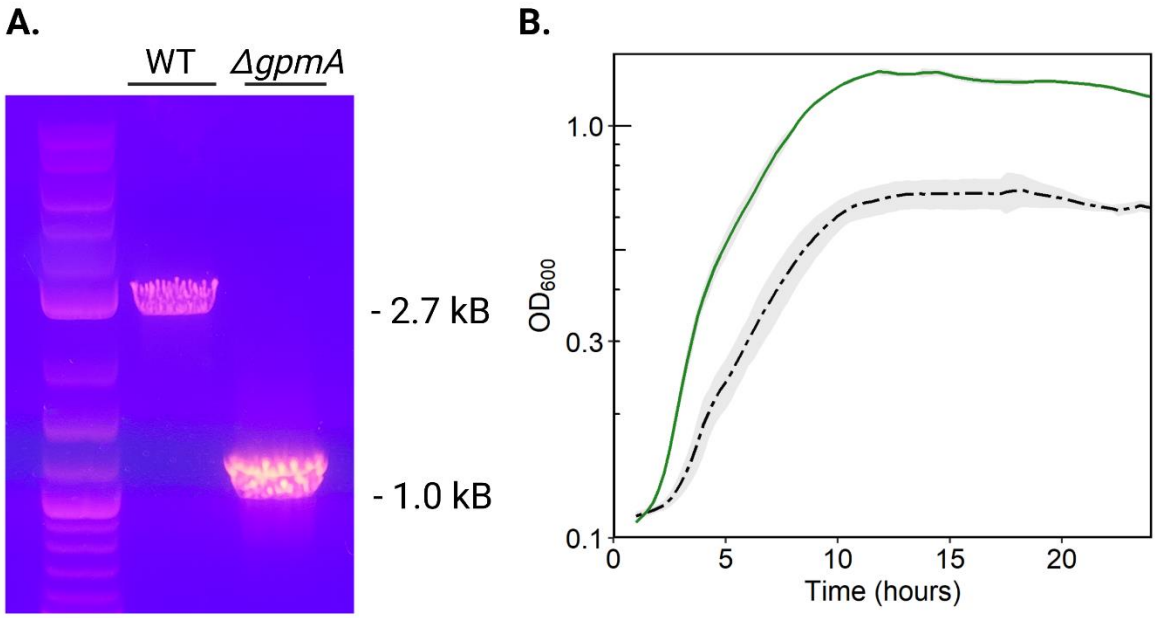

Figure 4.4 Identification and Aerobic growth of *S. oneidensis* WT vs. Δ*gpmA* cells in LB. (A) PCR amplification of the *gpmA* locus from WT *S. oneidensis* MR-1 and a *gpmA* deletion strain obtained by homologous recombination under modified conditions. Primers were located approximately 500 bp upstream and downstream of the coding region of the 1.7 kb gene. (B) Overnight cultures were used to inoculate 500 µl of LB in a 48-well plate for a starting OD_{600} of 0.1 in the wells. The plate was incubated with constant shaking at 30˚C in an aerobic plate reader, reading the OD_{600} every 15 mins. Lines represent the simple moving average of three biological replicates for WT cells (green, solid) and Δ*gpmA* cells (black, dashed), and grey ribbons represent standard deviation.

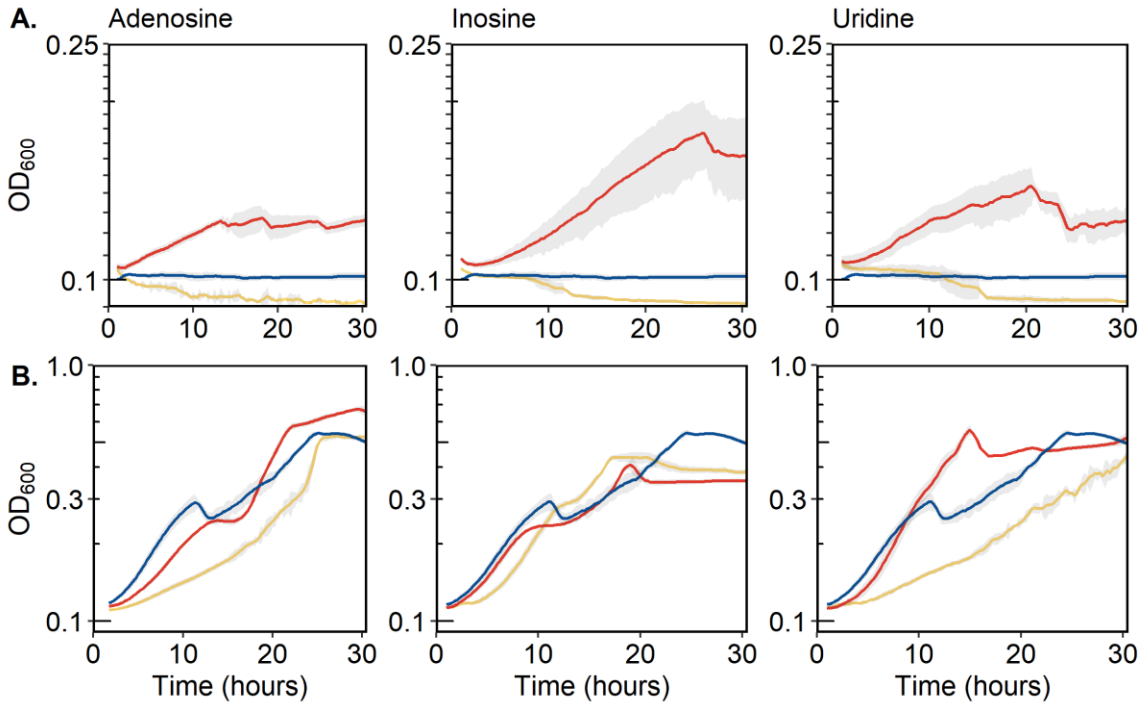

Figure 4.5 Experimental confirmation of growth capabilities of Δ*gpmA* cells grown in minimal medium with various substrates. M5 medium was prepared as described in the Materials and Methods. Growth of **(A)** Δ*gpmA***,** and **(B)** WT with lactate (blue), the designated nucleoside (yellow), or a combination of the two (red) (lactate results are repeated in each graph). The Δ*gpmA* cultures were grown overnight aerobically in LB at 30°C. Cells were normalized to an OD_{600} of 1.0 and 500 µl of each was inoculated into the M5 medium in a 48-well plate. The plate was incubated with constant shaking at 30°C in a plate reader, measuring the OD_{600} every 15 mins. Lines represent the simple moving average of three biological replicates, and grey ribbons represent the standard deviation.

We next measured growth of the mutant strain with the substrate combinations that were assessed by FBA. WT and Δ*gpmA* cultures were pre-grown in LB and washed with minimal medium with no carbon substrate or casamino acids. Cells were resuspended to an OD_{600} of 0.1 in M5 with either a single substrate or a combination of two substrates and incubated with shaking at 30°C. The Δ*gpmA* cells did not grow with any single substrate but did grow when provided two substrates (**Figure 4.5A**) while the WT culture grew under all conditions (**Figure 4.5B**). The highest final cell density of the Δ*gpmA* culture was observed with the combination of D,L-lactate and inosine. Cultures

provided solely nucleosides saw a decrease in OD_{600} while those provided D,L-lactate remained relatively stable at the starting density. This may be due to a small of amount of D,L-lactate being metabolized for energy but not for biomass, while nucleosides could not support any metabolic activity.

4.4 Discussion

Using computationally guided methods, we deleted *gpmA* from the *S. oneidensis* genome although it was previously classified as essential. We hypothesized that two carbon sources would be required to enable the Δ*gpmA* strain to grow based on previous results with *E. coli* and the FBA for *S. oneidensis* (**Figure 4.6**)[34]. While our experiments agreed with most FBA predictions, the model predicted that the Δ*gpmA* cells would grow solely on nucleoside substrates that enter metabolism 'above' GpmA. However, we observed experimentally that nucleosides alone did not support growth of the Δ*gpmA* strain. We hypothesize that this discrepancy was caused by unrealistic pathway flexibility in the model. Specifically, the predicted growth of Δ*gpmA* on nucleosides alone relied on conversion of 3-phosphoglycerate to serine, which was broken down to pyruvate that could be used in the TCA cycle. However, the required flux through this workaround pathway was ~10-fold higher than in the WT model and is likely infeasible *in vivo* without overexpression of the enzymes involved. Thus, *gpmA* deletion functionally blocks nucleosides from being fully oxidized although there were possible workarounds in the metabolic model. Therefore, even though the model predicts growth on nucleosides, we did not observe this outcome due to the energy limitations imposed by the cutoff of the TCA cycle and by extension, ATP generation by oxidative phosphorylation. In future work, this issue could be addressed through

refinement of the model through the inclusion of proteomic and transcriptomic data to better represent energy acquisition in cells during growth.

The inspiration for the project was to develop of a CO_2 fixing strain of *S. oneidensis* using a similar method to Antonovsky et a[15]l., however, crucial differences from *E. coli* created significant challenges. Specifically, *gpmA* deletion was difficult in *S. oneidensis* and this gene was classified as essential[34]. We utilized a gene knockdown system called ‘mobile CRISPRi’ to evaluate FBA predictions of conditions that would enable growth of a *gpmA* knockout strain. On LB, the phenotype for a *gpmA*-targeting sgRNA was comparable to that of an sgRNA targeting the essential gene *rpoC* (10^5-fold decrease in fitness), supporting the hypothesis that *gpmA* is essential for growth on LB. This explains why the transposon library used by Deutschbauer et al., did not contain any *gpmA* mutants, because the library was generated on LB[52]. Indeed, even an improved library preparation protocol starting with over 39,000 transposon mutants did not yield a *gpmA* disruption, likely because this method also generated the library on LB[53]. While transposon library sequencing is an immensely informative technique for genome annotation and fitness analysis, our results highlight the biases introduced by the library-generation conditions. The CRISPRi knockdown system utilized in this work could be a powerful tool towards expanding our knowledge of gene functionality built on the foundations created by transposon libraries. Namely, complementation of transposon mutagenesis libraries with CRISPRi knockdown libraries will enable high-throughput characterization of conditionally essential genes[38].

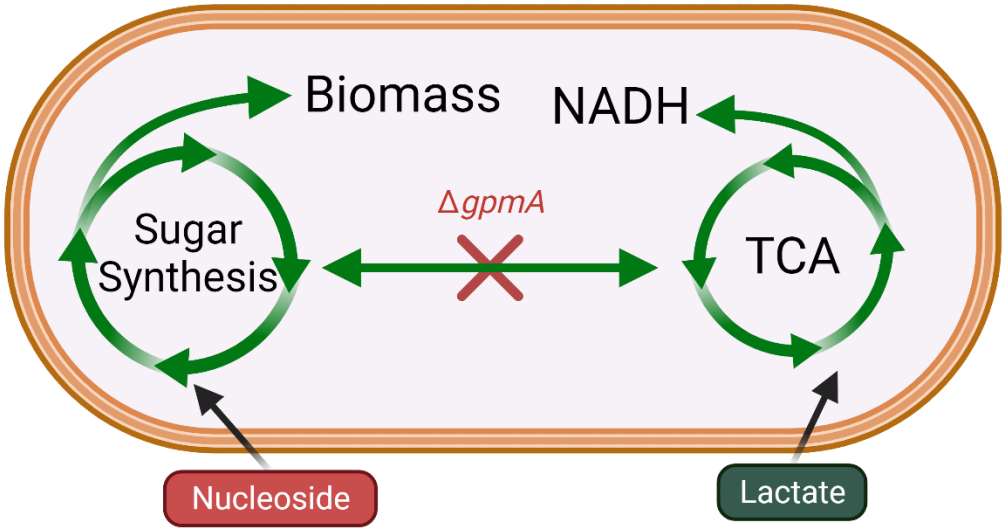

Figure 4.6 Metabolic strategy of MR-1 Δ*gpmA* cells. With the deletion of *gpmA*, metabolites entering the cell as a TCA cycle intermediate are cutoff from entering glycolysis to build biomass, and vice versa. To satisfy the cell requirements for growth, MR-1 Δ*gpmA* requires at least two carbon sources to grow; one entering 'above' *gpmA* to build biomass (nucleoside), and one entering 'below' *gpmA* to acquire energy and reducing equivalents (lactate).

While use of various existing genetic tools is a staple of synthetic biology work, there are gaps in the prospective scope of their implementation, such as using them for deletion of genes classified as essential. Through this work, we have devised a means to generate such a novel deletion. This both expands the bounds of potential synthetic biology applications in *S. oneidensis* and paves the way for development of a CO_2 fixing strain. Because the Δ*gpmA* mutant requires a sugar source, it can form the basis for laboratory evolution experiments to activate a heterologous pCBB pathway during growth with limiting sugar, as previously demonstrated by Antonovsky et al[15].

The pipeline developed here can be used to predict and characterize the potential phenotypes associated with deletion of conditionally essential genes, thereby informing strategies to construct the deletions. The use of FBA and CRISPRi analysis is a modular system that uses existing models and genetic tools and has high adaptability to

work in other common laboratory microorganisms. To our knowledge, this is the first instance of using these specific systems to generate difficult or otherwise infeasible gene deletions. This capability is especially useful for probing the effects of genes that are essential under typical laboratory conditions and opens the door to exploring the phenotypes of gene deletions previously thought to be lethal. Biotechnology research relies on the ability to manipulate microorganisms' genomes to perform a specific task, such as engineering carbon fixation in heterotrophs. Expanding our toolkit to include deletion of conditionally essential genes is a crucial step to achieving these goals.

4.5 Materials and Methods

Strains and Culture Media

Table 4.2 Strains and plasmids used in this study

Strain or Plasmid	Description	Source
E. coli		
WM3064	Cloning and conjugation strain for *S. oneidensis, dap-*	
WM6026	sJMP2644 – Tn7 Transposase donor strain, contains pJMP1039, *dap-*	Peters 2019
BW25141	sJMP2846 – CRISPRi transposon donor strain used for cloning sgRNA, contains pJMP2846	Peters 2019
S. oneidensis		
MR-1	Wild type	Meyers and Nealson, 1988
Δ*gpmA*	Mutant with gene deletion of *gpmA*	This study
sgRNA-*gpmA*	MR-1 strain containing the CRISPRi knockdown vector targeting *gpmA* (pJMP2846-*gpmA*)	This study
sgRNA-*rpoC*	MR-1 strain containing the CRISPRi knockdown vector targeting *rpoC* (pJMP2846-*rpoC*)	This study
sgRNA-EV	MR-1 strain containing the CRISPRi knockdown vector targeting no genes (pJMP2846)	This study
Plasmids		
pJMP1039	Tn7 transposase donor vector, amp^R	Peters 2019
pJMP2846	CRISPRi transposon donor plasmid, used for cloning sgRNA, kan^R	Peters 2019
pJMP2846-*gpmA*	CRISPRi transposon donor plasmid, knocks down *gpmA*	This study

Table 4.2 (cont'd)

pJMP2846-*rpoC*	CRISPRi transposon donor plasmid, knocks down *rpoC*	This study
pSMV3.0	Deletion vector, Kan^R, *sacB*	Saltikov and Newman 2003

Table 4.3 Primers used for making in-frame deletion mutants and CRISPRi knockdowns

	Primer	Primer Sequence
Deletions		
gpmA	FO	ACGAGGTCATGCCAGCATTGCA
	RO	GCACTTGTTGCTCGGCCATCAA
CRISPRi - knockdown		
gpmA	FWD	TAGTTCGAGGATCAACAACGCGAT
	REV	AAACATCGCGTTGTTGATCCTCGA
rpoC	FWD	TAGTGACCAAGAACGGATCAGATC
	REV	AAACGATCTGATCCGTTCTTGGTC

Strains and plasmids used are listed in Table 4.2 and primers in Table 4.3. This work was done in *Shewanella oneidensis* MR-1 and using *Escherichia coli* WM3064, WM6026, and BW25141 for plasmid construction and conjugation. Strains were grown using LB for growth curves and supplemented with 30 mM diaminopimelic acid (DAP), 50 μg/mL kanamycin (Kan) or 100 μg/mL ampicillin (Amp) as needed for construction of CRISPRi knockdown strains. M5 Minimal Medium (1.29 mM K_2HPO_4, 1.65 mM KH_2PO_4, 7.87 mM NaCl, 1.70 mM NH_4SO_4, 475 μM $MgSO_4 \cdot 7H_2O$, 10 mM HEPES, 1× Wolfe's mineral solution, and 1× Wolfe's vitamin solution), with pH adjusted to 7.2 with NaOH. Casamino acids and riboflavin were not included in the media. M5 medium was supplemented with various carbon sources to final concentrations of: 20mM D,L-lactate and 10mM nucleosides (adenosine, uridine, or inosine). Growth experiments were conducted in either 96- or 48-well plates and OD_{600} was read using an H1M BioTek

Plate Reader. *E. coli* strains were grown at 37°C with shaking, and MR-1 strains were grown at 30°C, with shaking, with a starting OD_{600} of 0.1.

Flux Balance Analysis

The genome-scale model of *S. oneidensis* MR-1's metabolic network was taken from Ong et al[54]. The ATP growth-associated maintenance (GAM) cost was removed from this version of the MR-1 model due to a lack of GAM measurements for other *S. oneidensis* strains that were being compared with MR-1. The GAM was added back in by referring to the information from an earlier iteration of the model[43]. The objective function for all optimizations was the maximization of flux through the model's biomass equation, followed by the minimization of the sum of all fluxes. All optimizations were performed in MATLAB (version 2019a) using the COBRA Toolbox[55] and version 8.1.1 of the Gurobi optimizer[42]. To model carbon utilization, specific uptake rates were set for each substrate, with lactate provided at two times the value (-20 mmol/gDW/hr) of the nucleosides (-10 mmol/gDW/hr) as done *in vivo*.

Design and Assembly of CRISPRi knockdown vectors

A complete list of knockdown vectors assembled are listed in Table 2. pJMP2846 was used as is for an 'empty vector' (EV) control, as it contains the CRISPRi knockdown system, but the sgRNA does not contain the gene-targeting tag. Gene-targeting plasmids were constructed as described in Peters et al. 2019. In short, to target either *gpmA* or *rpoC*, a 20bp region located near the 5' end of the ORF with BsaI generated sticky ends was constructed using annealed oligonucleotides synthesized by Integrated DNA Technologies and cloned into pJMP2846[38]. Target sites were selected using a publicly available script found at https://github.com/traeki/sgrna_design downloaded on

October 9th, 2020. Constructed plasmids were then transferred into MR-1 using a Tn7-based tri-parental mating protocol along with pJMP1039, which expresses the transposase transfer system (pJMP1039)[38]. Matings were re-streaked on LB with Kan plates without DAP to select for growth of MR-1 containing either pJMP2846, pJMP2846-*gpmA*, or pJMP2846-*rpoC.*

CRISPRi Knockdown Analysis

Strains carrying the knockdown vectors were pre-grown in LB with Kan and incubated with shaking for 16 h at 30°C. Overnight cultures were serially diluted in LB from 10^{-1} to 10^{-8} in a 96-well plate. 3 µL of each dilution was plated on LB with Kan or LB with Kan and 10mM IPTG in triplicate. Plates were incubated at 30°C for between 18 and 24 h, colonies were then counted, and plates imaged. When testing growth media to overcome the fitness defect of the sgRNA-*gpmA* knockdown strain, LB plates were additionally supplemented with either 20mM D,L-lactate, 10 mM uridine, or a combination of D,L-lactate and uridine.

Gene Deletion

Gene deletion was conducted as described in Blomfield et al. (1991). In short, two approximately 500bp regions of homology located immediately upstream and downstream of *gpmA* were cloned into the nonreplicating vector pSMV3.0[56]. This vector, containing the sucrose sensitivity gene *sacB,* was inserted into the chromosome at the site of *gpmA*. Cells were pre-grown in LB with Kan, then subcultured into LB without NaCl. After growing for 16 hours, cells were plated on LB without NaCl and with 10% sucrose was used to select cells that had resolved the vector. Resulting colonies were screened via patch plating onto LB with Kan plates then onto LB plates to screen

for colonies that lost resistance associated with pSMV3.0. Colonies that were kanamycin sensitive were screened via colony PCR for sizes corresponding to Δ*gpmA* (1 kB) or WT revertants (2.7 kB) using primers flanking the *gpmA* locus. Suspected mutants were then confirmed via Sanger Sequencing.

4.6 Acknowledgements

We thank Dr. Jason Peters and Dr. Amy Banta for providing the Mobile-CRISPRi knockdown system and helpful experimental suggestions. This material is based upon work supported by the National Science Foundation Graduate Research Fellowship under Grant No. (DGE-1848739) to K.C.F. and the 2018 Beckman Young Investigator Award to M.T. This work was supported by the U.S. Department of Energy, Office of Science, Office of Basic Energy Sciences, under Award Number DE-SC0018269 (J.A.M.K, Y.S.-H.). This work was supported, in part, by the NSF Research Traineeship Program (Grant DGE-1828149) to J.A.M.K. This publication was also made possible by a predoctoral training award to J.A.M.K. from Grant T32-GM110523 from National Institute of General Medical Sciences (NIGMS) of the NIH. Its contents are solely the responsibility of the authors and do not necessarily represent the official views of the NIGMS or NIH.

4.7 Author Contributions

K.C.F. and M.T. devised the project. K.C.F. planned and carried out the wet lab experiments. J.A.M.K. designed the computational framework for Flux Balance Analysis with conceptual ideas from Y.S.-H., and the modeling was carried out by K.C.F. K.C.F. and M.T. wrote the manuscript in consultation with J.A.M.K. and Y.S.-H.

REFERENCES

(1) Xu, J.-Z., and Zhang, W.-G. (2016) Strategies used for genetically modifying bacterial genome: site-directed mutagenesis, gene inactivation, and gene over-expression *. *J Zhejiang Univ-Sci B (Biomed Biotechnol) 17*, 83–99.

(2) Zeaiter, Z., Mapelli, F., Crotti, E., and Borin, S. (2018) Methods for the genetic manipulation of marine bacteria. *Electron. J. Biotechnol. 33*, 17–28.

(3) Bertels, L. K., Murillo, L. F., and Heinisch, J. J. (2021) The pentose phosphate pathway in yeasts–more than a poor cousin of glycolysis. *Biomolecules 11*.

(4) Papagianni, M. (2012) Recent advances in engineering the central carbon metabolism of industrially important bacteria. *Microb. Cell Fact. 11*.

(5) Francois, J. M., Alkim, C., and Morin, N. (2020) Engineering microbial pathways for production of bio-based chemicals from lignocellulosic sugars: Current status and perspectives. *Biotechnol. Biofuels 13*.

(6) Becker, J., and Wittmann, C. (2015) Advanced biotechnology: Metabolically engineered cells for the bio-based production of chemicals and fuels, materials, and health-care products. *Angew. Chemie - Int. Ed. 54*, 3328–3350.

(7) Xia, P. F., Zhang, G. C., Walker, B., Seo, S. O., Kwak, S., Liu, J. J., Kim, H., Ort, D. R., Wang, S. G., and Jin, Y. S. (2017) Recycling Carbon Dioxide during Xylose Fermentation by Engineered Saccharomyces cerevisiae. *ACS Synth. Biol. 6*, 276–283.

(8) Guadalupe-Medina, V., Wisselink, H. W., Luttik, M. A., De Hulster, E., Daran, J. M., Pronk, J. T., and Van Maris, A. J. A. (2013) Carbon dioxide fixation by Calvin-Cycle enzymes improves ethanol yield in yeast. *Biotechnol. Biofuels*.

(9) Gong, F., Zhu, H., Zhang, Y., and Li, Y. (2018) Biological carbon fixation: From natural to synthetic. *J. CO_2 Util. 28*, 221–227.

(10) Satanowski, A., Dronsella, B., Noor, E., Vögeli, B., He, H., Wichmann, P., Erb, T. J., Lindner, S. N., and Bar-Even, A. (2020) Awakening a latent carbon fixation cycle in Escherichia coli. *Nat. Commun. 11*.

(11) Mattozzi, M. d., Ziesack, M., Voges, M. J., Silver, P. A., and Way, J. C. (2013) Expression of the sub-pathways of the Chloroflexus aurantiacus 3-hydroxypropionate carbon fixation bicycle in *E. coli*: Toward horizontal transfer of autotrophic growth. *Metab. Eng. 16*, 130–139.

(12) Giessen, T. W., and Silver, P. A. (2017) Engineering carbon fixation with artificial protein organelles. *Curr. Opin. Biotechnol. 46*, 42–50.

(13) Baba, T., Ara, T., Hasegawa, M., Takai, Y., Okumura, Y., Baba, M., Datsenko, K. A., Tomita, M., Wanner, B. L., and Mori, H. (2006) Construction of Escherichia coli K-12

in-frame, single-gene knockout mutants: The Keio collection. *Mol. Syst. Biol. 2*, 1–11.

(14) Yamamoto, N., Nakahigashi, K., Nakamichi, T., Yoshino, M., Takai, Y., Touda, Y., Furubayashi, A., Kinjyo, S., Dose, H., Hasegawa, M., Datsenko, K. A., Nakayashiki, T., Tomita, M., Wanner, B. L., and Mori, H. (2009) Update on the Keio collection of *Escherichia coli* single-gene deletion mutants. *Mol. Syst. Biol. 5*, 335.

(15) Antonovsky, N., Gleizer, S., Noor, E., Zohar, Y., Herz, E., Barenholz, U., Zelcbuch, L., Amram, S., Wides, A., Tepper, N., Davidi, D., Bar-On, Y., Bareia, T., Wernick, D. G., Shani, I., Malitsky, S., Jona, G., Bar-Even, A., and Milo, R. (2016) Sugar Synthesis from CO_2 in *Escherichia coli*. *Cell 166*, 115–125.

(16) Herz, E., Antonovsky, N., Bar-On, Y., Davidi, D., Gleizer, S., Prywes, N., Noda-Garcia, L., Lyn Frisch, K., Zohar, Y., Wernick, D. G., Savidor, A., Barenholz, U., and Milo, R. (2017) The genetic basis for the adaptation of *E. coli* to sugar synthesis from CO_2. *Nat. Commun. 8*, 1–10.

(17) Gleizer, S., Ben-Nissan, R., Bar-On, Y. M., Antonovsky, N., Noor, E., Zohar, Y., Jona, G., Krieger, E., Shamshoum, M., Bar-Even, A., and Milo, R. (2019) Conversion of *Escherichia coli* to Generate All Biomass Carbon from CO_2. *Cell 179*, 1255-1263.e12.

(18) Fredrickson, J. K., Romine, M. F., Beliaev, A. S., Auchtung, J. M., Driscoll, M. E., Gardner, T. S., Nealson, K. H., Osterman, A. L., Pinchuk, G., Reed, J. L., Rodionov, D. A., Rodrigues, J. L. M., Saffarini, D. A., Serres, M. H., Spormann, A. M., Zhulin, I. B., and Tiedje, J. M. (2008) Towards environmental systems biology of *Shewanella*. *Nat. Rev. Microbiol. 6*, 592–603.

(19) Beliaev, A. S., Klingeman, D. M., Klappenbach, J. A., Wu, L., Romine, M. F., Tiedje, J. M., Nealson, K. H., Fredrickson, J. K., and Zhou, J. (2005) Global transcriptome analysis of *Shewanella oneidensis* MR-1 exposed to different terminal electron acceptors. *J. Bacteriol. 187*, 7138–7145.

(20) Schwalb, C., Chapman, S. K., and Reid, G. A. (2003) The tetraheme cytochrome CymA is required for anaerobic respiration with dimethyl sulfoxide and nitrite in *Shewanella oneidensis*. *Biochemistry 42*, 9491–9497.

(21) Tefft, N. M., and Teravest, M. A. (2019) Reversing an Extracellular Electron Transfer Pathway for Electrode-Driven Acetoin Reduction. *ACS Synth. Biol. 8*, 1590–1600.

(22) Baron, D., LaBelle, E., Coursolle, D., Gralnick, J. A., and Bond, D. R. (2009) Electrochemical measurement of electron transfer kinetics by *Shewanella oneidensis* MR-1. *J. Biol. Chem. 284*, 28865–28873.

(23) Marsili, E., Baron, D. B., Shikhare, I. D., Coursolle, D., Gralnick, J. A., and Bond, D. R. (2008) *Shewanella* secretes flavins that mediate extracellular electron transfer. *Proc. Natl. Acad. Sci. U. S. A. 105*, 3968–3973.

(24) Rabaey, K., and Rozendal, R. A. (2010) Microbial electrosynthesis - Revisiting the electrical route for microbial production. *Nat. Rev. Microbiol. 8*, 706–716.

(25) Prévoteau, A., Carvajal-Arroyo, J. M., Ganigué, R., and Rabaey, K. (2020, April 1) Microbial electrosynthesis from CO_2: forever a promise? *Curr Opin Biotechnol*. **62**, 48-57.

(26) Bajracharya, S., Ter Heijne, A., Dominguez Benetton, X., Vanbroekhoven, K., Buisman, C. J. N., Strik, D. P. B. T. B., and Pant, D. (2015) Carbon dioxide reduction by mixed and pure cultures in microbial electrosynthesis using an assembly of graphite felt and stainless steel as a cathode. *Bioresour. Technol. 195*, 14–24.

(27) Howard, E. C., Hamdan, L. J., Lizewski, S. E., and Ringeisen, B. R. (2012) High frequency of glucose-utilizing mutants in *Shewanella oneidensis* MR-1. *FEMS Microbiol. Lett. 327*, 9–14.

(28) Choi, D., Lee, S. B., Kim, S., Min, B., Choi, I. G., and Chang, I. S. (2014) Metabolically engineered glucose-utilizing *Shewanella* strains under anaerobic conditions. *Bioresour. Technol. 154*, 59–66.

(29) Nakagawa, G., Kouzuma, A., Hirose, A., Kasai, T., Yoshida, G., and Watanabe, K. (2015) Metabolic characteristics of a glucose-utilizing *Shewanella oneidensis* strain grown under electrode-respiring conditions. *PLoS One 10*, e0138813.

(30) Brutinel, E. D., and Gralnick, J. A. (2012) Preferential utilization of d-Lactate by *Shewanella oneidensis*. *Appl. Environ. Microbiol. 78*, 8474–8476.

(31) Pinchuk, G. E., Geydebrekht, O. V., Hill, E. A., Reed, J. L., Konopka, A. E., Beliaev, A. S., and Fredrickson, J. K. (2011) Pyruvate and lactate metabolism by *Shewanella oneidensis* MR-1 under fermentation, oxygen limitation, and fumarate respiration conditions. *Appl. Environ. Microbiol. 77*, 8234–8240.

(32) Pinchuk, G. E., Rodionov, D. A., Yang, C., Li, X., Osterman, A. L., Dervyn, E., Geydebrekht, O. V., Reed, S. B., Romine, M. F., Collart, F. R., Scott, J. H., Fredrickson, J. K., and Beliaev, A. S. (2009) Genomic reconstruction of *Shewanella oneidensis* MR-1 metabolism reveals a previously uncharacterized machinery for lactate utilization. *Proc. Natl. Acad. Sci. U. S. A. 106*, 2874–2879.

(33) Winn, S. I., Watson, H. C., Harkins, R. N., and Fothergill, L. A. (1981) Structure and activity of phosphoglycerate mutase. *Philos. Trans. R. Soc. Lond. B. Biol. Sci.*

(34) Deutschbauer, A., Price, M. N., Wetmore, K. M., Shao, W., Baumohl, J. K., Xu, Z., Nguyen, M., Tamse, R., Davis, R. W., and Arkin, A. P. (2011) Evidence-based annotation of gene function in *Shewanella oneidensis* MR-1 using genome-wide fitness profiling across 121 conditions. *PLoS Genet.* (Richardson, P. M., Ed.) *7*, e1002385.

(35) Yang, H., Krumholz, E. W., Brutinel, E. D., Palani, N. P., Sadowsky, M. J., Odlyzko, A. M., Gralnick, J. A., and Libourel, I. G. L. (2014) Genome-Scale Metabolic Network

Validation of *Shewanella oneidensis* Using Transposon Insertion Frequency Analysis. *PLoS Comput. Biol.* (Maranas, C. D., Ed.) *10*, e1003848.

(36) Blomfield, I. C., Vaughn, V., Rest, R. F., and Eisenstein, B. I. (1991) Allelic exchange in *Escherichia coli* using the *Bacillus subtilis* sacB gene and a temperature-sensitive pSC101 replicon. *Mol. Microbiol. 5*, 1447–1457.

(37) Hawkins, J. S., Wong, S., Peters, J. M., Almeida, R., and Qi, L. S. (2015) Targeted transcriptional repression in bacteria using CRISPR interference (CRISPRi). *Methods Mol. Biol. 1311*, 349–362.

(38) Peters, J. M., Koo, B. M., Patino, R., Heussler, G. E., Hearne, C. C., Qu, J., Inclan, Y. F., Hawkins, J. S., Lu, C. H. S., Silvis, M. R., Harden, M. M., Osadnik, H., Peters, J. E., Engel, J. N., Dutton, R. J., Grossman, A. D., Gross, C. A., and Rosenberg, O. S. (2019) Enabling genetic analysis of diverse bacteria with Mobile-CRISPRi. *Nat. Microbiol. 4*, 244–250.

(39) Rodionov, D. A., Yang, C., Li, X., Rodionova, I. A., Wang, Y., Obraztsova, A. Y., Zagnitko, O. P., Overbeek, R., Romine, M. F., Reed, S., Fredrickson, J. K., Nealson, K. H., and Osterman, A. L. (2010) Genomic encyclopedia of sugar utilization pathways in the *Shewanella* genus. *BMC Genomics 11*, 1–19.

(40) Chubiz, L. M., and Marx, C. J. (2017) Growth trade-offs accompany the emergence of glycolytic metabolism in *Shewanella oneidensis* MR-1. *J. Bacteriol. 199*.

(41) Groh, J. L., Luo, Q., Ballard, J. D., and Krumholz, L. R. (2007) Genes that enhance the ecological fitness of *Shewanella oneidensis* MR-1 in sediments reveal the value of antibiotic resistance. *Appl. Environ. Microbiol. 73*, 492–498.

(42) Gurobi Optimization, L. L. C. Gurobi Optimizer Reference Manual.

(43) Pinchuk, G. E., Hill, E. A., Geydebrekht, O. V., de Ingeniis, J., Zhang, X., Osterman, A., Scott, J. H., Reed, S. B., Romine, M. F., Konopka, A. E., Beliaev, A. S., Fredrickson, J. K., and Reed, J. L. (2010) Constraint-based model of *Shewanella oneidensis* MR-1 metabolism: A tool for data analysis and hypothesis generation. *PLoS Comput. Biol. 6*, 1–8.

(44) Duhl, K. L., Tefft, N. M., and TerAvest, M. A. (2018) *Shewanella oneidensis* MR-1 utilizes both sodium- and proton-pumping NADH dehydrogenases during aerobic growth. *Appl. Environ. Microbiol. 84*, e00415-18.

(45) Rodrigues, J. L. M., Serres, M. H., and Tiedje, J. M. (2011) Large-scale comparative phenotypic and genomic analyses reveal ecological preferences of *Shewanella* species and identify metabolic pathways conserved at the genus level. *Appl. Environ. Microbiol. 77*, 5352–5360.

(46) Driscoll, M. E., Romine, M. F., Juhn, F. S., Serres, M. H., McCue, L. A., Beliaev, A. S., Fredrickson, J. K., and Gardner, T. S. (2007) Identification of diverse carbon

utilization pathways in *Shewanella oneidensis* MR-1 via expression profiling. *Genome Inform.*

(47) Venkateswaran, K., Moser, D. P., Dollhopf, M. E., Lies, D. P., Saffarini, D. A., MacGregor, B. J., Ringelberg, D. B., White, D. C., Nishijima, M., Sano, H., Burghardt, J., Stackebrandt, E., and Nealson, K. H. (1999) Polyphasic taxonomy of the genus *Shewanella* and description of *Shewanella oneidensis* sp. nov. *Int. J. Syst. Bacteriol. 49*, 705–724.

(48) Nealson, K. H., and Scott, J. (2006) Ecophysiology of the Genus *Shewanella*. *The Prokaryotes* 1133–1151.

(49) Myers, C. R., and Nealson, K. H. (1988) Bacterial manganese reduction and growth with manganese oxide as the sole electron acceptor. *Sci. Sci. 240*, 1319–1321.

(50) Ringo, E., Stenberg, E., and Strom, A. R. (1984) Amino acid and lactate catabolism in trimethylamine oxide respiration of Alteromonas putrefaciens NCMB 1735. *Appl. Environ. Microbiol. 47*, 1084–1089.

(51) Serres, M. H., and Riley, M. (2006) Genomic analysis of carbon source metabolism of *Shewanella oneidensis* MR-1: Predictions versus experiments. *J. Bacteriol. 188*, 4601–4609.

(52) Oh, J., Fung, E., Price, M. N., Dehal, P. S., Davis, R. W., Giaever, G., Nislow, C., Arkin, A. P., and Deutschbauer, A. (2010) A universal tagmodule collection for parallel genetic analysis of microorganisms. *Nucleic Acids Res. 38*.

(53) Baym, M., Shaket, L., Anzai, I. A., Adesina, O., and Barstow, B. (2016) Rapid construction of a whole-genome transposon insertion collection for *Shewanella oneidensis* by Knockout Sudoku. *Nat. Commun. 7*.

(54) Ong, W. K., Vu, T. T., Lovendahl, K. N., Llull, J. M., Serres, M. H., Romine, M. F., and Reed, J. L. (2014) Comparisons of *Shewanella* strains based on genome annotations, modeling, and experiments. *BMC Syst. Biol. 8*, 31.

(55) Heirendt, L., Arreckx, S., Pfau, T., Mendoza, S. N., Richelle, A., Heinken, A., Haraldsdóttir, H. S., Wachowiak, J., Keating, S. M., Vlasov, V., Magnusdóttir, S., Ng, C. Y., Preciat, G., Žagare, A., Chan, S. H. J., Aurich, M. K., Clancy, C. M., Modamio, J., Sauls, J. T., Noronha, A., Bordbar, A., Cousins, B., El Assal, D. C., Valcarcel, L. V., Apaolaza, I., Ghaderi, S., Ahookhosh, M., Ben Guebila, M., Kostromins, A., Sompairac, N., Le, H. M., Ma, D., Sun, Y., Wang, L., Yurkovich, J. T., Oliveira, M. A. P., Vuong, P. T., El Assal, L. P., Kuperstein, I., Zinovyev, A., Hinton, H. S., Bryant, W. A., Aragón Artacho, F. J., Planes, F. J., Stalidzans, E., Maass, A., Vempala, S., Hucka, M., Saunders, M. A., Maranas, C. D., Lewis, N. E., Sauter, T., Palsson, B., Thiele, I., and Fleming, R. M. T. (2019) Creation and analysis of biochemical constraint-based models using the COBRA Toolbox v.3.0. *Nat. Protoc. 14*, 639–702.

(56) Saltikov, C. W., and Newman, D. K. (2003) Genetic identification of a respiratory

arsenate reductase. *Proc. Natl. Acad. Sci. U. S. A. 100*, 10983–10988.

Chapter 5: Engineering Strategy for a CO_2 Fixation Pathway in *S. oneidensis*

Kathryne C. Ford[1,2], Joshua A.M. Kaste[1,3], Yair Shachar-Hill[3], Michaela A. TerAvest[1]*

[1]Department of Biochemistry and Molecular Biology, Michigan State University, East Lansing, MI, 48824, USA

[2]Department of Microbiology and Molecular Genetics, Michigan State University, East Lansing, MI, 48824, USA

[3]Department of Plant Biology, Michigan State University, East Lansing, MI, 48824, USA

5.1 Introduction

The global effects of anthropogenic carbon emissions include damage to human and animal health, increased economic burden, and ecosystem destruction[1–5]. As efforts to phase out fossil fuels entirely becomes increasingly polarizing, researchers aim to develop more sustainable designs for existing infrastructure. One such effort relies on carbon capture, which would remove greenhouse gases like carbon dioxide (CO_2) from the atmosphere. Other methods rely on biotic generation of fuel products like ethanol. Biofuel usage would eliminate the need for fossil fuel extraction, itself an extremely pollutive process, while producing fuels that can be used in existing infrastructure. Early developments towards biofuels used ethanol derived from plants like switchgrass and corn. While plant-based biofuels have demonstrated success and already been deployed for commercial use, they can present problems related to land management and food resource availability. Therefore, our research aims to circumvent this problem by using the electroactive bacterium *Shewanella oneidensis* MR-1 to develop a platform for microbial electrosynthesis (MES). MES is a burgeoning biotechnology that uses microorganisms to convert electricity and CO_2 into useful chemical products like biofuels; this process can also be expanded to produce bioplastics, pharmaceuticals, and other specialty chemicals (**Figure 5.1**)[6–9]. However, to create this carbon-neutral platform using *S. oneidensis* MR-1, we must optimize the electron uptake pathway and install a carbon fixation module in this heterotrophic microbe. Work described in Chapters 2 and 3 focus on the former, while Chapter 4 lays out the initial steps taken towards engineering a strain of *S. oneidensis* MR-1 to be autotrophic. Here, I will describe the rationale behind our design strategy, what steps have been taken, and the future direction of this research.

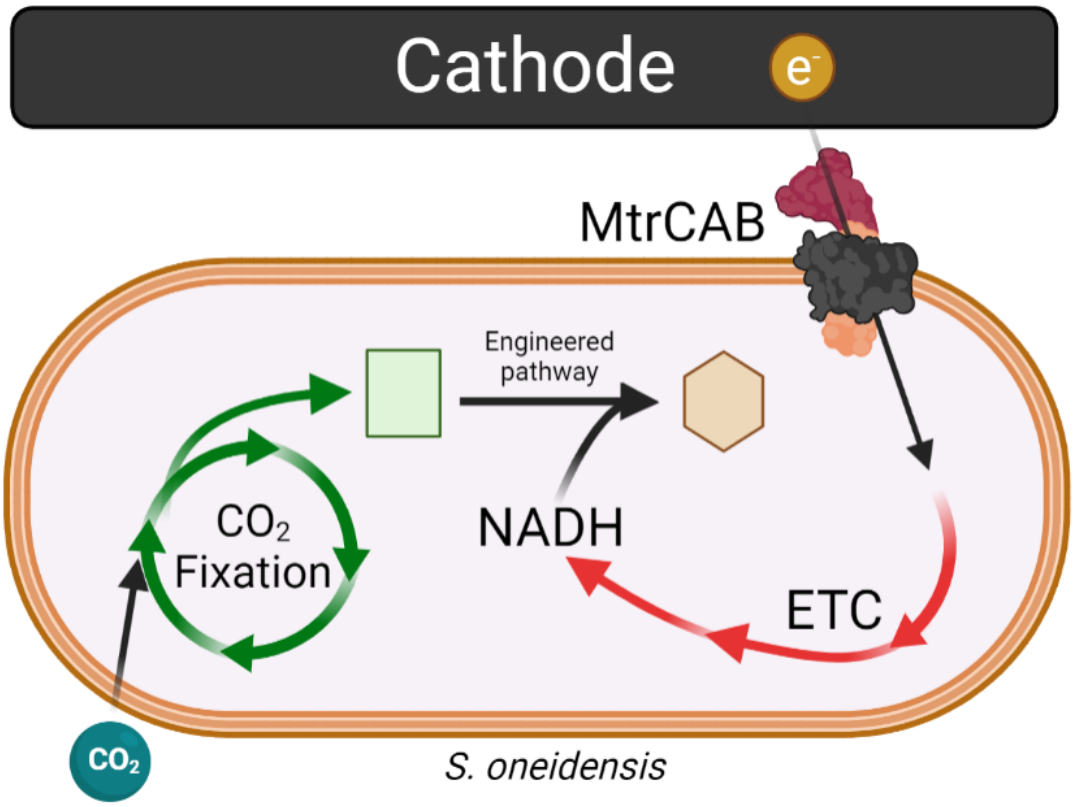

Figure 5.1 Electroautotrophic Strategy. To engineer an electroautotrophic metabolism in *S. oneidensis*, we created a strain that requires separate carbon sources to build biomass and gain energy and reducing power (Δ*gpmA*). This strain will be used to evolve a CO_2 fixation module for building biomass and be grown on a cathode to use electron uptake for NADH production. This strain will use solely electricity and CO_2 for growth. We can then implement an engineered bioproduction pathway, to produce useful chemicals from these minimal feedstocks.

Our design for engineering autotrophy in *S. oneidensis* was inspired by work from Antonovsky et al. and the subsequent related publications[10–15]. They expressed the genes encoding ribulose-1,5-bisphosphate carboxylase/oxygenase (RuBisCO), phosphoribulokinase (*prkA*), and a carbonic anhydrase (CA) in *Escherichia coli* from a vector (pCBB). These, together with the native *E. coli* enzymes, created an artificial Calvin-Benson-Bassham (CBB) cycle. RuBisCO and PrkA bridge the gap between ribulose 5-phosphate and 3-phosphoglycerate, while CA, an enzyme commonly found in carboxysomes alongside RuBisCO, could concentrate CO_2 in the cytosol (**Figure 5.2**).

Overexpression of these three genes was not sufficient to allow growth using solely CO_2 to build biomass, therefore the team utilized metabolic modeling to generate a strategy for deleting endogenous genes to force reliance on RuBisCO for growth. Results from modeling led them to generate a knockout of the two genes that each encode a 3-phosphoglycerate mutase (*gpmAM*). This deletion severed the flow of carbon between the artificial CBB cycle and the tricarboxylic acid (TCA) cycle, requiring this strain to be supplied with two carbon substrates. The Δ*gpmAM* pCBB strain was evolved in a chemostat, in medium supplemented with excess carbon to feed the TCA cycle (pyruvate) and limiting substrate for biomass synthesis (xylose) in a 10% CO_2 atmosphere. This way, strains that develop the ability to use RuBisCO and CO_2 to build biomass will have a fitness advantage over those that do not, and become the dominant phenotype in the community. This approach was successful in generating a strain of *E. coli* capable of growth with CO_2 as the sole substrate for biomass assimilation. We adapted this strategy to engineering autotrophic *S. oneidensis*. We were provided with the pCBB plasmid from the Milo Research Group and introduced it into WT *S. oneidensis*. Similar to results in *E. coli*, adding pCBB did not initially create an autotrophic phenotype in *S. oneidensis*. Proceeding forward, we applied the OptKnock program to an existing model of *S. oneidensis* metabolism to determine the best gene deletion strategy for our organism and the optimal mutant was generated[16]. The next steps of this research will focus on further developing this strain, including characterizing substrate usage, directed evolution to carbon fixation, and analysis of the acquired mutations in these lineages.

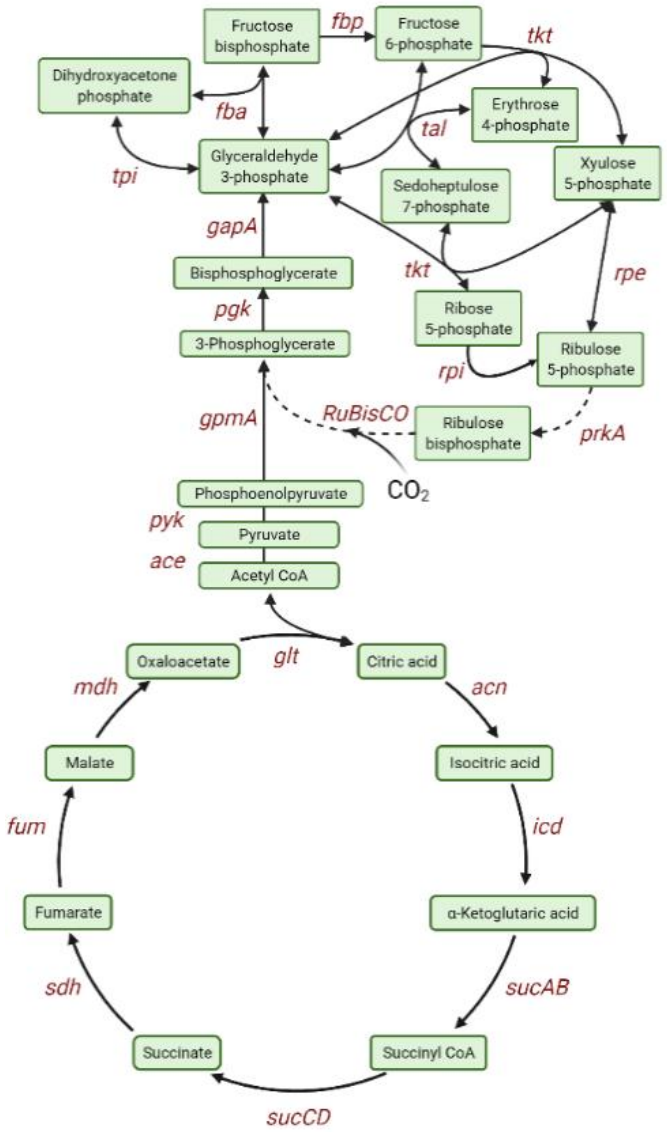

Figure 5.2 *S. oneidensis* central carbon metabolism amended with RuBisCO and PrkA. A metabolic map of central carbon metabolism, including the TCA cycle and an engineered Calvin-Benson Cycle. Solid lines represent enzymatic reactions native to *S. oneidensis*, dashed represent exogenous proteins, RuBisCO and PrkA, that are encoded by genes on pCBB. Adapted from Chapter 4 **Figure 4.1**.

5.2 Results

5.2.1 Determining Optimal Gene Knockout Strategy

Despite *S. oneidensis* being a γ-proteobacteria and close relative to *E. coli*, our aim was to explore novel gene deletion strategies *in silico* for *S. oneidensis*, rather than

duplicating what has been done in *E. coli*. To do this analysis, we utilized a MATLAB program called OptKnock[17]. As previously described in Chapter 4, this program allows us to examine the flux of carbon within central metabolism and how loss of different enzymatic reactions affects this flow. We applied this to a previously published model of *S. oneidensis* and set the parameters to optimize flux though the RuBisCO reaction, allow up to two deletions in a limited set of target reactions, and growth on nine different substrates and CO_2[18].

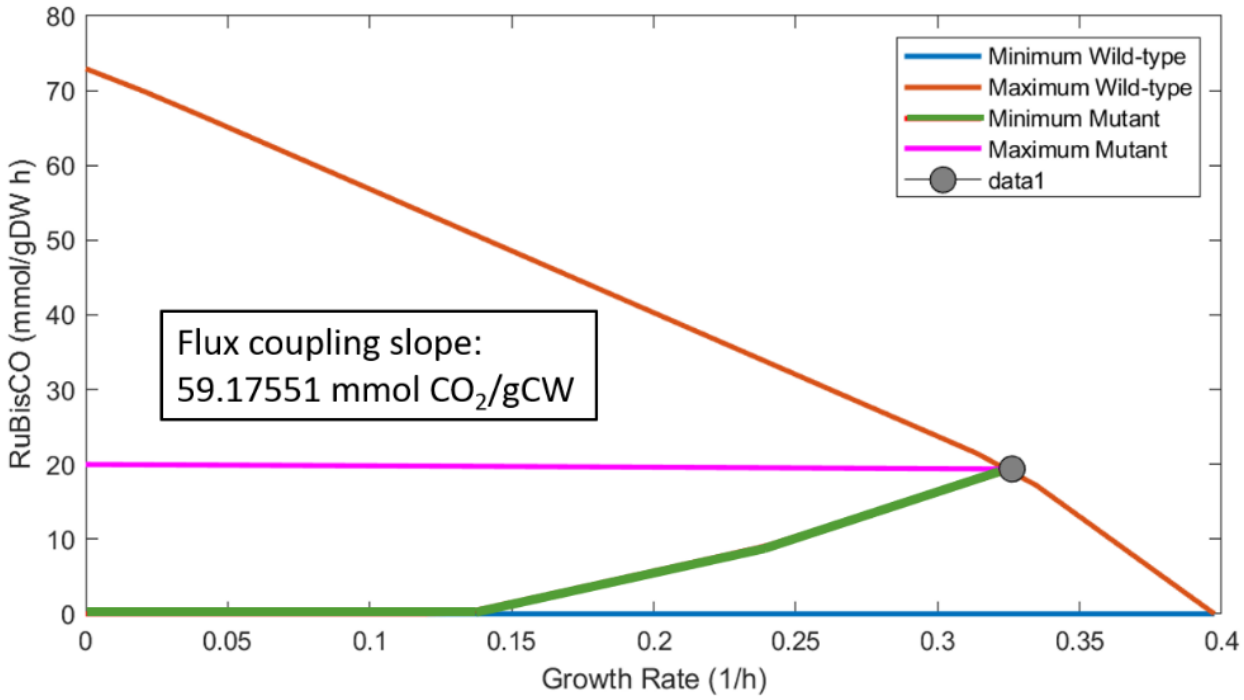

Figure 5.3 Example for Determining Flux Coupling Slope. For each gene deletion strategy, single and double knockouts, a graph was generated that compared the growth potential of the mutant to WT when growing on different substrates. This is an example for Δ*gapA* growing on inosine. When WT is growing on inosine, it can reach its maximum growth rate potential (0.4 1/h) without no carbon flux through (and therefore use of) RuBisCO (0.4, 0). Conversely, the Δ*gapA* mutant can only have a maximum growth rate up to 0.15 1/h without RuBisCO; any higher growth rate will require the cell to use RuBisCO (green line = Flux Coupling Slope). When deciding which gene knockouts were best suited for our needs, we looked for mutations that showed a > 0 value for RuBisCO flux for any given growth rate.

This output determined whether or not a specific mutant could feasibly grow on a specific substrate with CO_2, whether that growth would be dependent on the use of RuBisCO, and how much carbon would be fixed by RuBisCO, calculated as moles of CO_2 fixed per gram of cell weight per hour (mmol CO_2/gCWh) (**Figure 5.3**). This analysis was used to calculate the flux coupling slope (mmol CO_2/gCW) for each potential mutant, and strains capable of growth without RuBisCO were ruled out **(Figure 5.4**). From the strains that were dependent on RuBisCO, the mutant that had the highest growth potential for the greatest number of carbon sources was a *gpmA* knockout (annotated in program as PGM). This meant that the optimal strategy for generating a strain of *S. oneidensis* that was capable of building biomass via carbon fixation was Δ*gpmA* expressing pCBB, the same strategy used for *E. coli*. However, unlike in *E. coli*, the enzymatic reaction carried out by GpmA was considered essential for *S. oneidensis*. This was based on both computational modeling and failure to generate a transposon insertion mutant during library preparation[18]. Though initial attempts to delete this gene were unsuccessful, we developed a genetic engineering pipeline to eventually generate Δ*gpmA* pCBB. Details for this are outlined in Chapter 4.

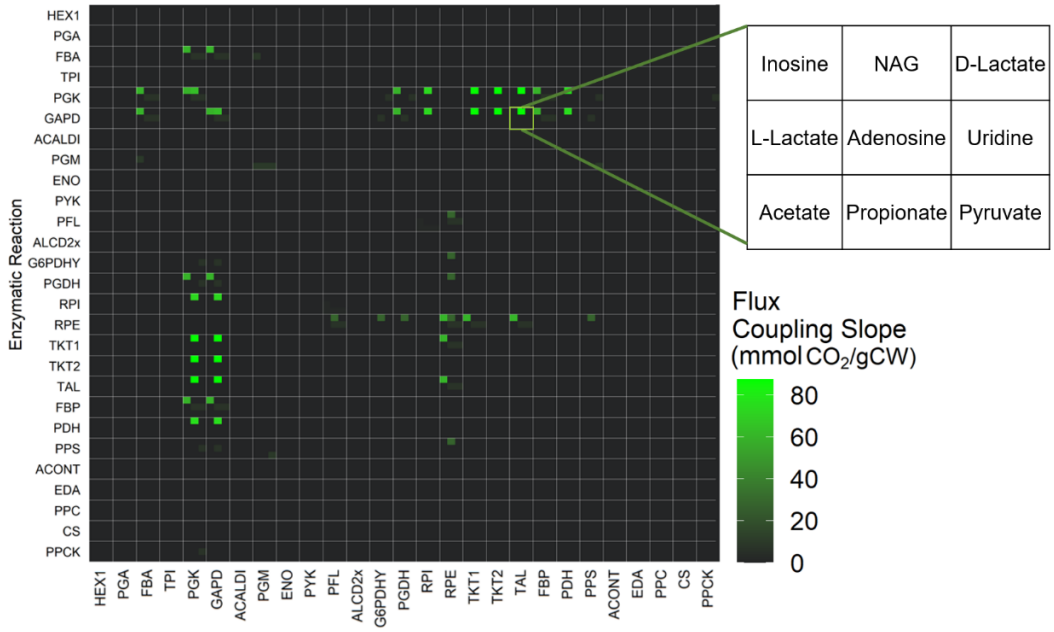

Figure 5.4 Results of Flux Balance Analysis. To identify a gene knockout strategy for optimizing flux of carbon through the RuBisCO reaction, we applied the OptKnock program to an existing metabolic map of *S. oneidensis*. We limited the scope of the program to only allow up to two knockouts of 27 central metabolic reactions. Intersections represent the two potential knockouts. Some reactions represent multiple genes that encode homologous proteins. The gradient represents the flux coupling slope in (mM CO_2)/gCW (grams of cell weight), which means the amount of carbon that will flow through RuBisCO in a mutant that will only grow if RuBisCO is present. Within each box, are the flux coupling slope for a given knockout strategy grown on one of 9 carbon substrates 9 (inset) with 10% atmospheric CO_2. See Abbreviations Table for the enzymes associated with these Enzymatic Reactions.

5.2.2 Investigating Growth Potential of ΔgpmA pCBB

Once we created the Δ*gpmA* pCBB, we characterized its growth potential on various carbon substrates. Because this mutation severs the flow of carbon between the energy module (TCA) from the biomass module (gluconeogenesis/CBB), we hypothesized that this strain would need a minimum of two carbon substrates to grow. We compared growth of this strain in LB and M5 minimal medium lacking casamino acids supplemented with various combinations of carbon sources that either enter metabolism though the TCA cycle (pyruvate, $_{D,L}$-lactate) or through glycolysis (adenosine, inosine,

uridine)[19]. These were compared to WT and WT expressing pCBB. Indeed, we observed that the OD_{600} of Δ*gpmA* pCBB only increased during growth in LB, or with two carbon sources, while WT and WT pCBB grew under all conditions (**Figure 5.5**). The most robust growth of Δ*gpmA* pCBB was observed using a combination of uridine and lactate, so these substrates were used in subsequent evolution experiments. The next step was to confirm that growth was due to consumption of both carbon substrates, as opposed to regulatory changes or other unintended effects.

WT, WT pCBB, and Δ*gpmA* pCBB cells were grown in medium with either 20 mM $_{D,L}$-lactate, 10 mM uridine, or both, and samples were taken for HPLC analysis at inoculation and when cultures reached maximum OD_{600}. When both substrates are provided, WT and WT pCBB consumed all provided D,L-lactate and uridine, while Δ*gpmA* pCBB consumed about ~25% and ~35% respectively (**Figure 5.6**). This confirmed that both substrates were consumed by Δ*gpmA* pCBB, and the decreased assimilation accounts for the lower maximum cell density. In the single carbon medium, both WT strains consumed all of the provided carbon, while Δ*gpmA* pCBB consumed none of the $_{D,L}$-lactate, and about ~25% of the uridine. It is likely that the small amount of uridine consumed went towards cellular maintenance and not biomass because there was no appreciable increase in OD_{600}.

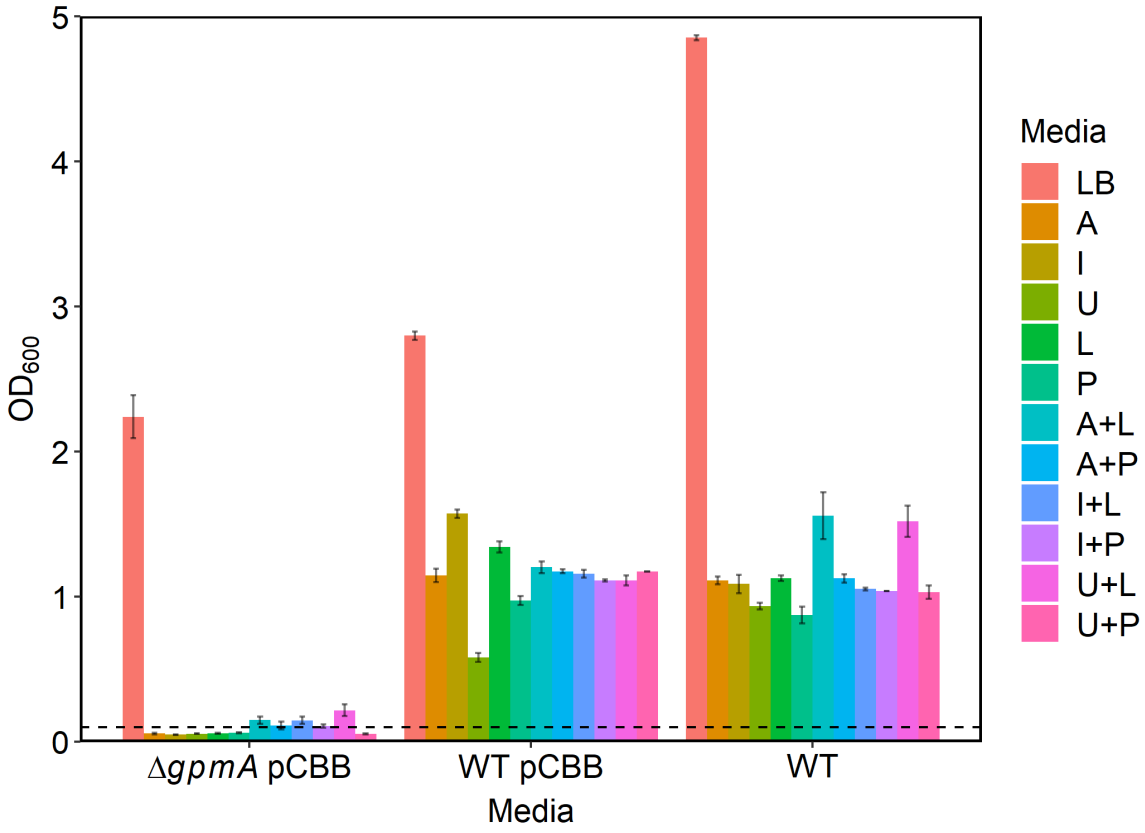

Figure 5.5 Growth of *S. oneidensis* Variants on Different Substrates. WT MR-1, WT pCBB, and Δ*gpmA* pCBB was grown overnight in LB (+Chl for strains with pCBB). Cells were washed and resuspended in 200 µL fresh LB, or M5 with one or two carbon substrates in a 96-well plate in triplicate (n=3). Medi key: LB = Lysogeny Broth, A = 10 mM adenosine, I = 10 mM inosine, U = 10 mM uridine, L = 20 mM $_{D,L}$-lactate, and P = 20 mM pyruvate. Dashed line represents OD_{600} at inoculation. Δ*gpmA* pCBB only increased in OD in LB, or when 2 carbon substrates were provided.

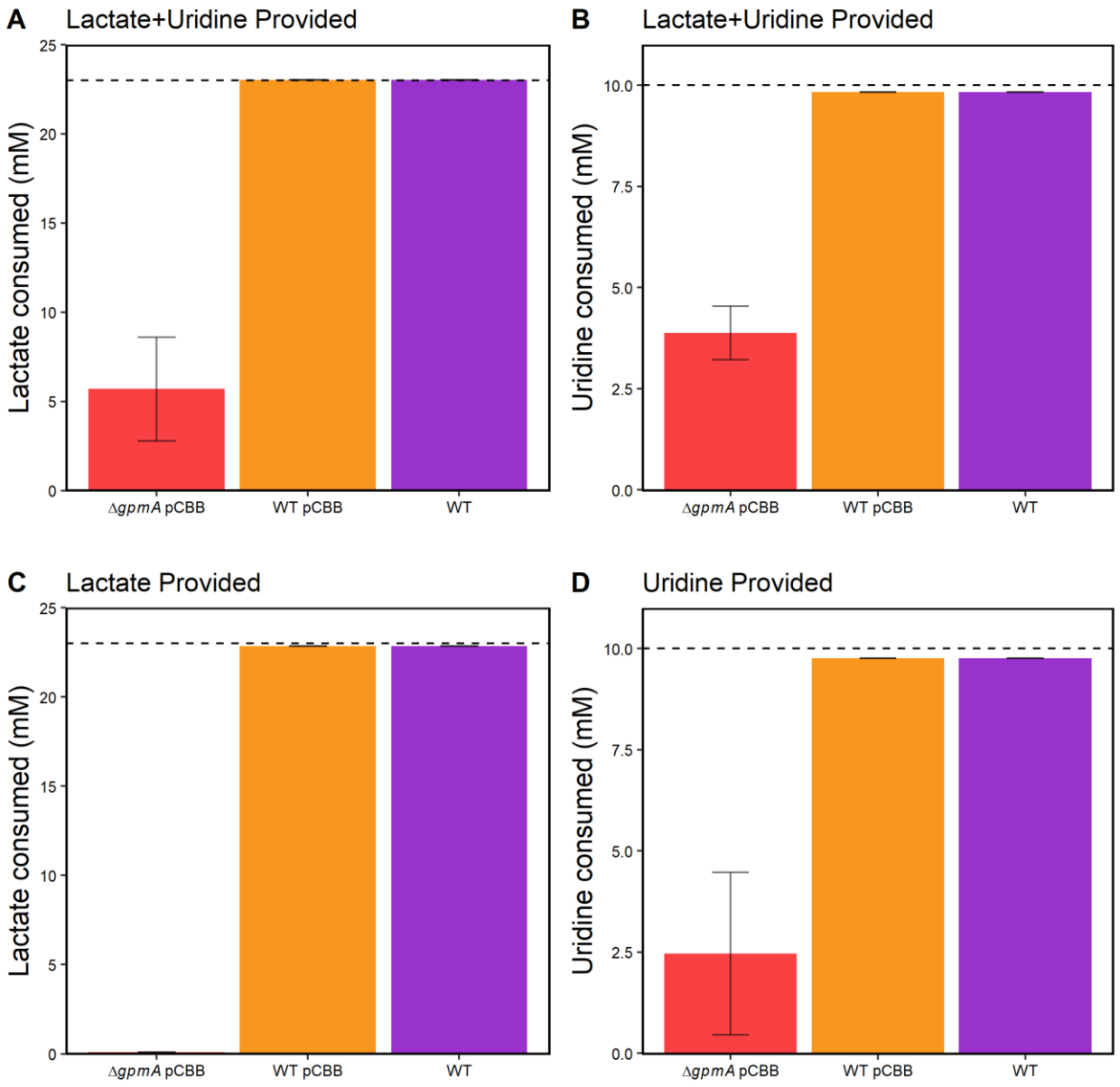

Figure 5.6 Carbon Consumption by Strain. WT, WT pCBB, and Δ*gpmA* pCBB were pre-grown in LB (+Chl for pCBB), washed, and resuspended in M5 minimal medium with no casamino acids, and either 20 mM lactate, 10 mM uridine, or both. Samples were taken at inoculation, and after cultures reached a max OD for HPLC analysis. Bars and error bars represent mean and standard error, respectively (n=3). When provided with both carbon sources, all strains consumed both substrates, in their entirety in the case of WT strains (A,B). When provided only lactate, Δ*gpmA* pCBB did not consume any, while WT and WT pCBB consumed it all (C). When provided only uridine, Δ*gpmA* pCBB consumed ~25% and WT and WT pCBB consumed it all (D). Δ*gpmA* pCBB may have consumed this small amount of uridine for cellular maintenance, but was unable to grow to an appreciable OD_{600} (**Figure 5.5**).

5.2.3 Designing a Directed Evolution Experiment

For chemostat evolution experiments, the medium is designed to ensure there is a fitness advantage for cells containing mutations that increase their use of RuBisCO. In Δ*gpmA* pCBB, $_{D,L}$-lactate is taken up into the cell and converted into pyruvate and subsequently enters the TCA cycle. Providing $_{D,L}$-lactate in excess ensures that the cells have ample reserves of NADH and ATP. Uridine is used to build biomass, and therefore will be the limiting factor for growth. This design ensures that Δ*gpmA* pCBB cannot reach its maximum growth rate, and that there is a selective pressure to utilize the other available carbon source, CO_2. Cells that use CO_2 will increase in growth rate and become the dominant phenotype in the culture.

The amount of uridine needed to sustain growth under limiting conditions was determined by calculating the substrate concentration constant (K_s). This value represents the concentration of the limiting substrate, in this case uridine, at half the maximum growth rate (μ_{max}) of a given strain when the limiting carbon is in excess. To determine this, Δ*gpmA* pCBB was grown in M5 minimal medium with no casamino acids, 20 mM $_{D,L}$-lactate, and varying concentrations of uridine. The maximum growth rate for each version of the medium was calculated and plotted as a factor of uridine concentration (**Figure 5.7**). Applying the Monod equation to these points, μ_{max} is calculated to be 0.1386 1/h, $\mu_{max}/2$ is 0.069 1/h, and K_s is 64.95 mg/L of uridine. Knowing these values, chemostat evolution experiments to develop a strain of Δ*gpmA* pCBB that grows by fixing CO_2 will use medium with 20 mM $_{D,L}$-lactate and 65 mg/L of uridine (~0.26 mM).

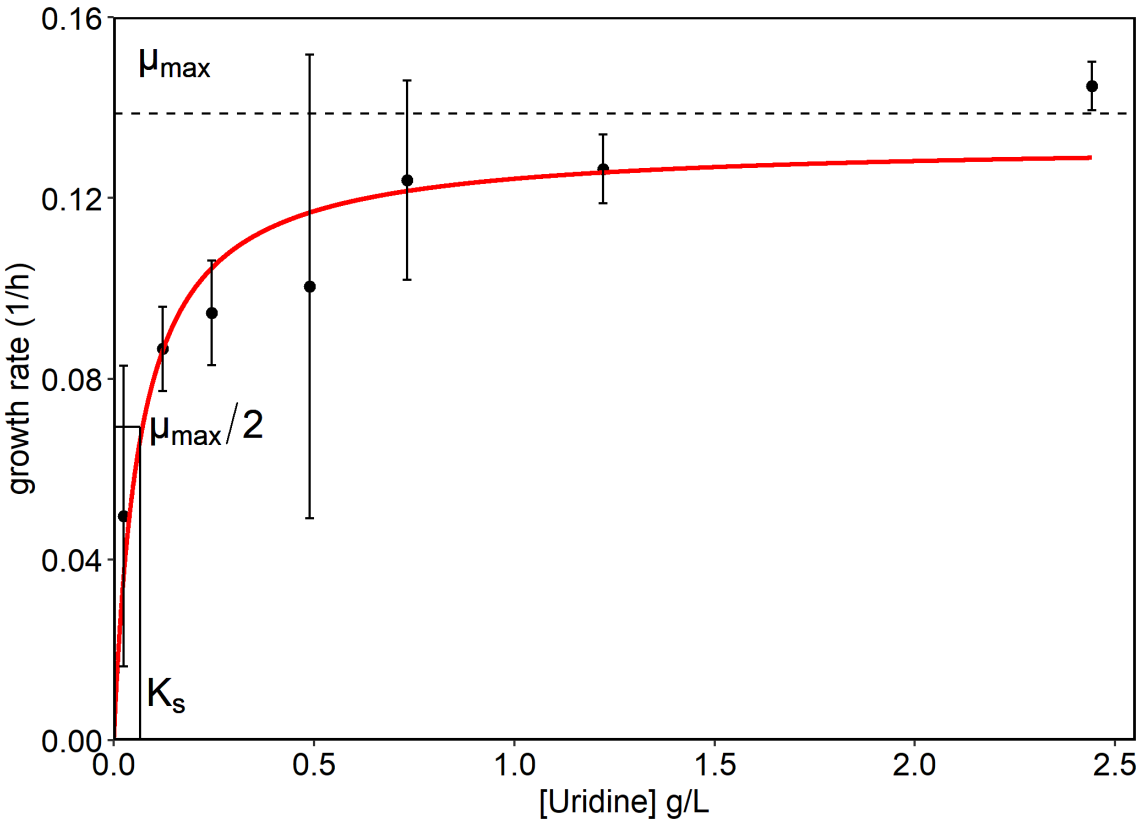

Figure 5.7 Growth Rate of Δ*gpmA* pCBB on Varying [uridine]. Δ*gpmA* pCBB cells were pre-grown in LB+Chl, washed, and resuspended in 2 mL of M5 without casamino acids, with 20 mM lactate and various concentrations of uridine, in a 24-well plate. OD_{600} was measured every 15 minutes until a maximum OD_{600} was reached for all wells. The max growth rate (1/h) was calculated and plotted against [uridine] g/L. Points and error bars represent average and standard error, respectively (n=3). Red line represents the calculated Monod Curve for this data, with μ_{max} being the maximum potential growth rate, $\mu_{max}/2$ being half the maximum potential growth rate, and K_s being the [uridine] at $\mu_{max}/2$.

5.3 Future Directions

From this work, we have everything needed to begin directed evolution to create a strain of *S. oneidensis* capable of fixing CO_2 for biomass. Evolution experiments with Δ*gpmA* pCBB will be carried out using a BIOSTAT-A Fermenter, with an excess of $_{D,L}$-lactate (20 mM) and limiting uridine (65 mg/L). The culture vessel will be regularly sampled to track substrate usage via HPLC, cell growth (OD_{600}), and ensure no

contamination. At the onset of the experiment, we expect the culture to grow denser with time before reaching a steady state OD_{600} where all uridine is being consumed, but there is still excess $_{D,L}$-lactate in the medium. Mutations will naturally occur within the cells, and any mutations that aid in fitness will be retained in subsequent generations. One such path for increasing fitness is being able to use the other available carbon source (CO_2) to build biomass. Consequently, genotypes that express and use RuBisCO and PrkA to fix carbon will outcompete others that do not. Because these cells use the CO_2 and uridine, they will simultaneously increase their consumption of $_{D,L}$-lactate. Therefore, we can infer the evolution of the desired phenotype when there is an increase in OD_{600} and decrease in residual $_{D,L}$-lactate from steady state. When the culture has reached a new, higher steady state OD_{600} where all $_{D,L}$-lactate is consumed, samples will be taken to identify isolates capable of growth using solely CO_2 and $_{D,L}$-lactate.

If multiple isolates with the CO_2 fixing phenotype are identified, it is unlikely that they will all have the same acquired mutations (genotype). Therefore, the next step is to perform whole genome sequencing on various isolates. This genomic data will provide insight regarding how the metabolome was fine-tuned to redirect the flow of carbon through RuBisCO. Additionally, we will observe any overlap in mutations between isolates, indicative of that specific mutation being a greater influence. The information can also be used, as in Herz et al, to build a version of this strain with the smallest number of required mutations[11]. To do this engineering, the acquired mutations of different isolates will be pooled and ranked based on frequency and proximity to carbon

metabolism. They would then be systematically reintroduced into an unevolved Δ*gpmA* pCBB until the phenotype is restored.

As this engineered strain will still require $_{D,L}$-lactate to grow, an important follow up to this work would be to ensure that the $_{D,L}$-lactate is being solely used for energy acquisition and not to build biomass. This assessment could be done using isotopically labeled CO_2 and $_{D,L}$-lactate to track which substrate is the building block for the synthesis of metabolites or cell components. This analysis will be crucial to using this strain for electroautotrophy. The intent with this design is to eventually replace the secondary carbon source ($_{D,L}$-lactate) with the cathode. Therefore, we must ensure that the cell is capable of growth using solely CO_2 for biomass synthesis, as the cathode will only facilitate NADH and ATP formation. Once autotrophy is confirmed, the bioengineered strain can be applied as a biocatalyst for a wide variety of MES applications.

5.4 Materials and Methods

Strains and Plasmids

Strains and plasmids used are listed in Table 5.1. *S. oneidensis* strains were grown at 30 °C and shaking at 275 rpm for aerobic growth. For growth curves, cells were pre-grown aerobically in 5 mL of lysogeny broth (LB) supplemented with 50 μg/mL chloramphenicol (Chl) for strains with pCBB, for inoculating minimal medium. For growth curves, cells were grown in M5 minimal medium containing: 1.29 mM K_2HPO_4, 1.65 mM KH_2PO_4, 7.87 mM NaCl, 1.70 mM NH_4SO_4, 475 μM $MgSO_4 \cdot 7\ H_2O$, 10 mM HEPES, 0.01% (w/v) casamino acids, 1× Wolfe's vitamin solution, and 1× Wolfe's mineral solution, then the pH adjusted to 7.2 with 5 M NaOH. After autoclaving, carbon

substrates were added depending on the experiment to final concentrations of: 20 mM D,L-lactate, 20 mM pyruvate, 10 mM uridine, 10 mM adenosine, or 10 mM inosine. Growth curves were performed in an aerobic plate reader (BioTek), grown in 2 mL of M5 (with appropriate carbon) in a 24-well plate. These were done in triplicate.

Table 5.1 Strains and Plasmids used in this study

Strain or Plasmid	Description	Source
S. oneidensis		
MR-1	Wild type *S. oneidensis*	Meyers and Nealson, 1988[20]
Δ*gpmA*	Mutant with gene deletion of SO_0049	This work
Plasmids		
pCBB	pZA11 vector expressing RuBisCO, *prkA*, and CA, Chl^R	Antonovsky et al. 2017[10]

HPLC analysis

HPLC analysis was performed as previously described (Tefft and TerAvest, 2019) with the amendments described in (Tefft et al., 2022)[9,10]. Sample analysis was performed on a Shimadzu 20A HPLC, using an Aminex HPX-87H (BioRad, Hercules, CA) column with a Microguard Cation H^+ guard column (BioRad, Hercules, CA) at 65 °C with a 0.5 ml/min flow rate.

Data analysis

Analysis of HPLC data, OD, current data, and growth curve data was done using RStudio using the following packages: ggplot2, dplyr, ggpubr, plyr, data.table, stringr, , and growthcurver[61–67].

Flux Balance Analysis

We used the genome-scale model of the metabolic network of *S. oneidensis* MR-1 from Ong et al[54]. The ATP growth-associated maintenance (GAM) cost was removed from

this version of the MR-1 model due to a lack of GAM measurements for other *S. oneidensis* strains that were being compared with MR-1. The GAM was added back in by referring to the information from an earlier iteration of the model[41]. All optimizations were performed in MATLAB (version 2019a) using the COBRA Toolbox[55] and version 8.1.1 of the Gurobi optimizer[40]. To model carbon utilization, specific uptake rates were set for each substrate (inosine, L-lactate, D-lactate, adenosine, uridine, acetate, N-acetyl glucosamine (NAG), propionate, pyruvate) in equal amounts. Using the OptKnock program, the number of potential mutations was limited to a maximum of two from a designated pool of enzymatic reactions, see Table 5.2. Reactions for RuBisCO and PrkA were added to the model, and RuBisCO was the reaction targeted for optimizing carbon flux. For each potential mutant and substrate combination, it was determined whether the growth was possible, and if so if it was non-linked (non-growth coupled), linked (growth coupled no unique), or dependent (growth coupled) on flux through RuBisCO. Additionally, we calculated the flux couple slope (mmol CO_2/gDW) for each mutant and substrate combination from the output, which is represented in the heatmap (**Figure 5.4**).

Table 5.2 Reactions Targeted as Potential Deletions[18]

Enzymatic Reaction	Enzyme	Reaction	Locus
ACALDI	acetaldehyde dehydrogenase	acetaldehyde + CoA+ NAD^+ -> acetoacetyl-CoA + H^+ + NADH	(SO2136)
ACONT	aconitase	citrate <=> isocitrate	(SO0432) or (SO0343)
ALCD2X	alcohol dehydrogenase (ethanol: NAD^+)	EtOH + NAD^+ <=> acetaldehyde + H^+ + NADH	(SO2136)
CS	citrate synthase	acetoacetyl-CoA + H_2O + oxaloacetate -> citrate + CoA+ H^+	(SO1926)

Table 5.2 (cont'd)

EDA	2-dehydro-3-deoxy-phosphogluconate aldolase	2-dehydro-3-deoxy-D-gluconate 6-phosphate -> glyceraldehyde 3-phosphate + pyruvate	(SO2486)
ENO	enolase	D-glycerate 2-phosphate <=> H_2O + phosphoenolpyruvate	(SO3440)
FBA	fructose-bisphosphate aldolase	D-fructose 1,6-bisphosphate <=> dihydroxyacetone phosphate + glyceraldehyde 3-phosphate	(SO0933)
FBP	fructose-bisphosphatase	D-fructose 1,6-bisphosphate + H_2O -> D-fructose 6-phosphate + Pi	(SO3991)
G6PDHY	glucose 6-phosphate dehydrogenase	D-glucose 6-phosphate + $NADP^+$ <=> 6-phospho-D-glucono-1,5-lactone + H^+ + NADPH	(SO2489)
GAPD	glyceraldehyde-3-phosphate dehydrogenase (NAD^+)	glyceraldehyde 3-phosphate + NAD^+ + Pi <=> 3-Phospho-D-glyceroyl phosphate + H^+ + NADH	(SO0538) or (SO2345) or (SO2347)
HEX1	hexokinase	ATP + D-glucose -> ADP + D-glucose 6-phosphate + H^+	(SO1656)
PDH	pyruvate dehydrogenase	CoA+ NAD^+ + pyruvate-> acetoacetyl-CoA+ CO_2 + NADH	(SO0424, SO0425, SO0426)
PGI	glucose-6-phosphate isomerase	D-glucose-6-phospate <=> D-fructose-6-phospate	(SO3547)
PGK	phosphoglycerate kinase	3-phospho-D-glyceroyl phosphate + ADP <=> 3-phospho-D-glycerate + ATP	(SO0932)
PGM	phosphoglycerate mutase	3-phospho-D-glycerate <=> D-glycerate 2-phosphate	(SO0049)
PGDH	phosphogluconate dehydrogenase	6-phospho-D-gluconate + $NADP^+$ -> CO_2 + NADPH + D-ribulose 5-phosphate	(SO1902)
PFL	Formate C-acetyltransferase	CoA + pyruvate <=> acetoacetyl-CoA + formate	(SO2912, SO2913)
PYK	pyruvate kinase	ADP + H+ + phosphoenolpyruvate -> ATP + pyruvate	(SO2491)
PPS	phosphoenolpyruvate synthase	ATP + H_2O + pyruvate -> AMP + 2 H^+ + phosphoenolpyruvate + Pi	(SO2644)

Table 5.2 (cont'd)

PPC	phosphoenolpyruvate carboxylase	CO_2 + H_2O + phosphoenolpyruvate -> H^+ + oxaloacetate + Pi	(SO0274)
PPCK	phosphoenolpyruvate carboxykinase	ATP + oxaloacetate -> ADP + CO_2 + phosphoenolpyruvate	(SO0162)
RPE	ribulose 5-phosphate 3-epimerase	D-ribulose 5-phosphate <=> D-xylulose 5-phosphate	(SO0292)
RPI	ribose-5-phosphate isomerase	α-D-ribose 5-phosphate <=> D-ribulose 5-phosphate	(SO1150)
TAL	transaldolase	glyceraldehyde 3-phosphate + sedoheptulose 7-phosphate <=> D-erythrose 4-phosphate + D-fructose 6-phosphate	(SO3546)
TKT1	transketolase	α-D-ribose 5-phosphate + D-xylulose 5-phosphate <=> glyceraldehyde 3-phosphate + sedoheptulose 7-phosphate	(SO0930)
TKT2	transketolase	D-erythrose 4-phosphate + D-xylulose 5-phosphate <=> D-fructose 6-phosphate + glyceraldehyde 3-phosphate	(SO0930)
TPI	triose-phosphate isomerase	dihydroxyacetone phosphate <=> glyceraldehyde 3-phosphate	(SO1200)

REFERENCES

(1) Lenoir, J., and Svenning, J. C. (2015) Climate-related range shifts - a global multidimensional synthesis and new research directions. *Ecography 38*, 15–28.

(2) Zarnetske, P. L., Skelly, D. K., and Urban, M. C. (2012, June 22) Biotic multipliers of climate change. *Science (1979)*. American Association for the Advancement of Science.

(3) Poloczanska, E. S., Brown, C. J., Sydeman, W. J., Kiessling, W., Schoeman, D. S., Moore, P. J., Brander, K., Bruno, J. F., Buckley, L. B., Burrows, M. T., Duarte, C. M., Halpern, B. S., Holding, J., Kappel, C. V., O'Connor, M. I., Pandolfi, J. M., Parmesan, C., Schwing, F., Thompson, S. A., and Richardson, A. J. (2013) Global imprint of climate change on marine life. *Nat Clim Chang 3*, 919–925.

(4) Pecl, G. T., Araújo, M. B., Bell, J. D., Blanchard, J., Bonebrake, T. C., Chen, I. C., Clark, T. D., Colwell, R. K., Danielsen, F., Evengård, B., Falconi, L., Ferrier, S., Frusher, S., Garcia, R. A., Griffis, R. B., Hobday, A. J., Janion-Scheepers, C., Jarzyna, M. A., Jennings, S., Lenoir, J., Linnetved, H. I., Martin, V. Y., McCormack, P. C., McDonald, J., Mitchell, N. J., Mustonen, T., Pandolfi, J. M., Pettorelli, N., Popova, E., Robinson, S. A., Scheffers, B. R., Shaw, J. D., Sorte, C. J. B., Strugnell, J. M., Sunday, J. M., Tuanmu, M. N., Vergés, A., Villanueva, C., Wernberg, T., Wapstra, E., and Williams, S. E. (2017, March 31) Biodiversity redistribution under climate change: Impacts on ecosystems and human well-being. *Science (1979)*. American Association for the Advancement of Science.

(5) Perera, F. P. (2017, February 1) Multiple threats to child health from fossil fuel combustion: Impacts of air pollution and climate change. *Environ Health Perspect*. Public Health Services, US Dept of Health and Human Services.

(6) Jourdin, L., and Burdyny, T. (2021) Microbial Electrosynthesis: Where Do We Go from Here? *Trends Biotechnol 39*, 359–369.

(7) Karthikeyan, R., Singh, R., and Bose, A. (2019) Microbial electron uptake in microbial electrosynthesis: a mini-review. *J Ind Microbiol Biotechnol 46*, 1419–1426.

(8) Rabaey, K., and Rozendal, R. A. (2010) Microbial electrosynthesis - Revisiting the electrical route for microbial production. *Nat Rev Microbiol 8*, 706–716.

(9) Nevin, K. P., Woodard, T. L., Franks, A. E., Summers, Z. M., and Lovley, D. R. (2010) Microbial Electrosynthesis: Feeding Microbes Electricity To Convert Carbon Dioxide and Water to Multicarbon Extracellular Organic Compounds. *mBio 1*, 1–4.

(10) Antonovsky, N., Gleizer, S., Noor, E., Zohar, Y., Herz, E., Barenholz, U., Zelcbuch, L., Amram, S., Wides, A., Tepper, N., Davidi, D., Bar-On, Y., Bareia, T., Wernick, D. G., Shani, I., Malitsky, S., Jona, G., Bar-Even, A., and Milo, R. (2016) Sugar Synthesis from CO_2 in *Escherichia coli*. *Cell 166*, 115–125.

(11) Herz, E., Antonovsky, N., Bar-On, Y., Davidi, D., Gleizer, S., Prywes, N., Noda-Garcia, L., Lyn Frisch, K., Zohar, Y., Wernick, D. G., Savidor, A., Barenholz, U., and Milo, R. (2017) The genetic basis for the adaptation of *E. coli* to sugar synthesis from CO_2. *Nat Commun 8*, 1–10.

(12) Gleizer, S., Ben-Nissan, R., Bar-On, Y. M., Antonovsky, N., Noor, E., Zohar, Y., Jona, G., Krieger, E., Shamshoum, M., Bar-Even, A., and Milo, R. (2019) Conversion of *Escherichia coli* to Generate All Biomass Carbon from CO_2. *Cell 179*, 1255–1263.

(13) Bar-Even, A., Noor, E., Lewis, N. E., and Milo, R. (2010) Design and analysis of synthetic carbon fixation pathways. *Proc Natl Acad Sci U S A 107*, 8889–8894.

(14) Bar-Even, A., Flamholz, A., Noor, E., and Milo, R. (2012) Thermodynamic constraints shape the structure of carbon fixation pathways. *Biochim Biophys Acta Bioenerg 1817*, 1646–1659.

(15) Antonovsky, N., Gleizer, S., and Milo, R. (2017) Engineering carbon fixation in *E. coli*: from heterologous RuBisCO expression to the Calvin–Benson–Bassham cycle. *Curr Opin Biotechnol 47*, 83–91.

(16) Ford, K. C., Kaste, J. A. M., Shachar-Hill, Y., and TerAvest, M. A. (2022) Flux-Balance Analysis and Mobile CRISPRi-Guided Deletion of a Conditionally Essential Gene in *Shewanella oneidensis* MR-1. *ACS Synth Biol 11*, 3405–3413.

(17) Burgard, A. P., Pharkya, P., and Maranas, C. D. (2003) OptKnock: A Bilevel Programming Framework for Identifying Gene Knockout Strategies for Microbial Strain Optimization. *Biotechnol Bioeng 84*, 647–657.

(18) Pinchuk, G. E., Hill, E. A., Geydebrekht, O. V., de Ingeniis, J., Zhang, X., Osterman, A., Scott, J. H., Reed, S. B., Romine, M. F., Konopka, A. E., Beliaev, A. S., Fredrickson, J. K., and Reed, J. L. (2010) Constraint-based model of *Shewanella oneidensis* MR-1 metabolism: A tool for data analysis and hypothesis generation. *PLoS Comput Biol 6*, 1–8.

(19) Rodrigues, J. L. M., Serres, M. H., and Tiedje, J. M. (2011) Large-scale comparative phenotypic and genomic analyses reveal ecological preferences of *Shewanella* species and identify metabolic pathways conserved at the genus level. *Appl Environ Microbiol 77*, 5352–5360.

(20) Myers, C. R., and Nealson, K. H. (1988) Bacterial manganese reduction and growth with manganese oxide as the sole electron acceptor. *Science Science 240*, 1319–1321.

Chapter 6: Conclusions and Future Directions

6.1 Conclusions and Significance

Understanding mechanisms of extracellular electron transfer (EET) in *S. oneidensis*, and harnessing synthetic biology techniques to optimize these mechanisms, is imperative for advancing microbial electrosynthesis (MES) and its applications in sustainable bioproduction and carbon capture. The work presented here contributes to this effort by employing an enzymatic system (Bdh) for reassessing the physiology energetics of inward electron transfer (Chapter 2 and 3),and using novel synthetic biology designs to implement an artificial carbon fixation pathway in *S. oneidensis* (Chapter 4 and 5).

6.1.1 Bidirectional Electron Transfer to Oxygen and NADH

Previous work published by our research group demonstrated that a proton and electrochemical gradient must be maintained across the inner membrane of *S. oneidensis* to sustain NADH generation from a cathode [1,2]. Through our investigation into sustained 2,3-butanediol production in *S. oneidensis* cells lacking the exogenous proton-pump proteorhodopsin (PR), we determined this was the result of coupling NADH generation to O_2 reduction. This bidirectional electron transfer (to O_2 and NAD^+) maintained the energetic balance needed to restore PMF via oxidases as it was being consumed by NADH dehydrogenases (NDHs). We first established this by confirming that *S. oneidensis* expressing butanediol dehydrogenase (Bdh) could reduce acetoin to 2,3-butanediol at a steady rate in a bioelectrochemical system (BES) being sparged with N_2. To investigate if bidirectional electron transfer was occurring under these conditions, we used a dissolved oxygen (DO) probe to determine the concentration of DO in the working chamber inoculated with *S. oneidensis.* We showed that despite N_2

sparging, there was ~ 1% DO (2 µM) present throughout the course of the experiment; the environment is microaerobic and not anaerobic. Reduction of one molecule of O_2 will translocate four protons across the inner membrane into the periplasm via *S. oneidensis*'s native oxidase (Cco, Cox). Similarly, four protons moving down the gradient into the cytoplasm are required to produce one NADH. Therefore, ~1% DO is more than sufficient to sustain the rate of 2,3-butanediol production that we observed. To confirm that the cells were using DO, we used a strain that is unable to reduce O_2 (Δ*cco*Δ*cyd*Δ*cox* pBDH). This strain showed a ~90% decrease in 2,3-butanediol accumulation compared to WT, and could be functionally complemented by expressing PR. Similarly, the current in Δ*cco*Δ*cyd*Δ*cox* pBDH decreased to approximately the same current observed in sterile BES, and was partially rescued by PR. Together, these results showed that *S. oneidensis* cells were using cathode-derived electrons to couple NADH generation to O_2 reduction in the microaerobic BES.

Interestingly, increasing DO via passive aeration negatively impacted 2,3-butanediol production. We determined this effect was due to the formation of reactive oxygen species (ROS) via interactions of O_2 with the cathode or reduced flavins. This ROS formation killed ~2.5 $\log_{10}$ cells within three hours of the onset of cathodic potential. Addition of catalase prior to cathodic potential reduced formation of H_2O_2 and mitigated the severity of cell death. We concluded that a microaerobic environment is optimal for bidirectional electron transfer for NADH generation under these conditions, as high O_2 levels have cytotoxic effects. There is room for continued optimization via modulation of DO %, as well as addition of other ROS-neutralizing enzymes such as superoxide dismutase. This will also be important for MES work that aims to operate in

an anaerobic environment. Careful attention must be paid to BES design to prevent oxygen intrusion as simply sparging with N_2 is insufficient to maintain true anaerobicity.

6.1.2 Flexibility of the EET Pathway

The EET pathway of *S. oneidensis* is a complex network of cytochromes, flavins and flavin associated proteins, that is heavily influenced by the environment.[3,4] Attempts to improve MES in *S. oneidensis* by increasing EET have heavily relied on electrical output to determine what is helpful or detrimental to this cause. However, this approach is susceptible to abiotic interference that can obscure what is happening biotically. Therefore, we reassessed the role of major EET pathway components during inward electron transfer. By expressing Bdh and adding acetoin, we can measure the 2,3-butanediol produced via acetoin reduction with NADH as a proxy for electron uptake to form NADH. This is less likely to be impacted by abiotic reactions than electrochemical measurements. Additionally, this approach will allow us to determine if there are any potential electron sinks that are diverting the flow of electrons away from the targeted reaction.

We first assessed EET via the Mtr pathway by comparing 2,3-butanediol accumulation between WT and Δ*mtrA*. This mutant showed a ~95% decrease in production and had cathodic current as low as abiotic BESs, confirming previous reports showing MtrCAB as essential for EET[3]. Similarly, results from a *cymA* deletion mutant were in alignment with the literature. The Δ*cymA* strain showed a decrease but not complete loss of both current and 2,3-butanediol. Recent reports have shown evidence for a CymA-independent pathway for electrons to enter the quinol pool from Mtr/periplasmic shuttles, and this work supports those findings; CymA is likely the

primary inner membrane electron hub, but other proteins can partially compensate its role[5–7].

We next examined the role of exogenous and endogenous flavins during EET. A strain unable to export flavins (Δ*bfe*) showed a significant decrease in current and 2,3-butanediol accumulation. Somewhat surprisingly, the phenotype for 2,3-butanediol production could not be complemented with exogenous flavin mononucleotide (FMN) or riboflavin (RF). However, we showed that exogenous flavins did increase the cathodic current. We hypothesize that this was due to abiotic reactions of free flavins with the cathode and photooxidation of the flavins. The discrepancy between current generation and bioproduction highlights the need to use quantifiable, biological outputs and not only current to assess the efficiency of EET, especially because the impact of flavins on EET has been debated. There is evidence suggesting flavins mediate EET over long distances as free flavins, aid in direct electron transfer as outer membrane cytochrome (OMC) cofactors, and influence regulation of biofilms and pili[8–10]. We investigated the latter by pre-growing Δ*bfe* cells with exogenous flavins, but saw similar results as without, suggesting they do not greatly alter the proteome under these conditions. Because our BES operates with stationary phase cells with no substrate, we cannot entirely rule out regulation being important. Additionally, this environment may also impact OMC binding or flavin diffusion through the biofilm.

Finally, we showed evidence that the native hydrogenases (Hyd, Hya) are important for increasing cell survival during stationary phase, in agreement with the literature[11]. We previously showed that deletion of the hydrogenases improved inward electron transfer to 2,3-butanediol. However, after modifying the experimental protocol

to remove residual organic matter, we saw their absence caused a decrease in production. In the initial design, the hydrogenases acted as an electron sink, siphoning electrons away from NADH, whereas in the absence of carbon they aid in survival, potentially by modulating the redox state of the quinol pool.

6.1.3 Synthetic Biology Strategies

S. oneidensis is a genetically tractable organism, so there are a wide range of bioengineering techniques that can be applied for improving performance in MES. We developed a pipeline that combines existing techniques from *E. coli* and *in silico* modeling to generate a novel mutation in a conditionally essential gene, *gpmA*[12–14]*.* This mutant was selected as a starting point for evolution of a carbon fixation pathway in *S. oneidensis* as outlined in Chapter 5[15–17]. The *gpmA* gene was considered essential based on metabolic modeling and failure to isolate a transposon insertion at this site during library preparation[18]. This was believed because GpmA connects the flow of carbon between gluconeogenesis and the tricarboxylic acid (TCA) cycle, and without GpmA cells either cannot build biomass or make ATP when given a single carbon source. To overcome this lethal phenotype, we used flux balance analysis to examine the growth potential of Δ*gpmA* with different carbon substrates. The results of the modeling were compared to phenotypes of a *gpmA* knockdown strain grown with different substrates. We determined that providing the cells with two substrates, one to build biomass and one to gain energy, restores growth phenotype of a *gpmA* knockdown to WT. Therefore, including additional substrate in the medium during the gene deletion protocol allowed strains that retain the mutation to compete with WT

revertants, resulting in a 44% rate of success in isolating a Δ*gpmA* mutant. This design can be implemented to generate other difficult genetic modifications.

6.1.4 Engineering Carbon Fixation in S. oneidensis

Finally, this dissertation outlines the initial steps we have taken towards using the Δ*gpmA* mutant as a basis for carbon fixation in *S. oneidensis.* Chapter 5 lays out how we used flux balance analysis to identify this mutant, as it showed the highest reliance on using CO_2-fixing RuBisCO to grow. We then further characterized this strain in relation to WT, and WT expressing the carbon fixation genes (pCBB). This strain (Δ*gpmA* pCBB) was unable to grow without two substrates, whereas WT with and without pCBB showed robust growth regardless of the carbon source. The mutant only consumed $_{D,L}$-lactate as a substrate and increased in OD_{600} when uridine was also available. This information will be the basis for directed evolution to generate a CO_2 fixing strain of *S. oneidensis.*

6.2 Future directions

This dissertation lays out the framework for building a chassis for carbon-neutral biofuel production using *S. oneidensis*. However, there is still a long road from where we are now to industrial application. As discussed in Chapter 2, the presence of oxygen, even at low levels, can have a large impact on the efficiency of MES systems. We showed that bubbling the BES working chamber with N_2 creates a microaerobic atmosphere, with enough oxygen to sustain bidirectional electron transport without generating ROS. However, as the DO level measured in the BES was a by-product of our design, there is room to improve this model. From an engineering perspective, more control over the DO concentrations can be achieved by using copper tubing instead of

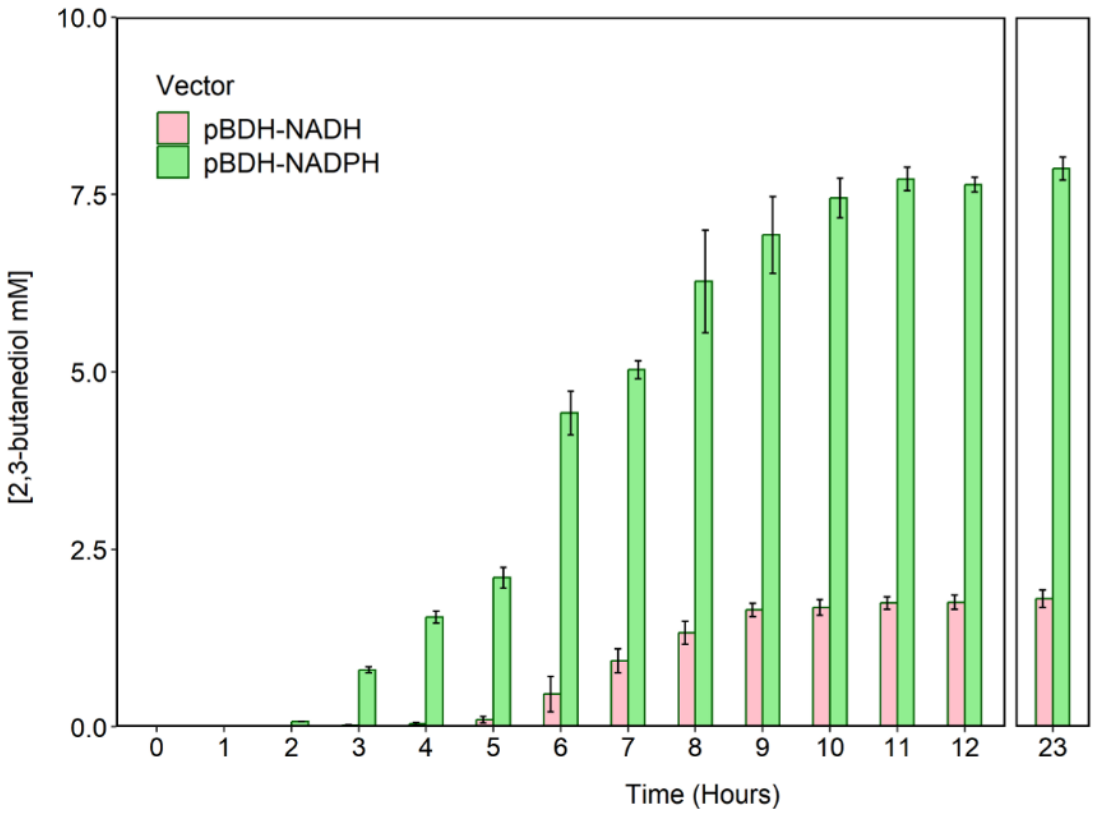

Figure 6.1 Comparing NADH and NADPH as Redox Partners with Bdh. Measurements of 2,3-butanediol accumulation in WT MR-1 expressing either a Bdh from *Enterobacter cloacae* (pBDH-NADH) or *Clostridium ljungdahlii* DSM 13528 (pBDH-NADPH) from an IPTG inducible promoter. Strains were pre-grown in LB, washed and resuspended in M5 medium with 20mM lactate, 10 mM acetoin, and 100 µM IPTG at an OD_{600} of 0.01. Samples were taken for OD_{600} readings (data not shown) and HPLC analysis every hour for twelve hours, then a final time point at 23 hours. The 2,3-butanediol accumulation in MR-1 pBDH-NADPH rapidly outpaced MR-1 pBDH-NADH, converting almost 80% of the acetoin in 23 hours, compared to less than 25%.

neoprene, crimping caps to tighten the stopper seals, and using specialized gas mixes (e.g., 1% O_2: 99% N_2). Additionally, the medium could be amended with oxygen scavengers (e.g., sodium sulfite, ascorbic acid) or other antioxidants (e.g., superoxide dismutase, N-acetyl cysteine). The *S. oneidensis* genome encodes three oxidases (Cyd, Cco, Cox) that are expressed under different conditions, have varying affinities for O_2, and different mechanisms for proton translocation. To determine if there is a specific oxidase, or combination of two oxidases, that work best for bidirectional electron

transfer, we would compare the current and 2,3-butanediol formation of single (Δ*cyd,* Δ*cco,* Δ*cox*) and double (Δ*cyd*Δ*cco,* Δ*cyd*Δ*cox,* Δ*cco*Δ*cox*) oxidase deletion mutants. Additionally, there is interest in using bidirectional electron transfer to generate NADPH, so we have made a vector that expresses a Bdh from *Clostridium ljungdahlii* DSM 13528 which uses NADPH instead of NADH. Preliminary data show that this version is functional in *S. oneidensis* and is more effective than the NADH version (**Figure 6.1**). If *S. oneidensis* can drive cathode-dependent 2,3-butanediol production with NADPH, the higher rate of activity of this enzyme could make it easier to discern smaller differences between experimental conditions.

The EET network in *S. oneidensis* has been well characterized in the context of power density and current generation. In few cases has this information been directly translated into impacts in MES. Therefore, expanding on the work in Chapter 3 would entail examining how other EET proteins contribute to 2,3-butanediol production. This approach could be done through a combination of gene deletion or overexpression, such as the mutant designed by Sun et al. that showed significantly higher current (Δ*fccA*Δ*napB*Δ*tsdB* pHGEN-Ptac-cctA)[19]. The Bdh system could be used to confirm the conclusions drawn for any mutant or engineered strain. Similarly, as we failed to rescue the phenotype of Δ*bfe* through exogenous flavins, there are still questions as to the scope of flavin influence on EET. Our data indicate that the origin of the flavins is crucial, which could point to a regulatory role. We ruled out a role for flavins to impact regulation during pre-growth, but their influence may not be enacted until contact with the cathode and by this time the cells have entered stationary phase and fail to shift their proteome. To test this hypothesis, we can compare the proteomes of cell

population at different stages of the experiment to look at differences in proteins known to be regulated by flavins, such as biofilm formation in WT versus Δ*bfe* and cytochrome expression profiles. Finally, to better understand the role of hydrogenases in EET, experiments should compare hydrogen formation during the experiment between WT and single and double hydrogenase knockouts (Δ*hydA,* Δ*hyaB,* Δ*hydA*Δ*hyaB*).

The work described in Chapter 4 and Chapter 5 lays the foundation for engineering an electroautotrophic *S. oneidensis.* As previously described, the next steps will be to design and implement laboratory directed evolution using Δ*gpmA* pCBB, a 10% CO_2 atmosphere, and medium supplemented with excess $_{D,L}$-lactate and limiting uridine. This will be done in a BIOSTAT-A fermenter operating as a chemostat, with samples taken daily to track metabolite concentration, OD_{600}, and check for contamination. Once the culture reaches a steady state, we expect the onset of a CO_2-fixing phenotype to be indicated by a rise in OD_{600} and a decrease in $_{D,L}$-lactate concentration. This outcome indicates that there is a population of cells that is using the other available carbon source (CO_2) and will therefore be consuming more $_{D,L}$-lactate and have a fitness advantage over cells that are not. Then, CO_2 fixing CFUs can be isolated and characterized. The next steps would be to replace the reliance on $_{D,L}$-lactate for ATP and NADH with a cathode. This process will result in a strain of *S. oneidensis* capable of electroautotrophy and be the basis for a carbon-neutral MES system.

REFERENCES

(1) Tefft, N. M., and TerAvest, M. A. (2019) Reversing an Extracellular Electron Transfer Pathway for Electrode-Driven Acetoin Reduction. *ACS Synth Biol 8*, 1590–1600.

(2) Tefft, N. M., Ford, K., and TerAvest, M. A. (2022) NADH dehydrogenases drive inward electron transfer in *Shewanella oneidensis* MR-1. *Microb Biotechnol 00*, 1–9.

(3) Coursolle, D., and Gralnick, J. A. (2010) Modularity of the Mtr respiratory pathway of *Shewanella oneidensis* strain MR-1. *Mol Microbiol 77*, 995–1008.

(4) Marsili, E., Baron, D. B., Shikhare, I. D., Coursolle, D., Gralnick, J. A., and Bond, D. R. (2008) *Shewanella* secretes flavins that mediate extracellular electron transfer. *Proc Natl Acad Sci U S A 105*, 3968–3973.

(5) Marritt, S. J., Lowe, T. G., Bye, J., Mcmillan, D. G. G., Shi, L., Fredrickson, J., Zachara, J., Richardson, D. J., Cheesman, M. R., Jeuken, L. J. C., and Butt, J. N. (2012) A functional description of CymA, an electron-transfer hub supporting anaerobic respiratory flexibility in *Shewanella*. *Biochemical Journal 444*, 465–474.

(6) Xiao, X., Li, C. X., Peng, J. R., Fan, Y. Y., and Li, W. W. (2023) Dynamic roles of inner membrane electron-transfer hub of *Shewanella oneidensis* MR-1 in response to extracellular reduction kinetics. *Chemical Engineering Journal 451*.

(7) Rowe, A. R., Salimijazi, F., Trutschel, L., Sackett, J., Adesina, O., Anzai, I., Kugelmass, L. H., Baym, M. H., and Barstow, B. (2021) Identification of a pathway for electron uptake in *Shewanella oneidensis*. *Commun Biol 4*, 1–10.

(8) Xu, S., Jangir, Y., and El-Naggar, M. Y. (2016) Disentangling the roles of free and cytochrome-bound flavins in extracellular electron transport from *Shewanella oneidensis* MR-1. *Electrochim Acta 198*, 49–55.

(9) Zhang, Y. T., Zhang, Y., and Peng, L. (2021) Electrochemical fluorescence microscopy reveals insignificant long-range extracellular electron transfer in *Shewanella oneidensis* anodic processes. *Electrochim Acta 398*, 1–7.

(10) Edwards, M. J., White, G. F., Norman, M., Tome-Fernandez, A., Ainsworth, E., Shi, L., Fredrickson, J. K., Zachara, J. M., Butt, J. N., Richardson, D. J., and Clarke, T. A. (2015) Redox Linked Flavin Sites in Extracellular Decaheme Proteins Involved in Microbe-Mineral Electron Transfer. *Sci Rep 5*, 1–11.

(11) Joshi, K., Kane, A. L., Kotloski, N. J., Gralnick, J. A., and Bond, D. R. (2019) Preventing Hydrogen Disposal Increases Electrode Utilization Efficiency by *Shewanella oneidensis*. *Front Energy Res 7*, 95.

(12) Pharkya, P., Burgard, A. P., and Maranas, C. D. (2003) Exploring the Overproduction of Amino Acids Using the Bilevel Optimization Framework OptKnock. *Biotechnol Bioeng 84*, 887–899.

(13) Burgard, A. P., Pharkya, P., and Maranas, C. D. (2003) OptKnock: A Bilevel Programming Framework for Identifying Gene Knockout Strategies for Microbial Strain Optimization. *Biotechnol Bioeng 84*, 647–657.

(14) Peters, J. M., Koo, B. M., Patino, R., Heussler, G. E., Hearne, C. C., Qu, J., Inclan, Y. F., Hawkins, J. S., Lu, C. H. S., Silvis, M. R., Harden, M. M., Osadnik, H., Peters, J. E., Engel, J. N., Dutton, R. J., Grossman, A. D., Gross, C. A., and Rosenberg, O. S. (2019) Enabling genetic analysis of diverse bacteria with Mobile-CRISPRi. *Nat Microbiol 4*, 244–250.

(15) Gleizer, S., Ben-Nissan, R., Bar-On, Y. M., Antonovsky, N., Noor, E., Zohar, Y., Jona, G., Krieger, E., Shamshoum, M., Bar-Even, A., and Milo, R. (2019) Conversion of *Escherichia coli* to Generate All Biomass Carbon from CO_2. *Cell 179*, 1255–1263.

(16) Herz, E., Antonovsky, N., Bar-On, Y., Davidi, D., Gleizer, S., Prywes, N., Noda-Garcia, L., Lyn Frisch, K., Zohar, Y., Wernick, D. G., Savidor, A., Barenholz, U., and Milo, R. (2017) The genetic basis for the adaptation of *E. coli* to sugar synthesis from CO_2. *Nat Commun 8*, 1–10.

(17) Antonovsky, N., Gleizer, S., Noor, E., Zohar, Y., Herz, E., Barenholz, U., Zelcbuch, L., Amram, S., Wides, A., Tepper, N., Davidi, D., Bar-On, Y., Bareia, T., Wernick, D. G., Shani, I., Malitsky, S., Jona, G., Bar-Even, A., and Milo, R. (2016) Sugar Synthesis from CO_2 in *Escherichia coli*. *Cell 166*, 115–125.

(18) Pinchuk, G. E., Hill, E. A., Geydebrekht, O. V., de Ingeniis, J., Zhang, X., Osterman, A., Scott, J. H., Reed, S. B., Romine, M. F., Konopka, A. E., Beliaev, A. S., Fredrickson, J. K., and Reed, J. L. (2010) Constraint-based model of *Shewanella oneidensis* MR-1 metabolism: A tool for data analysis and hypothesis generation. *PLoS Comput Biol 6*, 1–8.

(19) Sun, W., Lin, Z., Yu, Q., Cheng, S., and Gao, H. (2021) Promoting Extracellular Electron Transfer of *Shewanella oneidensis* MR-1 by Optimizing the Periplasmic Cytochrome *c* Network. *Front Microbiol 12*, 1–13.